Engineering cell-based patches as controlled VEGF-releasing devices for therapeutic angiogenesis

Inauguraldissertation

zur

Erlangung der Würde eines Doktors der Philosophie

vorgelegt der

Philosophisch-Naturwissenschaftlichen Fakultät der Universität Basel

von

EMANUELE GAUDIELLO

Von Italien

Basel, 2017

Genehmigt von der Philosophisch-Naturwissenschaftlichen Fakultät

auf Antrag von

Prof. Dr. Markus Affolter

Dr. Andrea Banfi

Dr. Martin Ehrbar

Basel, 20.09.2016

Prof. Dr. J. Schibler

The dean of the Faculty

Table of Contents

Chapter I: Introduction

The introduction is structured in four main sections. The first one reviews the pathological features of the Myocardial Infarction (MI), the unmet clinical needs and the strategies that are currently under investigation, focusing in particular on therapeutic angiogenesis. Thus, section two is a deep insight into the biological mechanisms of blood vessels growth, with a particular attention to the role of the Vascular Endothelial Growth Factor (VEGF). Section three gives a general overview of the several VEGF-delivery strategies to induce therapeutic angiogenesis with a conclusive deeper focus on the cell based gene therapy approach which ultimately leads to the aim of the thesis, described in section four.

1 Myocardial infarction: clinical needs and innovative treatments

1.1 Cardiovascular ischaemic diseases: a general overview

According to the last updated report published in 2014 by the World Health Organization (Global Health Estimates: Deaths by Cause, Age, Sex and Country 2000-2012), in 2012 an estimated number of 17.2 M of people died because of Cardiovascular Diseases (CVD) (1). Among them, the major number of deaths, about 14 M, were due to an ischaemic event (Cardiovascular Ischaemic Disease, CID), which is generally caused by a chronic atherosclerotic condition (2). Atherosclerosis defines the build-up of fatty deposits on the inner walls of the blood vessels, resulting in a progressive shortening of oxygen and nutrients to the downstream tissue (3). Depending from the affected district of the body, CID are divided in Peripheral Artery Disease (PAD, legs and arms), Coronary Artery Disease (CAD, heart) or cerebrovascular disease (brain, generally referred as stroke). CAD and stroke are the most severe conditions, resulting in about 30% of death during the acute phase.

1.2 Ischaemic heart disease: current treatment and unmet clinical needs

About 7.4 M of people die annually because of Coronary Artery disease (CAD), also known as Ischemic Heart Disease (IHD), making it the number-one cause of death globally. Although in developed countries the risk of death from CAD for a given age has decreased between 1980 and 2010 (1), mostly due to the prevention actuated to reduce some risk factor behaviours (smoking, lack of exercise, obesity, poor diet and excessive alcohol), severe morbidity and high mortality upon treatments are still common situations. In particular, management of Myocardial Infarction (MI), the most relevant disease in CAD, represents a major issue and, in most cases, current therapies

can only limit but not prevent the progression to an end-stage of Heart Failure (HF) (4). During MI, the shortage of oxygens and nutrients occurring in the downstream tissue upon a blockage in the coronary circulation leads to an ischaemic event and necrosis of the affected area. This event is responsible for the loss of cardiomyocytes, the contractile cells of the myocardium supporting the pumping of the heart, impairing the normal functionality of the organ. The severity of the clinical outcome depends on the extension and the location of the coronary blockage. Occlusions occurring in a minor coronary, or moderately in a major artery, result in a partial thickness damage of heart muscle, a condition known as NSTEMI (Non–ST-segment elevation myocardial infarction) accounting for about 30% of the total cases. On the other hand, STEMI (ST-segment elevation myocardial infarction), which represents the other 70%, occurs by developing the complete occlusion of a major coronary artery, causing a whole thickness-damage of the cardiac wall. It is crucial to distinguish between the two conditions because although similar, the treatment is different. Surgical and non-surgical neovascularization strategies aiming at restoring the blood flow to the ischemic tissue (such as Coronary Artery Bypassing Graft or Percutaneous Coronary Intervention) represent the first line treatments, together with pharmacological therapies such as antiplatelets, anticoagulants, beta-blockers, nitrate, statins, angiotensin-converting-enzyme inhibitors or angiotensin II receptor blockers. However, many patients still experience a negative outcome at long-term period. This is a direct consequence of the low capacity of human adult cardiomyocytes in re-entering in the cell cycle and

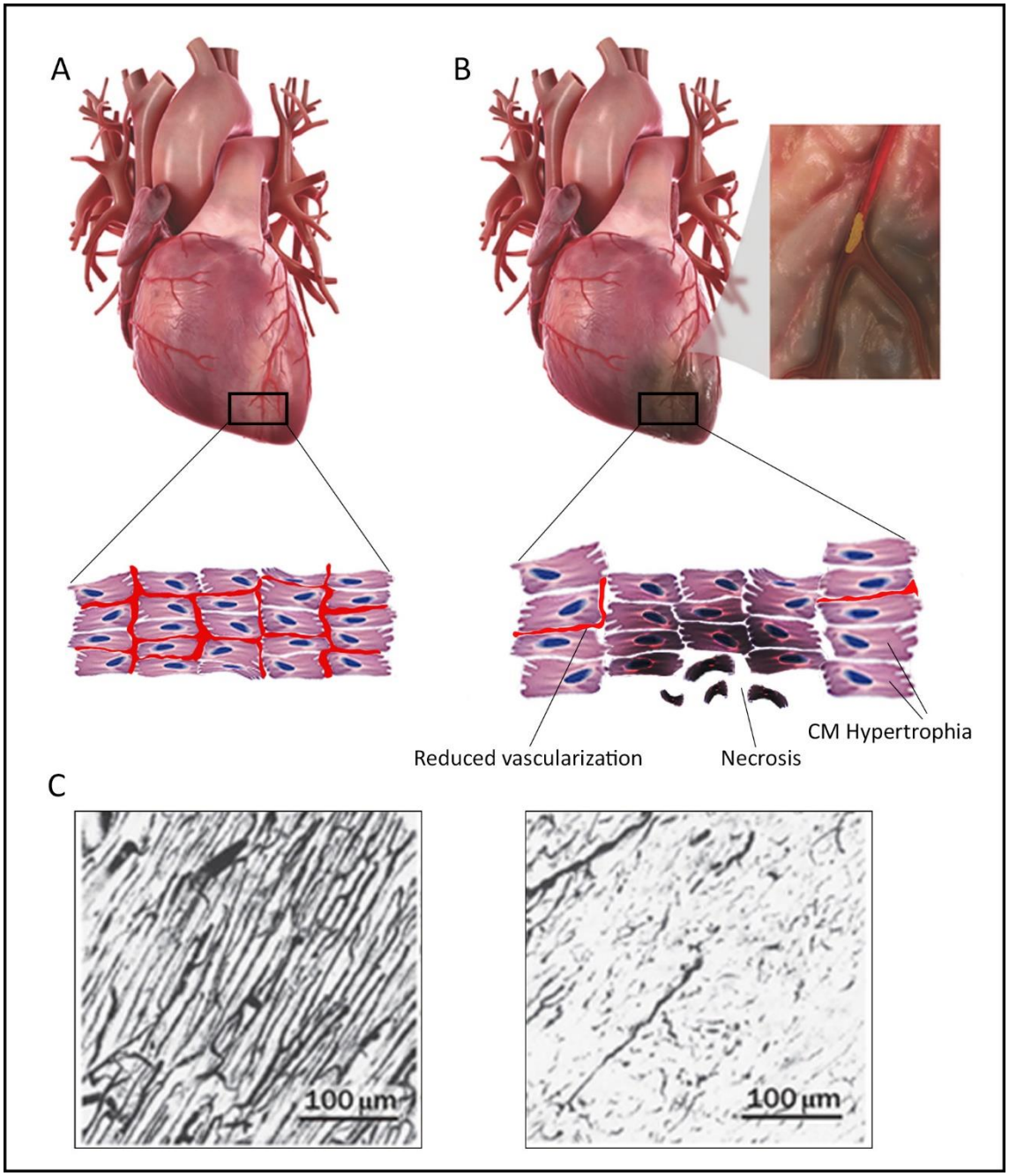

Fig. 1 Myocardial infarction (MI). **A)** Normal heart with functional cardiomyocytes supported by an adequate functional micro-vasculature. **B)** The occlusion of the coronary circulation results in necrosis of the downstream myocardium with a rarefaction of capillary network, a consistent loss of functional cardiomyocytes in the infarcted area and a hypertrophic reaction of the survived cells at the border zone. **C)** Histological evidence of the microvascular damaged in a rat heart after successful coronary reperfusion following MI (No-reflow phenomenon). Figure modified from: Forte G., et al **Stem Cell Rev.** *2013*; O'Neill H.S., et al **Adv. Mater**. *2016*; O'Farrell F.M. et al **Nat. Rev. Cardiol.** *2014.*

proliferating, thus regenerating the damaged tissue (5). Hence, in case of a grave ischemic event the heart replaces the huge loss of cardiomyocytes with a connective fibrotic tissue, which is not contractile and displays inadequate elastic and electro-conductive properties. To compensate, the remained cardiomyocytes at the border zone of the infarcted area undergo a hypertrophic process, which at long-term results in the disassembling of the sarcomere units and the consequent dysfunction of the organ. On the other hand, a spare destruction of the capillary network responsible for the exchange of oxygen and nutrients occurs in the affected area ( ) (6). Consequently, even in cases of re-established coronary circulation, incomplete or partial reperfusion of the ischaemic tissue is often observed and this disorder is known as no-reflow phenomenon (7). This continuous chronic situation is often associated with an increase in the size of the infarcted area and a faster progression to the end stage of heart failure (6). All these events are part of the post-infarct phase, known as ventricular remodelling that, in a long-term period, leads the heart to an end-stage of failure. While the current treatments (revascularization strategies and pharmacological therapies) aim on one hand to restore the coronary circulation and on the other hand to prevent the build of a new atherosclerotic plaque (8), the regeneration of the myocardium still remain an unmet clinical need (9). In order to restore completely the functionality of the infarcted myocardium, research has focus in finding novel strategies to replace the damaged tissue.

1.2.1 Novel biological-based treatment strategies

Since the early 90's, the group of Anversa conducted pioneer studies to investigate the latent mitotic capacity of adult mammalian cardiomyocytes (10). In 2009, an elegant

study carried on at the Karolinska Institute in Stockholm confirmed that human adult cardiomyocytes undergo a renewing process at the rate of c.a 1% per year at the age of 25 decreasing until 0.45% at the age of 75 (5). This observation drastically switched the paradigm considering the heart a terminal differentiated organ and represented the demonstration of a concept that for long time has been rejected by a great part of the scientific community (11). However, the origin of the new cardiomyocytes is still highly debated (12). The concept of using "stem cell therapy" to remuscularize the damaged myocardium captured the attention of investigators, which focused in identifying the "optimal" stem cell source, such as satellite cells, able to colonize and differentiate in functional cardiomyocytes (13). The identification in the mouse heart of resident adult cardiac progenitor cells (CPC) opened the new perspective to isolate, expand and re-inject *in loco* a cell population already committed towards a mature cardiac phenotype (14). Moreover, some studies reported the recruitment and partial trans-differentiation in cardiomyocytes of bone marrow-derived mesenchymal stem cells (MSC) in the area of the infarction (15) further supporting the rationale that cell-based therapies could be the solution for the heart repair. Nevertheless, the beneficial effects of injection of bone marrow–derived mononuclear cell (BMMNC) or MSC, although evident in preclinical animal models, became strongly controversial in the numerous clinical trials launched since the early 2000's, hence questioning their real therapeutic potential (16). A recent study with 1 year follow-up coordinated by the University Hospital of Zurich demonstrated no effect of BM-MNC injection in 200 patients affected by MI (17), further confirming the results of a previous independent study (18). Beyond the general poor cell survival, mainly due to inadequate delivery

strategies, serious doubts rose around the initial hypothesis of a direct contribution of the transplanted cells through an acquisition of cardiac phenotype (19). On the opposite, the rare poor improvements observed in some patients were often described as the results of cardioprotective/cardiorestorative effects triggered by factors secreted by the adult stem cell population, such as vascular endothelial growth factor (VEGF), basic fibroblast growth factor (bFGF), hepatocyte growth factor (HGF), insulin-like growth factor (IGF)-I, interleukin (IL)-1β and tumour necrosis factor (TNF)-α (20). These proteins are responsible for pro-angiogenic and anti-inflammatory stimuli associated with the reduction of scar and an amelioration of the overall cardiac functionality (21). This speculation found further support in a recent study performed in mice that deeper investigated the secretome profile of progenitor cells and the effects of a MSC conditioned media on myocardial infarction (22). Several groups developed trans-differentiation protocols to translate the cell therapy to a cell source with the unequivocal ability in differentiating in fully functional cardiomyocytes, like Embryonic Stem Cells (ESC) (23) or induced Pluripotent Stem Cells (iPSC) (24). However, the safety of these approaches still needs to be completely verified, and the usage of embryonic stem cells still brings unsolved ethical concerns (25).

In conclusion, these findings changed the conceptual mechanisms through which the infarcted area might benefit from cell therapy. Research moved from cell-based remuscularization strategies towards a restoring of innate tissue regeneration processes triggered by paracrine factors (19). Therefore, several approaches, including molecular medicine and gene therapies, have been developed either as standard technique alone or combined with stem cell therapies, to activate or enhance such

physiological mechanisms. In this context, one of the most studied approaches is the induction of therapeutic angiogenesis through the *in situ* delivery of pro-angiogenic factors.

1.3 Clinical need of therapeutic angiogenesis

As previously mentioned, in the clinical context of MI, the extension of the affected area depends on several factors, among which time and efficiency of blood flow reinstatement are critical aspects. Notably, some patients experience a non-adequate restoration of perfusion, known as no-reflow phenomenon, despite a successful primary surgical/pharmacological intervention, which correlates with a faster progression to an end-stage of heart failure (6). Such effect seems due to a rarefaction and dysfunction of the microvascular circulation occurring in the ischaemic tissue (26). Therefore, after MI, growth of new capillaries from the ischaemic border zone into the affected myocardium appears to be crucial for rescuing myocardial areas ("Hibernating Myocardium" or HM), which are still viable but in a chronic condition of inadequate blood supply (Fig 2) (27). Physiologically, perfusion can be re-established by two different mechanisms: angiogenesis and arteriogenesis. Angiogenesis is a process that is induced per se by the ischemic event and is characterized by the sprouting of new blood vessels from the pre-existing ones. On the other hand, arteriogenesis refers to a transformation of smaller arterioles into bigger arteries; it occurs following a variation of the fluid shear stress in small arterioles, in response to a change in the pressure caused by the occlusion of an upstream artery. Recently it was shown that pro-angiogenic stimuli occurring in the ischaemic tissue cause a back forward signalling which is responsible for the opening of

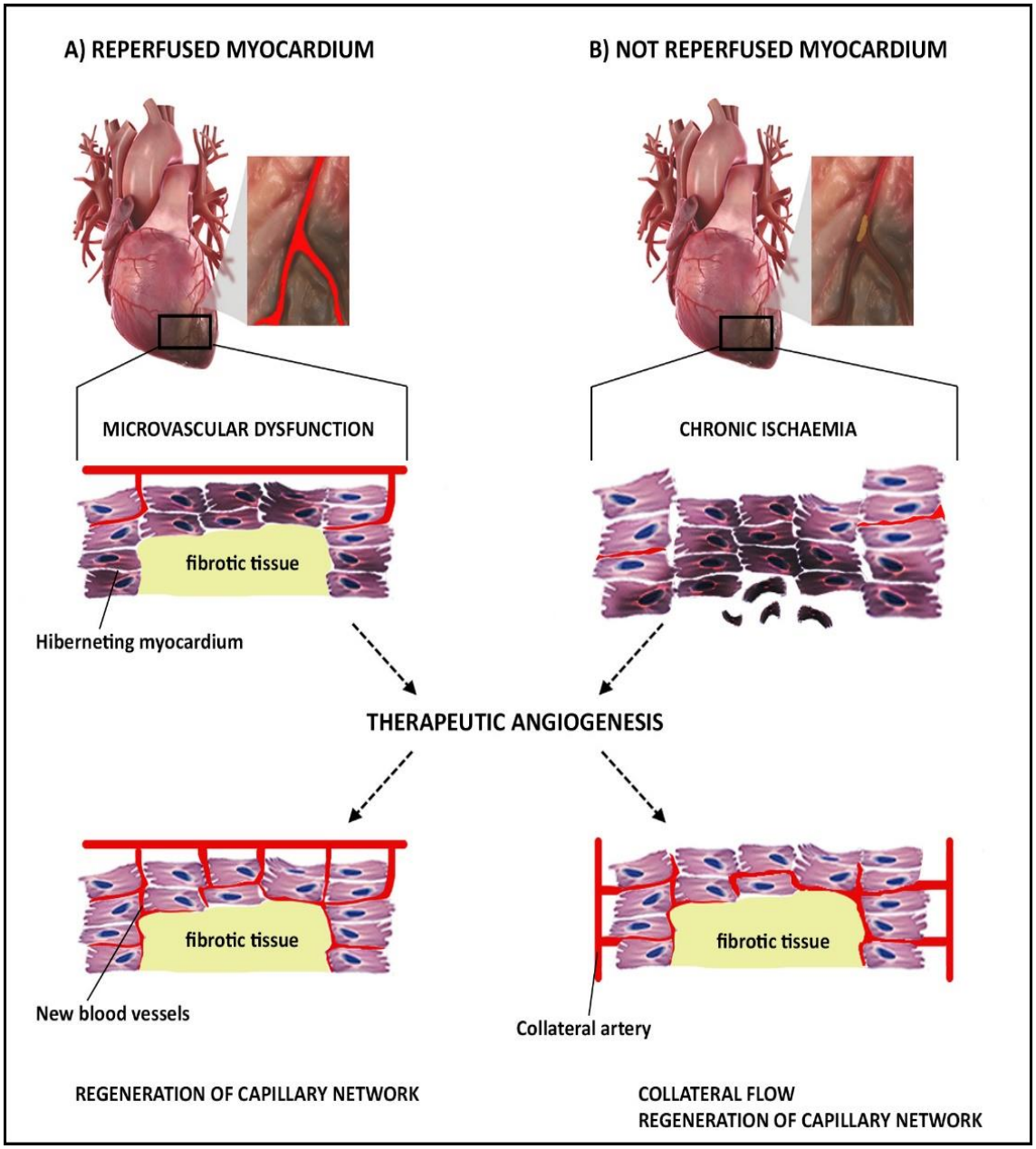

Fig. 2 Clinical need of therapeutic angiogenesis. A) In a condition of reperfused myocardium after MI, the rarefaction of the capillaries could generate a circumstance where cardiomyocytes are "hibernating", namely still alive but with a reduced functionality due to the inadequate supply of nutrients. In this context, therapeutic angiogenesis could rescue survived CM by restoring microvascular network. **B)** In a condition of chronic ischaemia, when the patient is not a good candidate for current revascularization strategies, proangiogenic stimuli in loco could be exploited to open collateral arteries and re-establish the coronary circulation. Figure modified from: O'Neill H.S., et al **Adv. Mater**. *2016.*

collateral arteries, namely tubes that are not functional in the physiological condition but become perfused following an ischaemic event (28). In this context, boosting the pro-angiogenic physiological response could be efficient in re-establishing the blood perfusion by inducing the growth of the new vessels as well as by triggering pro-arteriogenic signalling (Fig. 2). In perspective, it could be used as standard therapy e.g. in some clinical cases which are not suitable candidates for the currently available revascularization strategies, or in combination with cell based or tissue engineering approaches.

2 Biological mechanisms of blood vessel growth

2.1 Development of circulatory system

The cardiovascular system is responsible for supplying oxygen and nutrients and removing metabolic wastes from the tissues; two organs complete these functions: the heart and the blood vessels, which are respectively the blood-pumping unit and the tubes of the system. Blood vessels are divided in five different tubes: arteries: I) and veins II) which are the biggest in size and bring the blood from the heart to the main compartments of the body and vice versa. Arterioles III) and venules IV) instead connect the larger vessels with the capillaries (V) that are responsible of the nutrients exchange. In order to adequately reach and cover all the organs of a healthy human being, the heart pumps about 7.5l of blood every day, within almost 100.000 km length of blood vessels. In the adult organism, only two districts are avascular: the crystalline in the eye and the hyaline cartilage; cells from all the other types of tissues strictly relied on vascularisation. In tissues with a high metabolic demand, such as the myocardium, skeletal muscle or bone marrow, the distance from the cells to the closest capillary is rarely more than 200 µm (29) (30). Such a dense complex structure is the result of dynamic changes in assembling, expansion and remodelling of blood vessels, which start during the embryogenesis, and is maintained during all the life in response of pathophysiological stimuli.

2.1.1 Vasculogenesis

In vertebrates, the development of the cardiovascular system is one of the first events that take place during the organogenesis and starts with the biological process of vasculogenesis, during which mesoderm derived endothelial precursors assembly in

the primitive vascular network. In the past years, many studies on transgenic mice models helped in determining the key pathways responsible for the guide of de novo blood vessel formation during gastrulation, such as Vascular Endothelial Growth Factor (VEGF) and its receptor flk-1 (VEGFR-2). Notably, VEGF knockout is lethal in the early stage of the gastrulation also in a heterozygosis showing that this signal is haploinsufficient (31). Equally, mutation of flk-1 is fatal within the first 9 days of development due to the inability of the embryo in forming blood vessels and hematopoietic compartment (32). Morevoer, Flk-1 is an early marker of the primitive angioblasts and appears on a subset of Brachyury-positive cells in the primitive streak. It has been shown that these cells are able to give raise to either endothelial or hematopoietic lineages (33). In response to a basic Fibroblast Growth Factor (bFGF) and bone morphogenetic protein 4 (BMP-4) mediated signals, hemangioblasts migrate in the extra-embryonic ectoderm yolk sac and start to aggregate in clusters (blood islands) where the inner cells proceed towards a haematopoietic lineage whereas the external ones fuse, forming the first capillary plexus. On the other hand, mesoderm progenitors that disperse intra-embryonic, driven by sonic hedgehog (SHH), Notch and VEGF signals, assemble the dorsal aorta and the cardinal vein. These two distinct events together establish the initial primitive vascular network (34), which then undergoes expansion, remodelling and stabilization to form a mature circulation during the process named angiogenesis. VEGF is the main regulator of this event, but angiopoietins, platelet-derived growth factor (PDGF-B) and Transforming Growth Factor (TGF-B) are critical for the mobilization of endothelial cells (hence the growth of new capillaries) and the recruitment of pericytes that are responsible to stabilise the

newly formed blood vessels (35). Notably, most of the signalling pathways governing the assembling and the vasculature expansion during embryo development are recapitulated in a situation of neo-angiogenesis in the adult (36).

2.1.2 Arterial-venous specification

As vessels begin to remodel and grow towards the different compartment of the body, they simultaneously need to be specified as arterial or venous phenotype, which are interconnected but maintain different structures and functions. In fact, unlike veins, arteries are subjected to high blood pressure of systole; therefore, a thick layer of smooth muscle cells and connective tissue surround their endothelium. Based on this concept, initially it has been thought that hemodynamic forces could drive specification of the arterial-venous phenotype soon after the starting of the circulation in the yolk sac. Consistent with this hypothesis, Le Noble and colleagues showed that manipulation of the blood flow in the yolk sac of the chick causes simultaneously the downregulation the arterial marker EphrinB2, and the conversion to venous endothelial phenotype (EphB4) (37).

On the other hand, interfering with the Notch-Gridlock signalling in zebrafish before the onset of a functional circulation causes a progressively reduction of the artery regions, simultaneously expanding area of the vein, shown by an increase in expression of EphB4 receptor (ephb4) and contiguous decrease of the arterial marker Ephrin-B2 (38). Moreover, it is well-known that in the mice embryo the complementary and mutually expression of EphrinB2 and EphB4 on angioblasts occurs already during early stage of vasculogenesis (39). Another independent study showed that the vascular plexus already contains a mix of angioblasts positive for Neuropilin1 (NP1) or NP2

expression, which are specific markers for arterial or venous phenotype respectively (40). These studies taken together suggest a prior key role of a genetic selection for the specification of arterial-venous phenotype, which however can be further shaped by haemodynamic forces during the early vasculature expansion.

2.2 Angiogenesis

Angiogenesis is the biological process during which new blood vessels grow and expand from the pre-existing vasculature. It occurs throughout the entire life of the organism: starting during the early phase of embryo development until the old age. During embryogenesis, angiogenesis is responsible for the expansion and maturation of a functional circulatory system as well as is essential to provide fundamental morphogenic instructions for the correct development of some organs such as liver and bone (41). However, in the adulthood most of the blood vessels remain in a quiescent state with some physiological exceptions like in the placenta during the pregnancy, in the cycling ovary and the wound healing process (42). Nevertheless, all the endothelial cells maintain their ability in re-entering in the cell cycle and proliferating in response to proangiogenic stimuli triggered by specific growth factors. The mechanisms occurring during the angiogenesis process can be summarize in two main steps: I) tube and lumen formation and II) blood vessel maturation and stabilization. Mural cells (either pericytes or smooth muscle cells), play a key role in both phases by surrounding quiescent blood vessels and cross-talk with endothelial cells modulating their proliferation and survival. In response to a pro-angiogenic stimulus they detach from the endothelium and degrade the basement membrane, through secretion of Matrix Metalloproteinases (MMPs), allowing the migration of the

endothelial cells. Subsequently, mural cells are recruited through a Platelet-derived Growth Factor-B (PDGF-B) gradient on the wall of the newly formed blood vessel guaranteeing the maturation and stabilization of the vessels by depositing new ECM to restore the basal membrane. Formally, by definition a new vessel is stable when becomes independent from the pro-angiogenic stimulus (42). Angiogenesis is a process tuned by balanced secretion of different growth factors; therefore, once this balance is lost, this process can became a severe pathological condition such as in intraocular neovascular disorders, immunogenic rheumatoid arthritis and psoriasis (36). Moreover, solid neoplasia benefits of an uncontrolled and leaky angiogenesis to deliver nutrients in the core of the mass which otherwise would became necrotic. Several families of different growth factors have been identified in being able to stimulate the proliferation of endothelial cells such as VEGF, FGF and HGF (43). Nevertheless, vascular endothelial growth factor family predominantly represents the master regulator of angiogenesis process.

2.2.1 Vascular endothelial growth factor

VEGF has been identified for the first time in 1983 as a microvascular permeability protein in the guinea pigs, hamsters, and mice tumour ascites fluids (44); several years later, Ferrara and Henzel purified from a medium conditioned by bovine pituitary follicular cells a novel growth factor specific for endothelial cells (45). In mammals the VEGF family includes 5 members (VEGF-A, -B, -C, -D and the Placenta Growth Factor) and is part of the PDGF superfamily growth factors, which are secreted as dimeric proteins (Fig. 3).

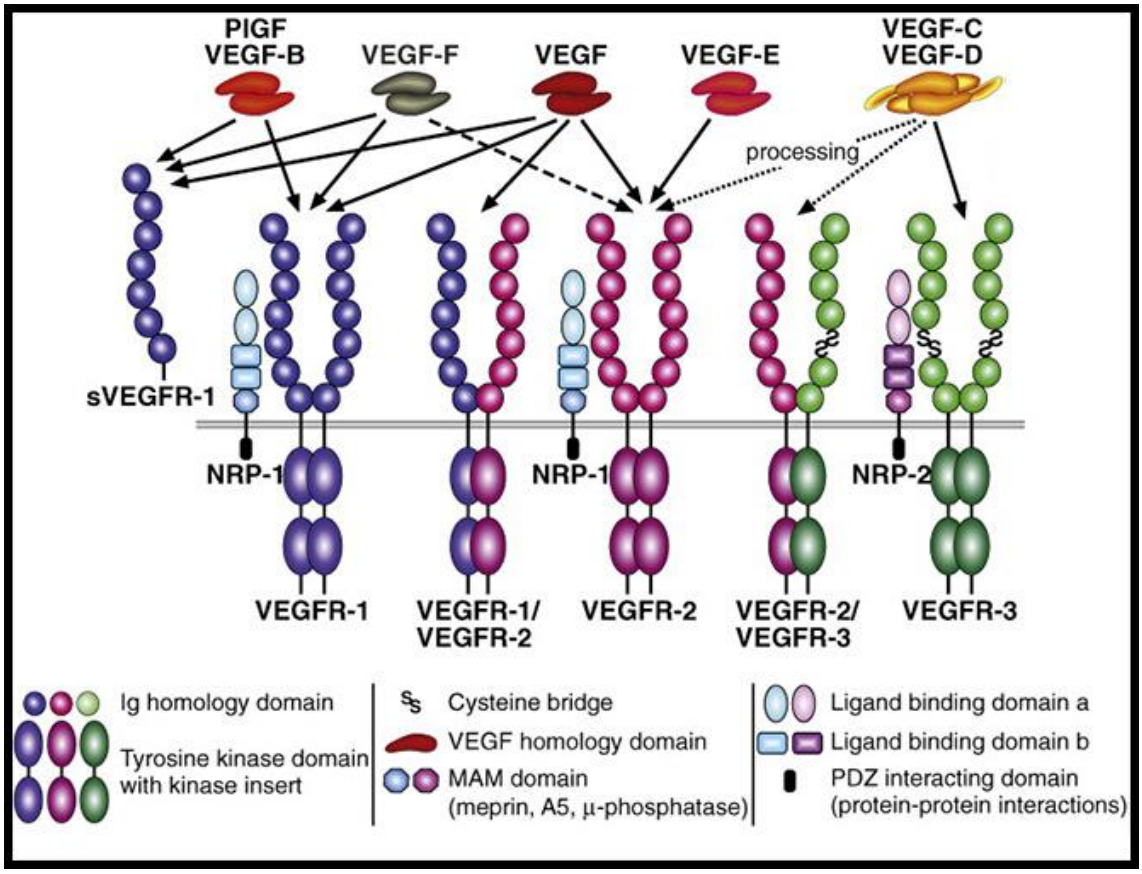

Fig. 3 Structure and interactions of VEGFs with VEGFRs and their neuropilin (NRP) co-receptors. The arrows indicate the varying specificities of VEGF growth factors bind to their receptors. The N-terminal and C-terminal of VEGF-C and VEGF-D can be processed to interact with VEGFR-2. The binding of the dimeric VEGF ligands stimulates receptor dimerisation with a consequent autophosphorylation, triggering the downstream signalling. In addition to the five VEGF members known in mammals, other two VEGF homologues have been identified: one produced by Orf viruses (VEGF-E) and one isolated from snake venom (VEGF-F). Figure modified from: Lohela M., et al **Curr. Opin. Cell. Biol.** *2009*.

VEGF-A is the main family member responsible for mitosis and migration of endothelial cells, also functioning as a vasodilator through a nitrox oxide signal cascade; on the opposite, VEGF-B has a less predominant role in triggering pro-angiogenic signals and is rather involved in preservation of existing blood vessels (46). VEGF-C and -D are mainly responsible for the development and repair of the lymphatic circulatory system; it has been shown that VEGF-C is required for sprouting of the first lymphatic vessels from embryonic veins and VEGF-$C^{-/-}$ in mice results to be lethal at a prenatal

stage (47). Moreover, VEGF-C can also modulate the vascular permeability and promotes the growth of blood vessels. (48). PlGF is mainly express by the placental trophoblast during embryogenesis and is important for vasculogenesis; nevertheless, it plays a role as well in regulating angiogenesis response during ischemia, inflammation and wound healing. Interestingly, secretion of PlGF is associated with a promotion of atherosclerotic intimal thickening and macrophage accumulation (49).

2.2.1.1 VEGF receptors

The various VEGF ligands interact with different affinity and defined specificity with three transmembrane tyrosine kinase receptors (VEGFRs): I) VEGFR-1 also known as fms-like tyrosine kinase 1 (Flt-1), II) VEGFR-2 defined as human kinase insert domain receptor (KDR)/mouse fetal liver kinase 1 (Flk1) and III) VEGFR-3 described as fms-like tyrosine kinase 4 (Flt4) (Fig. 3). All VEGFRs have an extracellular portion consisting of 7 immunoglobulin-like domains, a single transmembrane spanning region and an intracellular portion containing a split tyrosine-kinase domain. Interaction with the ligand causes the dimerization and activation through transphosphorylation signal. Beyond the Tyrosine Kinase Receptors (TKRs), Neuropilin 1 and 2 (NRP1 and NRP2), originally identified as semaphorin receptors, have also affinity for specific VEGF isoforms and they function mostly as co-receptors rather than directly transducing the signal (50). For example, NRP1 selectively enhances VEGF-A binding to VEGFR-2, by presenting the protein to the receptor, increasing the downstream signal (51). Moreover, in the cornea has been identified a soluble form of VEGFR-1 (sVEGFR-1), a VEGFR-1 splice variant having a potent anti-angiogenic activity, which contributes in maintaining the area avascular (52). While PlGF/VEGF-B and VEGF-D bind selectively

VEGFR-1 and VEGFR-3 respectively, receptor specificity of VEGF-C is regulated by proteolytic processings (53); VEGF-A displays high affinity for both VEGFR-1 and VEGR-2. Signaling of VEGF-A through VEGFR-2 is the major pathway that activates angiogenesis by inducing the proliferation and migration of endothelial cells (54).

2.2.1.2 Role and regulation of VEGF-A isoforms

VEGF-A is encoded in humans by the *VEGFA* gene located on the chromosome 6p21.3 which is governed by upstream factors include oxygen tension through the signal triggered by the Hypoxia inducible factor (HIF), beyond several cytokines, chemokines and growth factors. The gene contains 8 exons separated by 7 introns; the alternative splicing occurring for exons 6a and 7 results in the generation of four principal isoforms, having 121, 165, 189, and 206 amino acids, respectively, after the cleavage of the signal sequence ($VEGF_{121}$, $VEGF_{165}$, $VEGF_{189}$, $VEGF_{206}$). Less frequent splice variants have been recently identified, including $VEGF_{145}$, $VEGF_{183}$, and $VEGF_{162}$ (55). Moreover, in human it has been also reported a second category of isoforms generated by a distal splice-site selection (DSS) of the exon 8 which paradoxically results in a generation of anti-angiogenic VEGFxxxb versions (56). VEGF isoforms are typically secreted as cysteine linked antiparallel dimers. Binding to the VEGFRs is mediated at the exon 3 and 4 (VEGFR1 and 2 respectively), whereas the exons 6 and 7 contain sequences of basic amino acids, (heparin binding domain, HBD) which are responsible for the interaction of the VEGF with heparan-sulphate proteoglycans (HSPGs). Importantly, the exon 7 contains also some regions important for the binding with NRP1. Since the splicing involves these sequence of the protein, isoforms $VEGF_{121}$ (which lacks both the exons 6 and 7) and $VEGF_{165}$ (where the exon 6 is absent) display no- or reduced

interaction with extracellular matrix HSPGs e.g. perlecans and agrins, as compared to the longer versions 189 and 206 (57). VEGFs bind to the ECM close to the producing cells and diffuse around, forming a spatial gradient, which is responsible of driving the growth of blood vessels. Larger VEGF isoforms that tightly bind the ECM show steeper gradients, suggesting that heparin interactions per se slow the molecule diffusion. Nevertheless, computational studies on VEGF diffusion in vivo demonstrated that ECM sequestration alone could not be the responsible for generation of the protein gradient. This process is rather controlled by several balanced biological events including VEGF cleavage or degradation and sequestration on cell surface by membrane HSPGs (e.g. syndecans) (58). In this context, $VEGF_{189/206}$ might represent storage isoforms of the growth factor, which can be released after specific pro-angiogenic cleavage process such as the proteolytic cascade of plasminogen activation (59). Importantly, several studies suggested that $VEGF_{165}$, due to the intermediate ECM-binding properties and the affinity with the NRP1 has the ideal characteristics of bioavailability and biological potency (59). Remarkably, expression of only $VEGF_{120}$ (isoforms in mice are one amino acids shorter than in human) in mice resulted to be lethal prenatally, with a general reduced vascular complexity, leaky vessels because of poor pericytes coverage and ischemic cardiomyopathy (60). In addition, also mice expressing $VEGF_{188}$ showed impaired angiogenesis with an excess of thin and disorganized vascular branches and several muscle disorders, resulting in affected growth and poor survival (60). On the other hand, homozygotes expression restricted to $VEGF_{164}$ displayed a normal vessel phenotype with apparently any problem in survival (61).

2.2.2 Mechanisms of blood vessel expansion

Angiogenesis can occur mainly through two different mechanisms: sprouting or intussusception. High debate still exists around the recruitment of bone marrow derived cells (BMCs) or circulating endothelial progenitor cells and their incorporation into the growing vessels (a process known as "postnatal vasculogenesis") (62). Sprouting has been the first hypothesized and observed mechanism of blood vessel growth, occurring in response to a gradient of VEGF; the sequential steps of branching and the molecular mechanisms behind have been extensively investigated. As previously mentioned, in the adult under physiological conditions the blood vessels are maintained in a quiescent state; vascular homeostasis and survival are triggered by an autocrine endothelial cell VEGF-mediated signal (63). Moreover, endothelial cells are equipped with a system that represses their proliferation while allowing them in responding promptly to proangiogenic stimulus; this event is controlled mainly by the cross talk at the gap junctions of endothelial cells via the Angiopoietin (ANG)–Tie signalling. Briefly, mural cells secrete ANG-1, which clusterises the Tie2 receptor in a *Trans* configuration at the gap junctions of two adjacent endothelial cells, transducing pro-survival and anti-mitotic signal. On the opposite, the pro-angiogenic signals causes the release of ANG-2 from pericytes as well as from intracellular storage of endothelial cells, that acts as competitor of ANG-1, liberating Tie2, resulting in migration and proliferation signals (64). Branching and migration of the new blood vessel towards the source of the pro-angiogenic stimulus is a process that is guided by so called tip cell, which tests the environment with extruded filopodia, providing guidance cues (65). Following the angiogenic signalling at the onset of the sprouting, pericytes start to

degrade the basement membrane that surrounds quiescent blood vessels, liberating the endothelial cells (66). The process is actuated through secretion of metalloproteinases (MMPs) and is further controlled by the tip cells during the growth of the new tube (Fig. 4A). Importantly, extracellular matrix degradation also liberate pro-angiogenic growth factors (67). Sprout elongation and lumen formation is supported by the proliferation of stalk cells, which follow the tip guide. Selection of the tip cell and the subsequent specification of the next stalk endothelial cells is a process that is fine regulated by the Notch pathway.

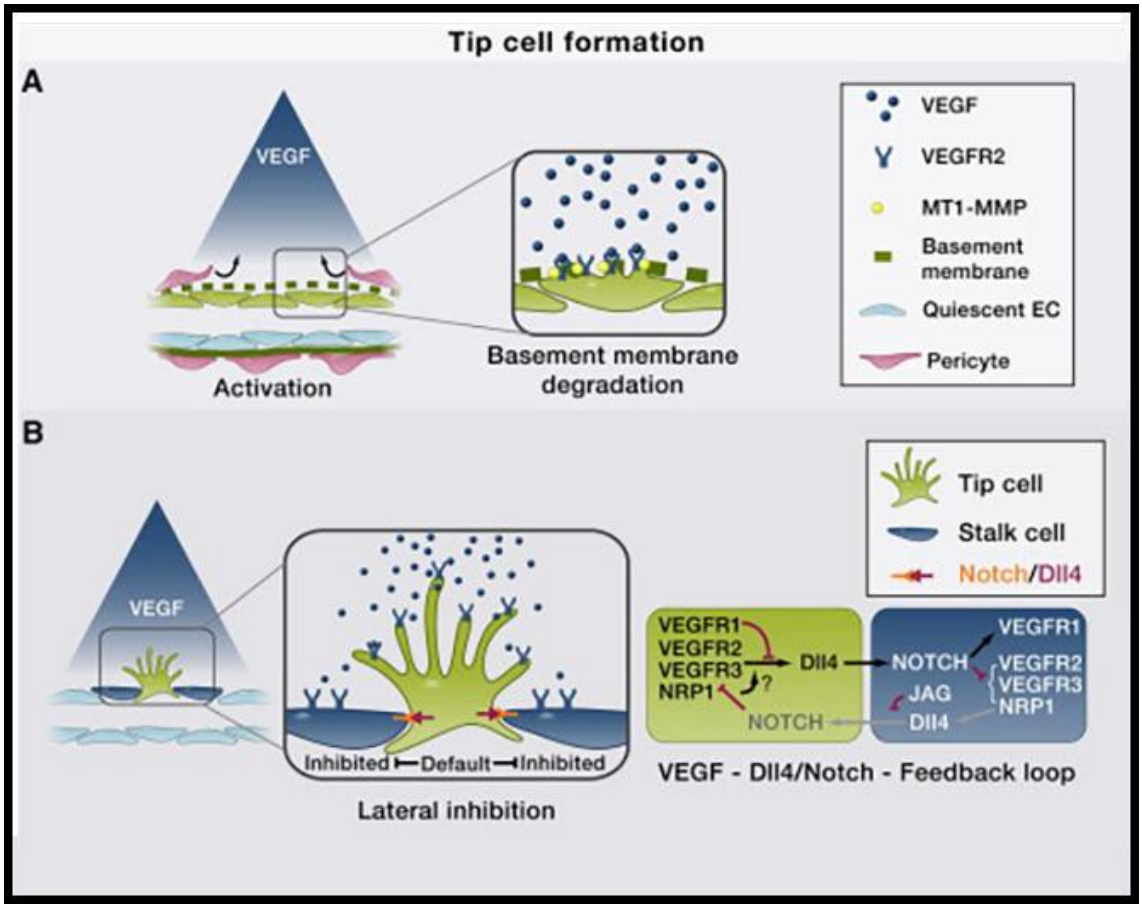

Fig. 4 Sprouting angiogenesis and tip-stalk cells regulation. A) VEGF stimulation causes the activation of endothelial cells (EC), which start to degrade the basement membrane. Pericytes detach from the vascular structures, allowing EC to migrate and elongate the new blood tube. **B)** Selected tip cells prevent the adjacent endothelial cells in acquiring tip features through the Notch/Dll4 lateral inhibition pathway, which is responsible for suppression of VEGFR2 and concomitant activation of cell cycle. Figure modified from: Potente M., et al **Cell** *2011.*

In particular, VEGF signal on tip cells stimulate the expression of Dll4, activating the notch signalling on the adjacent cells. In response, notch supresses the tip cell phenotype in the stalk cells by decreasing the expression of VEGFR2 and increasing VEGFR1. In contrast, tip cells receive high JAGGED1 signal, a second ligand for notch with opposing functional roles in the vasculature, which maintaining the high expression of NRP1 and VEGFR2 (68). Selection of the tip cell depends on small differences in the expression or activity of VEGFR2 on endothelial cells or microenvironmental discrepancy in the concentration of VEGF, which could give an initial advantage to some individual cells to become the tip (Fig.4B) (69). The end step of the sprouting angiogenesis includes contact between tip cells from different sprouts to form new vessel circuits, and lumen formation that can occurs through different mechanisms such as cell hollowing (70). After the structure of the new vessel is established, the process of maturation must start (explained more in detailed in the next paragraph). So far, most of the knowledge about molecular mechanisms regulating angiogenesis have been studied in and refereed to the sprouting model. Nevertheless, the alternative vessel-growth process known as intussusception, takes a significant part in patho-physiological process, including cancer and embryogenesis (71) (72). Moreover, it has been observed that upon VEGF overexpression in rodent models, intussusception is the predominant mechanism through which angiogenesis occurs (73). It consists in the longitudinal splitting of two blood vessels from an existing one and occurs through the formation and subsequent fusion of aligned transversal holes within the blood vessel wall (Fig. 5). These gaps are known as vessel pillars and are considered the hallmarks of the intussusception mechanism. The formation

includes 4 consequential steps during which I) activated endothelial cells start to protrude an intralumen process towards the opposite vessel wall, until a contact is established with and opposite protrusion; then a perforation occurs II) and the interstitial hole is immediately invaded by perycites III); through the deposition of extracellular matrix the pillar is re-shaped until it fuses with the close one, resulting in the splitting of the vessel (Fig. 5).

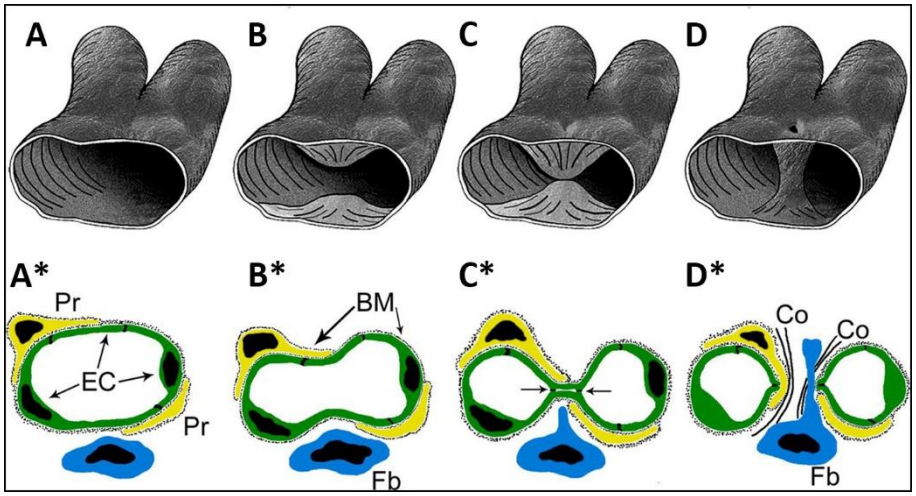

Fig. 5 Morphogenic features of pillar formation. A–D) 3D graphic reconstruction of transluminal pillar formation. **A*–D*)** 2D transversal images of the relatives events (A)–(D). Endothelial cells (EC) on the opposite sides of a capillary protrude into the lumen until they make contact with each other. The formation of endothelial junctions reinforces and maintains the contact until the endothelial bilayer is perforated centrally. Fibroblasts (Fb) and pericytes (Pr) invade the newly formed pillar being invaded and start todeposit collagen fibrils (Co). BM, basement membrane. Figure modified from: Djonov V., et al. **Cell Tissue Reearch** *2003*

Induction of pillar formation is an aspect that still needs to be fully elucidated, although recent evidences showed that haemodynamic variations occurring in areas characterized by low shear stress and turbulent flow conditions play a key role (74).

2.2.3 Maturation process

Upon activation of endothelial cells and the consequent growth (or split) of the capillary network, the newly formed blood vessels need to mature in order to become persistent (75) and acquire tissue specific differentiation adapting the local

homeostatic demands (76). Recruitment of mural cells surrounding the new capillaries is a fundamental step for vessel maturation. Pericytes are mainly guided by the adequate secretion of PDGF-BB from endothelial tip cells that acts as chemoattractant, stimulating the proliferation and migration of the mural cells (77). Notably, mice lacking of *pdgfβ or pdgfrβ* display affected pericytes function resulting in persistent endothelial proliferation and vascular abnormalities with consequent bleeding (78). Once the pericytes take contact with the wall of the blood vessel, they induce endothelial differentiation and growth arrest by both cell-cell direct interactions and expression of paracrine factors. In particular, TGF-*β* is important for the deposition of ECM around the blood vessel to reconstitute the basement membrane, an event that is crucial for the stabilization process, and acts as autocrine factor to stimulate the proliferation of mural cells (79). Loss of function of TGF-*β* receptor 2 in mice results in vessel instability due to the affected pericytes development (79). Another pathway that has been shown to be critical for endothelial cells/pericytes interaction is the EphrinB2 expression, necessary to guarantee the anchor of mural cells on the vessel wall (80). Pericytes can also be recruited by an indirect mechanism through the action of immuno-cells. It is well-known that populations of bone marrow (BM)-derived mononuclear cells also are recruited to the sites of angiogenesis in adult tissues, triggering pro-angiogenic effects by secreting paracrine factors (81) (82). In particular, a population of monocytes, expressing both CD11b and the NRP1, stimulate pericytes and smooth muscle cell recruitment by secreting transforming growth factor-β (TGF-β) and platelet-derived growth factor-BB (PDGF-BB) (83), leading also to normalization of tumour vessels and inhibiting tumour growth (84). In this context, our group recently

demonstrated that increasing doses of VEGF negatively regulated vascular stabilization in a dose-dependent fashion, without affecting pericytes recruitment and maturation, but rather by directly inhibiting endothelial expression of the NRP1 ligand Semaphorin3A (Sema3A) and the NEM/TGF-β1 paracrine axis (85).

3 VEGF-based strategies for therapeutic angiogenesis

3.1 First generation of VEGF delivery approaches and limitations: transgene expression efficacy, duration and dose

The concept of delivering VEGF to induce therapeutic angiogenesis rose two decades ago as a novel and promising strategy to treat ischaemic limb, as largely supported by numerous preclinical studies. In two independent pilot trials in patients suffering of peripheral arterial disease, the arterial or intramuscular injection of a DNA plasmid harbouring $VEGF_{165}$ gene resulted in angiogenesis and collateral vessel development respectively (86) (87). First evidences that delivery of proangiogenic factors could bring benefits to patients affected by congestive heart failure were reported in 1998. The study involved the injection of a DNA plasmid containing the gene for the VEGF (88). In parallel, Schumacher and colleagues demonstrated that the administration of recombinant human FGF in proximity of the site of anastomosis, provided revascularization of affected tissue by promoting capillary growth from the area of injection towards the periphery (89). Based on these encouraging results, several clinical trials started with the aim to confirm the initial observations. First-generation studies involved the direct injection of the recombinant protein or a gene therapy strategy based on the delivery of naked DNA or the use of adenovirus to overexpress the factor in situ (Fig. 6A). The VIVA (VEGF in Ischaemia for Vascular Angiogenesis) trial was the initial attempt to investigate the efficiency of injecting the recombinant protein in patients with CAD. Unfortunately, although safe, the study was stopped in phase II because the proved inefficacy of the treatment, most likely due to the very short half-life of the protein and the insufficient myocardial uptake (90). It was clear

that most of these limitations could be overcome by providing to the myocardium the VEGF-gene instead of the recombinant protein (91). Nevertheless, two clinical trials, EUROINJECT-ONE and NORTHERN performed on patients affected by stable severe ischaemic heart disease with no other options, showed no effects of naked $VEGF_{165}$ plasmid injection at long-term time points, despite some benefits in terms of myocardial perfusion were reported at 3 months upon the treatments (92) (93). While safe and relative low cost, the efficiency of the DNA uptake is poor. Moreover, preclinical studies showed that the duration of the expression of the gene delivered in form of DNA naked plasmid is limited to the first two weeks (91), which might be too short to induce the stabilization of the neovasculature, as previously mentioned, could affect. Of note, taking advantage of a transgenic system for conditional switching of VEGF, an elegant study showed that switching off the expression before 4 weeks caused a reproducible regression of the newly formed blood vessels (94). Two additional studies failed as well in achieving convincing clinical benefits, although they were designed to improve the VEGF plasmid activity by mobilizing putative angiogenic precursor cells from the bone marrow or by FGF-2 co-delivering (91). Similar discouraging results were registered in the KAT angiogenesis trial, investigating the effects of the injection of adenoviral vector harbouring $VEGF_{165}$ gene (95); remarkably, same outcomes were obtained in patients treated with a different isoform of VEGF (121) or different members of FGF family. The main reason for the failure of the first-generation adenoviral vectors is their inflammatory and immunogenic potential that, in addition to several safety concerns, limits also the time expression of the transgene in vivo at maximum two weeks (96) (97). It is important to highlight that the majority

of clinical trials have been conducted mainly on severely affected patients at an advanced stage of the disease, who might not have the capacity to respond optimally to the therapies. Moreover major cardiac adverse events, mortality and other very challenging clinical end points have been used in relatively small patient populations. In the next studies, it might be useful to enrol less severely affected patients using also more informative read out (98). However, taken together, the results from human studies suggest that the different approaches used in delivering or expressing the VEGF are not efficient in achieving a level of expression able to trigger the therapeutic effect (96). On the other hand, animal studies showed that high and uncontrolled over-expression of VEGF might induce the growth of angioma-like vascular tumours. Such events have been observed in the myocardium (99) (100), but also in skeletal muscle (101) (102), subcutaneous fat (103) and liver (94). These preclinical experimental results suggest the existence of a therapeutic window for VEGF gene delivery with lower doses being inefficacious and higher ones causing aberrant vascular growth (104). Moreover, since VEGF remains tightly localized in tissue after being secreted, as already discussed in the previous chapter, this therapeutic window of VEGF does not depend on the total dose administered, but rather on its level of release in the microenvironment. This biological concept has been elucidated and elegantly proved by the group of Helen Blau, taking advantage of a well-characterized cell-based platform for controlled gene delivery, in which clonal populations of transduced myoblasts were used to homogeneously express specific VEGF doses *in vivo* (102). Although observed only animals, these findings add a level of complexity in setting the approach for therapeutic angiogenesis, stating that an optimization is needed not only

on the efficacy and on the duration of VEGF expression but also on the level that is produce by the single cells.

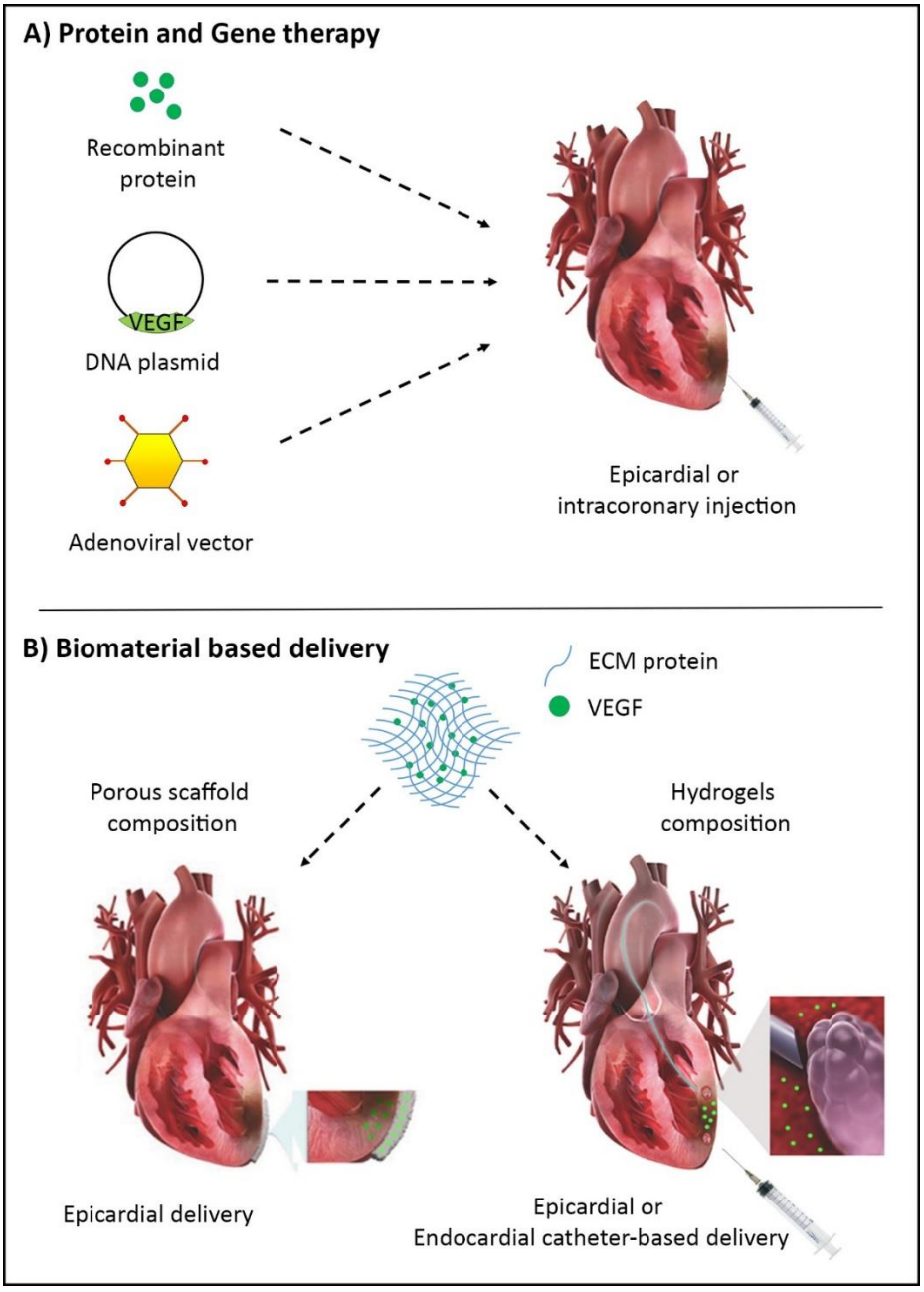

Fig. 6 VEGF delivery approaches. A) Direct endocardial/Intracoronary injection of recombinant VEGF or adenoviral vectors or naked-DNA plasmid harbouring VEGF were among the first strategies used to induce therapeutic angiogenesis in the myocardium. **B)** Novel biomaterial-based approaches rely on the possibility to link the VEGF to ECM protein fibers assembled in form of porous scaffold (e.g. collagen sponge) and delivered epicardially. Upon implantation, the VEGF migrates and diffuses in the underneath myocardium. Alternatively, VEGF can be add to hydrogel compositions and delivered directly into the myocardium via epicardial or catheter-based endocardial injections. Figure modified from: O'Neill H.S., et al **Adv. Mater**. *2016*

3.2 New technologies and alternative approaches

Besides the canonical gene therapy strategies, investigators attempt in finding new methods to deliver VEGF at a sustained level for an adequate time. An interesting approach to improve the efficacy of the therapeutic angiogenesis that is now in phase I clinical trial is represented by the possibility to increase the expression of the endogenous VEGF gene through the use of zing-finger (ZFP) proteins targeting activators on the gene promoter (105). Another possibility is to take advantage of the numerous drug delivery systems (DDS) that have been recently developed, including the possibility of enriching scaffolds, or trapping proteins in micro or nanoparticles. In order to increase the half-life of the protein and to localize its diffusion, in this context it is crucial to optimize the loading capacity, the distribution of the protein, the binding affinity that allows an adequate release profile and the ability to maintain the protein stability and bioactivity. (106). Loading of VEGF on scaffolds is the most studied strategy and so far, many different biological materials such as hydrogels made of ECM proteins such as collagen and fibrin have been tested as delivery system alone or in combination with functionalizing sequences to increase the interaction or to better control the release of the VEGF (106). Hydrogels are particularly advantageous as carrier systems because they are structurally similar to the tissue extracellular matrix (ECM) and can be designed to degrade in a timely fashion that coincides with the angiogenic process (107). Our lab recently optimized a fibrin platform for controlling delivery of recombinant VEGF, by fusing to the N-terminal of Murine $VEGF_{164}$ a sequence derived from α2-plasmin inhibitor (α2-PI1–8), which is a substrate for the coagulation factor XIIIa, to allow its covalent cross-linking into fibrin hydrogels and

release only by enzymatic cleavage (108). This approach resulted in a gradual release of the protein in vivo with a subsequent sustained expression of the protein over the entire 4 weeks.

Although promising, biomaterial mediated delivery of VEGF reacquires deeper investigation of the releasing profile *in vivo*, since this approach rely mostly on the reabsorption of the scaffolds occurring mainly by the enzymatic digestion triggered by the cells of the innate immunoresponse (109). To date, gene therapy is still the most affordable and suitable strategy to be tested in humans (91). In this context, the development of adeno-associated viral vectors (AAV) could represent a step forward in the clinical setting of therapeutic angiogenesis for cardiovascular disorders. This system in fact displays several advantages as compared to previous gene therapy methods, including no immunogenicity, hence no inflammatory response at the site of injection, and the capacity to transduce cells at high multiplicity of infection. It is reasonable to expect that such viral vectors will play a central role in the future not only restricted at the cardiovascular medicine field. (110). First preclinical investigations already showed a vascular regeneration in a clinical relevant animal model of ischemic hind limb by delivery of AAV expressing conditionally silenced VEGF (111).

3.3 Cell-based delivery

An effective strategy to control and optimize the expression of a transgene is represented by the possibility to exploit alive biological material as delivery platform, by using an autologous cell population previously modified genetically *in vitro* to over-express the VEGF. The cell-based gene therapy has the potential to address some of

the critical issues that limit the efficacy of VEGF gene therapy: the procedure of DNA uptake can be controlled and optimized *in vitro* and the approach guarantees a sustained expression of the protein if the cells are able to engraft permanently in the host tissue. In this context, the use of VEGF-expressing myoblasts has been extensively investigated and optimized to treat ischaemia and several preclinical studies showed their ability in integrating in the host tissues inducing robust and stable angiogenesis in skeletal muscle and in the myocardium (112) (113). More recently, several groups, including our, translated this approach to endothelial progenitor and mesenchymal stromal cells from bone marrow or adipose tissue (114) (115) (116) (117). The use of stromal cells as delivery platform offers several advantages for a cardiac application compared to myoblast: I) myoblast transplantation in the heart causes arrhythmias due to their inability to electrically integrate with the host myocardium; II) the production of synergistic paracrine factors by the delivered progenitors addresses several pathophysiological processes including inflammation and scar deposition as previously discussed. To date, it is well accepted that adipose derived mesenchymal stromal cells represented an "optimal" cell source as drug delivering system for cardiac applications (118). Studies reported an increased angiogenic response in both ischaemic skeletal muscle and myocardial infarction treated with MSC genetically modified with AAV (115) or baculovirus (114) respectively to over-express VEGF. Recent data from our group showed that VEGF release from retrotransduced human adipose tissue-derived MSC induced stable angiogenesis in both normal and ischemic myocardium, and prevented deterioration of cardiac function after coronary artery ligation (119). Nevertheless, besides functional angiogenesis, delivery of VEGF resulted

also in the spot formation of aberrant structures due to the uncontrolled expression, in line with what has been reported by our and other groups (119).

In order to have a precise control over the microenvironmental distribution of level expression in vivo, we recently developed a high-throughput, Fluorescence Activated Cell Sorting (FACS)-based technology to identify and purify cells expressing a specific range of VEGF level (120). This was achieved by linking VEGF expression to that of a FACS-quantifiable syngenic cell surface marker (truncated CD8a), so that the amount of CD8 on the cell surface reflects the level of VEGF secreted. Taking advantage of this technology, we generated purified populations of bone marrow- and adipose-derived mesenchymal progenitors expressing specific VEGF levels (116). Remarkably, the injection of purified VEGF expressing cells in skeletal muscle (121) and in the heart induced robust angiogenesis preventing at the same time the formation of aberrant structures (119). However, a still unresolved issue, limiting the efficacy of both cell therapy and cell-based gene therapy approaches, is the poor engraftment of injected cells in the myocardium (122).

4 Aim of the thesis

An adequate reperfusion of the infarcted tissue upon remains a formidable challenge in the management of MI. The concept of inducing angiogenesis for a therapeutic purpose aims at meeting this specific clinical need. Direct delivery of VEGF by a gene therapy approach has been for over 15 years the most investigated strategies and, although promising, presents still major limitations, due to the inefficiency of current transgene vectors in guaranteeing adequate and sustained expression levels of the VEGF triggering safe, mature and stable angiogenesis. In this context, optimizing *ex vivo* the VEGF transgene expression from a cell population suitable to be re-injected in vivo could offer a superior control over the genetic manipulation procedure. Nevertheless, this approach is still limited by major unsolved issues mostly related to the transplantation of the cell population *in vivo*. In particular, although still inadequate for the treatment of MI, direct epicardial or intracoronary injections still represent the standard methods for cell delivery in the myocardium. Beyond the poor cell engraftment that it has been observed in several independent studies, these delivery systems restrict the effect area to the injection site limiting the portion of the tissue that could receive benefits from the treatment. On the other hand, an epicardial delivery of a preformed tissue could cover homogeneously the affected area rather than having only scattered spots treated. In this context, the generation of proto-engineered tissue (patch) *in vitro* could also favour the cell survival upon implantation, as observed in previous studies performed by our and other groups (123)(124). Therefore, in my PhD project I focused on the use of engineered tissues (patch) as

VEGF delivery system to trigger an efficient pro-angiogenic signal able to induce a safe and mature vasculature.

In order to induce a safe vasculature and prevent the formation of aberrant structures caused by high doses of VEGF, it is crucial to control the expression of the protein at the microenvironmental level. As previously described, this can be achieved by controlling the VEGF expression of every single cell transplanted through a FACS based purification technique.

Hence, the first part of the thesis aimed at generating the patch by seeding a population of ASC purified to express safe levels of VEGF on a type I collagen scaffold, and give the "proof of principle" of its efficiency in inducing extrinsic angiogenesis (CHAPTER II).

$VEGF_{164}$ interacts with Extracellular matrix proteins through its heparin-binding domain. Therefore, the microenvironmental concentration depends, at least in part, from the composition and the abundance of heparin enriched ECM proteins (as previously discussed in the section 2.2.1.2). In this context, a scaffold made of type I collagen that has no affinity for VEGF could modulate the concentration of the protein around the seeded cells, acting as a diffusion system. Based on the hypothesis that the biological composition of the scaffolds allows VEGF to diffuse, normalizing the deleterious effect uncontrolled VEGF overexpression, in the second part of the work we investigated the possibility to obtain a safe and functional patch by seeding not purified VEGF expressing ASC (CHAPTER III).

5 References

1. *World Health Organization. Media centre/fact sheet.* **Website World Health Organization. (Online) 2015**. http://www.who.int/mediacentre/factsheets/fs317/en/.

2. *Pathophysiology of coronary artery disease.* **Libby P. and Theroux P.** 2005, Circulation 111, 3481-3488.

3. *Atherosclerosis - An Inflammatory Disease.* **Ross R.** 1999, New England Journal of Medicine 340, 115-126.

4. *Acute myocardial infarction.* **White H.D. and Chew D.P.** 2008, Lancet 372, 570–584.

5. *Evidence for cardiomyocyte renewal in humans.* **Bergmann O., et al.** 2009, Science 324, 98-102.

6. *A role for pericytes in coronary no-reflow.* **O'Farrell F.M. and Attwell D.** 2014, Nat. Rev. Cardiol. 11, 427-432.

7. *Myocardial no-reflow in humans.* **Niccoli G., et al.** 2009, J. Am. Coll. Cardiol. 54, 281-292.

8. *Heart failure.* **McMurray J.J. and Pfeffer M.A.** 2005, Lancet 365, 1877-1889.

9. *Regeneration of the heart.* **Steinhauser M.L. and Lee R.T.** 2011, EMBO Mol. Med. 3, 701-712.

10. *Ventricular myocytes are not terminally differentiated in the adult mammalian heart*. **Anversa P. and Kajstura J.** 1998, Circ. Res. 83, 1-14.

11. *Cardiovascular regenerative medicine: the developing heart meets adul heart repair*. 2009, Circ. Res. 105, 1041-1043.

12. *Origin of cardiomyocytes in the adult heart.* **Leri A., et al.** 2015, Circ. Res. 116, 150-166.

13. *Cell transplantation for myocardial repair: an experimental approach*. **Marelli D., et al.** 1992 Cell Transplant., 1, 383-390.

14. *Myocyte renewal and ventricular remodelling.* **Anversa P. and Nadal-Ginard B.** 2002, Nature 415, 240-243.

15. *Bone marrow cells regenerate infarcted myocardium*. **Orlic D., et al.** 2001, Nature 410, 701-705.

16. *The winding road to regenerating the human heart.* **Gerbin K.A. and Murry C.E.** 2015, Cardiovasc. Pathol. 24, 133-140.

17. *The Effect of Bone Marrow Derived Mononuclear Cell Treatment, Early or Late After Acute Myocardial Infarction: Twelve Months CMR and Long-Term Clinical Results*. **Suerder D., et al.** 2016, Circ. Res. (Epub ahead of print).

18. *One-year follow-up of intracoronary stem cell delivery on left ventricular function following ST-elevation myocardial infarction*. **Traverse J.H., et al.** 2014, JAMA 311, 301-302.

19. *Cell therapy for cardiac repair--lessons from clinical trials*. **Behfar A., et al.** 2014, Nat. Rev. Cardiol. 3, 232-246.

20. *Paracrine mechanisms in adult stem cell signaling and therapy*. **Gnecchi M., et al.** 2008, Circ Res. 103, 1204-1219.

21. *Cardiac cell therapy: lessons from clinical trials.* **Menasche P.** 2011, J. Mol. Cell. Cardiol. 50, 258-265.

22. *Bone-derived stem cells repair the heart after myocardial infarction through transdifferentiation and paracrine signaling mechanisms*. **Duran J.M., et al.** 2013, Circ. Res. 113, 539-552.

23. *Human embryonic-stem-cell-derived cardiomyocytes regenerate non-human primate hearts*. **Chong J.J., et al.** 2014, Nature 510, 273-277.

24. *Cardiac repair in a porcine model of acute myocardial infarction with human induced pluripotent stem cell-derived cardiovascular cells*. **Ye L., et al.** 2014, Cell Stem Cell 6, 750-761.

25. *Human embryonic stem cells vs human induced pluripotent stem cells for cardiac repair*. **Barad L., et al.** 2014, Can. J. Cardiol., Vol. 30, pp. 1279-1287.

26. *Targeting angiogenesis to restore the microcirculation after reperfused MI*. **Van der Laan A.M., et al.** 2009, Nat. Rev. Cardiol. 6, 515-523.

27. *Angiogenesis in wound healing.* **Tonnesen M.G.,et al.** 2000, J. Investig. Dermatol. Symp. Proc. 5, 40-46.

28. *Therapeutic angiogenesis for critical limb ischaemia*. **Annex B.H.** 2013, Nat. Rev. Cardiol. 10, 387-396.

29. *The number and distribution of capillaries in muscles with calculations of the oxygen pressure head necessary for supplying the tissue*. **Krogh, A.** 1919, J. Physiol. 52, 409–415.

30. *Modeling pO(2) distributions in the bone marrow hematopoietic compartment. I. Krogh's model*. **Chow D.C., et al.** 2001, Biophys J. 81, 675-684.

31. *Abnormal blood vessel development and lethality in embryos lacking a single VEGF allele*. **Carmeliet P., et al.** 1996, Nature 380, 435-439.

32. *Failure of blood-island formation and vasculogenesis in Flk-1-deficient mice*. **Shalaby F., et al.** 1995, Nature 376, 62-66.

33. *A common progenitor for haematopoietic and endothelial lineages in the zebrafish gastrula*. **Vogeli K.M., et al.** 2006, Nature 443, 337-339.

34. *Endothelial cells and VEGF in vascular development*. **Coultas L., et al.** 2005, Nature 438, 937-945.

35. *Molecular regulation of vessel maturation*. **Jain R.K.** 2003, Nat. Med. 9, 685-693.

36. *Developmental and pathological angiogenesis.* **Chung A.S. and Ferrara N.** 2011, Annu. Rev. Cell. Dev. Biol. 27, 563-584.

37. *Flow regulates arterial-venous differentiation in the chick embryo yolk sac*. **Le Noble F., et al.** 2004, Development 131, 361-375.

38. *Gridlock signalling pathway fashions the first embryonic artery*. **Zhong, T.P., et al**. 2001, Nature 414, 216-220.

39. *Molecular distinction and angiogenic interaction between embryonic arteries and veins revealed by ephrin-B2 and its receptor Eph-B4*. **Wang H.U. et al.** 1998, Cell 93, 741-753.

40. *Segregation of arterial and venous markers in subpopulations of blood islands before vessel formation*. **Herzog Y., et al.** 2005, Dev. Dyn. 232, 1047-1055.

41. *Morphological and molecular aspects of physiological vascular morphogenesis*. **Ribatti D., et al.** 2009, Angiogenesis 12, 101-111.

42. *Angiogenesis in life, disease and medicine*. **Carmeliet P.** 2005, Nature 438, 932-936.

43. *Vascular-specific growth factors and blood vessel formation*. **Yancopoulos G.D., et al.** 2000, Nature 407, 242-248.

44. *Tumor cells secrete a vascular permeability factor that promotes accumulation of ascites fluid*. **Senger D.R., et al.** 1983, Science 219, 983-985.

45. *Pituitary follicular cells secrete a novel heparin-binding growth factor specific for vascular endothelial cells*. **Ferrara N. and Henzel W.J.** 1989, Biochem. Biophys. Res. Commun. 161, 851-858.

46. *VEGF-B is dispensable for blood vessel growth but critical for their survival, and VEGF-B targeting inhibits pathological angiogenesis*. **Zhang F., et al.** 2009, Proc. Natl. Acad. Sci. U S A 106, 6152-6157.

47. *Vascular endothelial growth factor C is required for sprouting of the first lymphatic vessels from embryonic veins*. **Karkkainen M.J., et al.** 2004, Nat. Immunol. 5, 74-80.

48. *Blocking VEGFR-3 suppresses angiogenic sprouting and vascular network formation.* **Tammela T., et al.** 2008, Nature 454, 656–660.

49. *Placental growth factor promotes atherosclerotic intimal thickening and macrophage accumulation*. **Khurana R., et al.** 2005, Circulation 111, 2828–2836.

50. *Common mechanisms of nerve and blood vessel wiring.* **Carmeliet P. and Tessier-Lavigne M.** 2005, Nature 436, 193-200.

51. *Neuropilin-1 is expressed by endothelial and tumor cells as an isoform-specific receptor for vascular endothelial growth factor*. **Soker S., et al.** 1998, Cell 92, 735-745.

52. *Corneal avascularity is due to soluble VEGF receptor-1*. **Ambati B.K., et al.** 2006, Nature 443, 993–997.

53. *Proteolytic processing regulates receptor specificity and activity of VEGF-C*. **Joukov V., et al.** 1997, EMBO J. 16, 3898-3911.

54. *VEGFs and receptors involved in angiogenesis versus lymphangiogenesis*. **Lohela M., et al.** 2009, Curr Opin Cell Biol. 21, 154-165.

55. *Vascular endothelial growth factor: basic science and clinical progress.* **Ferrara, N.** 2004, Endocr. Rev. 25, 581-611.

56. *Expression of pro- and anti-angiogenic isoforms of VEGF is differentially regulated by splicing and growth factors*. **Nowak D.G., et al.** 2008, J. Cell Sci. 121, 3487-3495.

57. *Dual regulation of vascular endothelial growth factor bioavailability by genetic and proteolytic mechanisms*. **Houck K.A., et al.** 1992, J. Biol. Chem. 267, 26031-26037.

58. *Extracellular regulation of VEGF: isoforms, proteolysis, and vascular patterning*. **Vempati P., et al.** 2014, Cyt. Gro.Fac. Rev., Vol. 25, pp. 1-19.

59. *Binding to the extracellular matrix and proteolytic processing: two key mechanisms regulating vascular endothelial growth factor action*. **Ferrara N.** 2010, Mol. Biol. Cell. 21, 687-690.

60. *Spatially restricted patterning cues provided by heparin-binding VEGF-A control blood vessel branching morphogenesis*. **Ruhrberg C.**, **et al.** 2002, Genes Dev., 16, 2684-2698.

61. *Arteriolar and venular patterning in retinas of mice selectively expressing VEGF isoforms*. **Stalmans I., et al.** 2002, J. Clin. Invest., 109, 327-336.

62. *Molecular mechanisms and clinical applications of angiogenesis*. **Carmeliet P. and Jain R.K.** 2011, Nature 473,298-307.

63. *Autocrine VEGF signaling is required for vascular homeostasis*. **Lee S., et al.** 2007, Cell 130, 691-703.

64. *Control of vascular morphogenesis and homeostasis through the angiopoietin-Tie system*. **Augustin H.G., et al.** 2009, Nat. Rev. Mol. Cell. Biol. 10, 165-177.

65. *VEGF guides angiogenic sprouting utilizing endothelial tip cell filopodia*. **Gerhardt, H., et al.** 2003, J. Cell Biol. 161, 1163-1177.

66. *The extracellular matrix of blood vessels.* **Eble J.A. and Niland S.** 2009, Curr. Pharm. Des. 15, 1385-1400.

67. *Extracellular matrix, inflammation, and the angiogenic response.* **Arroyo A.G. and Iruela-Arispe M.L.** 2010, Cardiovasc. Res. 86, 226-235.

68. *The notch ligands Dll4 and Jagged1 have opposing effects on angiogenesis*. **Benedito R., et al.** 2009, Cell 137, 1124–1135.

69. *VEGF and Notch in tip and stalk cell selection.* **Blanco R. and Gerhardt H.** 2013, Cold Spring Harb. Perspect. Med. 3, 1-19.

70. *Basic and therapeutic aspects of angiogenesis.* **Potente M., et al.** 2011, Cell 146, 873-887.

71. *Escape mechanisms after antiangiogenic treatment, or why are the tumors growing again*? **Hlushchuk R., et al.** 2011, Int. J. Dev. Biol. 55, 563-567.

72. *Intussusceptive angiogenesis: its role in embryonic vascular network formation*. **Djonov V., et al.** 2000, Circ. Res. 86, 286-292.

73. *VEGF over-expression in skeletal muscle induces angiogenesis by intussusception rather than sprouting*. **Gianni-Barrera R., et al.** 2013, Angiogenesis 16, 123-136.

74. *Blood flow shapes intravascular pillar geometry in the chick chorioallantoic membrane*. **Lee G.S., et al.** 2010, J. Angiogenes. Res. 2.

75. *Mechanisms of Vessel Pruning and Regression.* **Korn C. and Augustin, H.G.** 2015, Dev. Cell 34, 5-17.

76. *Brothers and sisters: molecular insights into arterial-venous heterogeneity*. **Aitsebaomo J., et al.** 2008, Circ. Res. 103, 929-939.

77. *Molecular regulation of vessel maturation*. **Jain R.K.** 2003, Nat Med. 9, 685-93.

78. *Role of platelet-derived growth factors in physiology and medicine*. **Andrae J., et al.** 2008, Genes Dev. 22 , 1276-312.

79. *Signaling by members of the TGF-beta family in vascular morphogenesis and disease*. **Pardali E., et al.** 2010, Trends Cell Biol. 20, 556-567.

80. *Eph/ephrin molecules--a hub for signaling and endocytosis*. **Pitulescu M.E., et al.** 2010, Genes Dev. 24, 2480-2492.

81. *VEGF-induced adult neovascularization: recruitment, retention, and role of accessory cells*. **Grunewald M., et al.** 2006, Cell 124, 175-189.

82. *VEGF-A and PDGF-B combination gene therapy prolongs angiogenic effects via recruitment of interstitial mononuclear cells and paracrine effects rather than improved pericyte coverage of angiogenic vessels*. **Korpisalo P., et al.** 2008, Circ. Res. 103, 1092-1099.

83. *Bone marrow cells recruited through the neuropilin-1 receptor promote arterial formation at the sites of adult neoangiogenesis in mice*. **Zacchigna S., et al**. 2008, J. Clin. Invest. 118, 2062-2075.

84. *Neuropilin-1 identifies a subset of bone marrow Gr1- monocytes that can induce tumor vessel normalization and inhibit tumor growth*. **Carrer A., et al.** 2012, Cancer Res. 72, 6371-6381.

85. *VEGF dose regulates vascular stabilization through Semaphorin3A and the Neuropilin-1+ monocyte/TGF-β1 paracrine axis*. **Groppa E., et al.** 2015, EMBO Mol. Med. 7, 1366-1384.

86. *Clinical evidence of angiogenesis after arterial gene transfer of phVEGF165 in patient with ischaemic limb*. **Isner J.M., et al.** 1996, Lancet 348, 370-374.

87. *Constitutive expression of phVEGF165 after intramuscular gene transfer promotes collateral vessel development in patients with critical limb ischemia*. **Baumgartner I., et al.** 1998, Circulation 97, 1114-1123.

88. *Gene therapy for myocardial angiogenesis: initial clinical results with direct myocardial injection of phVEGF165 as sole therapy for myocardial ischemia*. **Losordo D.W., et al**. 1998, Circulation 98, 2800-2804.

89. *The stimulation of neoangiogenesis in the ischemic human heart by the growth factor FGF: first clinical results*. **Schumacher B., et al.** 1998, J. Cardiovasc. Surg. (Torino) 39, 783-789.

90. *The VIVA trial: Vascular endothelial growth factor in Ischemia for Vascular Angiogenesis.* **Henry T.D., et al.** 2003, Circulation 107, 1359-1365.

91. *VEGF gene therapy: therapeutic angiogenesis in the clinic and beyond*. **Giacca M. e Zacchigna S.** 2012, Gene Ther. 19, 622-629.

92. *Direct intramyocardial plasmid vascular endothelial growth factor-A165 gene therapy in patients with stable severe angina pectoris A randomized double-blind placebo-controlled study: the Euroinject One trial*. **Kastrup, J., et al.** 2005, J. Am. Coll. Cardiol. 45, 982-988.

93. *VEGF gene therapy fails to improve perfusion of ischemic myocardium in patients with advanced coronary disease: results of the NORTHERN trial*. **Stewart D.J., et al.** 2009, Mol. Ther. 17, 1109-1115.

94. *Conditional switching of VEGF provides new insights into adult neovascularization and pro-angiogenic therapy*. **Dor Y., et al.** 2002, EMBO J. 21, 1939-1947.

95. *Safety and feasibility of catheter-based local intracoronary vascular endothelial growth factor gene transfer in the prevention of postangioplasty and in-stent restenosis and in the treatment of chronic myocardial ischemia: phase II results of the KAT.* **Hedman M., et al.** 2003, Circulation 107, 2677-2683.

96. *Therapeutic angiogenesis for myocardial ischemia revisited: basic biological concepts and focus on latest clinical trials*. **Gilgenkrantz H., et al.** 2012, Angiogenesis 15, 1–22.

97. *Cardiovascular gene therapy for myocardial infarction.* **Scimia, M.C., et al.** 2014, Expert Opin. Biol. Ther. 14, 183-195.

98. *Current gene therapy trials for vascular diseases.* **Halonen P.J., et al.** 2014, Expert Opin. Biol. Ther. 14, 327-336.

99. *Evaluation of the effects of intramyocardial injection of DNA expressing vascular endothelial growth factor (VEGF) in a myocardial infarction model in the rat--angiogenesis and angioma formation*. **Schwarz E.R., et al.** 2000, J. Am. Coll. Cardiol. 35, 1323–1330.

100. *VEGF gene delivery to myocardium: deleterious effects of unregulated expression.* **Lee, R.J., et al**. 2000, Circulation, Vol. 102, p. 898–901.

101. *Long-term VEGF-A expression promotes aberrant angiogenesis and fibrosis in skeletal muscle*. **Karvinen H., et al.** 2011, Gene Ther. 18, 1166-1172.

102. *Microenvironmental VEGF concentration, not total dose, determines a threshold between normal and aberrant angiogenesis*. **Ozawa C.R., et al.** 2004, J. Clin. Invest. 113, 516–527.

103. *Heterogeneity of the angiogenic response induced in different normal adult tissues by vascular permeability factor/vascular endothelial growth factor*. **Pettersson A., et al.** 2000, Lab Invest. 80, 99–115.

104. *Critical role of microenvironmental factors in angiogenesis.* **Banfi A., et al.** 2005, Curr. Atheroscler. Rep. 7, 227-234.

105. *Regulation of an endogenous locus using a panel of designed zinc finger proteins targeted to accessible chromatin regions. Activation of vascular endothelial growth factor A*. **Liu P.Q., et al.** 2001, J. Biol. Chem. 276, 11323-11334.

106. *Vascular endothelial growth factor-delivery systems for cardiac repair: an overview*. **Simón-Yarza T., et al.** 2012, Theranostics, 2, 541-552.

107. *Hydrogels for therapeutic cardiovascular angiogenesis.* **Rufaihah A.J. and Seliktar D.** 2016, Adv. Drug. Deliv. Rev. 96, 31-39.

108. *Long-lasting fibrin matrices ensure stable and functional angiogenesis by highly tunable, sustained delivery of recombinant VEGF164*. **Sacchi V., et al.** 2014, Proc. Natl. Acad. Sci. U S A 111, 6952-6957.

109. *The host response to allogeneic and xenogeneic biological scaffold materials*. **Keane T.J. Badylak S.F.** 2015, J. Tissue Eng. Regen. Med. 9, 504-511.

110. *Gene therapy returns to centre stage.* **Naldini L**. 2015, Nature, 526, 351–360.

111. *Vascular Regeneration in Ischemic Hindlimb by Adeno-Associated Virus Expressing Conditionally Silenced Vascular Endothelial Growth Factor*. **Boden J., et al.** 2016, J. Am. Heart Assoc. 5.

112. *Myoblast-mediated gene transfer for therapeutic angiogenesis and arteriogenesis*. **von Degenfeld G., et al**. 2003, Br. J. Pharmacol. 140, 620-626.

113. *Cell transplantation for the treatment of acute myocardial infarction using vascular endothelial growth factor-expressing skeletal myobla*sts. **Suzuki K., et al.**, 2001, Circulation 104, 207-212.

114. *Baculovirus-transduced, VEGF-expressing adipose-derived stem cell sheet for the treatment of myocardium infarctio*n. **Yeh T.S., et al.**, 2014, Biomaterials 35, 174-184.

115. *Transplantation of modified human adipose derived stromal cells expressing VEGF165 results in more efficient angiogenic response in ischemic skeletal muscle*. **Shevchenko E.K., et al.** 2013, J. Transl. Med. 6, 138.

116. *Generation of human adult mesenchymal stromal/stem cells expressing defined xenogenic vascular endothelial growth factor levels by optimized transduction and flow cytometry purification*. **Helmrich U., et al.** 2012, Tissue Eng. Part C Methods. 18, 283-292.

117. *Vascular endothelial growth factor-expressing mesenchymal stem cell transplantation for the treatment of acute myocardial infarction*. **Matsumoto R., et al.** 2005, Arterioscler. Thromb. Vasc. Biol. 25, 1168-1173.

118. *Mesenchymal stem/stromal cells as a delivery platform in cell and gene therapies*. **D'souza N., et al.** 2015, BMC Med. 13.

119. *Controlled angiogenesis in the heart by cell-based expression of specific vascular endothelial growth factor levels.* **Melly L.F., et al.** 2012, Hum. Gene Ther. Methods. 23, 346-356.

120. *High-throughput flow cytometry purification of transduced progenitors expressing defined levels of vascular endothelial growth factor induces controlled angiogenesis in vivo*. **Misteli H., et al.** 2010, Stem Cells 28, 611–619.

121. *FACS-purified myoblasts producing controlled VEGF levels induce safe and stable angiogenesis in chronic hind limb ische*mia. **Wolff T., et al.** 2012, J. Cell. Mol. Med. 16, 107–117.

122. *Cell and gene therapy approaches for cardiac vascularization*. **Melly L., et al.** 2012, Cells 1, 961–975.

123. *Improving cell engraftment with tissue engineering.* **Suuronen E.J., et al.** 2008, Semin. Thorac. Cardiovasc. Surg. 20, 110-114.

124. *How to Improve the Survival of Transplanted Mesenchymal Stem Cell in Ischemic Heart?* **Liangpeng L., et al**. Stem Cells Int. 22, 9682757.

Chapter II: Engineered mesenchymal cell-based patches as controlled VEGF delivery systems to induce extrinsic angiogenesis

The data presented in this chapter have been published in *Acta Biomaterialia,* doi: 10.1016/j.actbio.2016.07.041

1 Introduction

Promising pro-angiogenic strategies based on the delivery of potent angiogenic factors, as the vascular endothelial growth factor-A (VEGF), have been investigated to induce growth of blood vessels in ischemic tissues (1) (2). Rapid and efficient restoration of the microvasculature is particularly crucial and challenging after a myocardial infarction to rescue organ function (3). Phase I and II clinical studies based on VEGF gene therapy showed inconsistent outcomes in cardiac functionality in patients after myocardial infarction, likely due to the low local transfection efficacy, resulting in limited amount and duration of the protein expression (4)(5). In fact, VEGF expression needs to be controlled within a defined therapeutic window (6) and sustained for a period of at least four weeks to allow the maturation and the stabilization of the newly formed blood vessels (7). Control over the dose and timing of VEGF release could be achieved by functionalized biomaterials (8) (9) (10) though with some shortcomings with regard to the limited factor supply and the unforeseeable potency of the local host immune reaction (11). A cell-based gene therapy approach could overcome such limitations by inducing a suitable cell population to overexpress the specific angiogenic gene (12). However, the microenvironmental dose of VEGF needs to be controlled in order to avoid the growth of aberrant vascular structures and angioma-like tumors, which would jeopardize clinical benefit (13) (14). In order to ensure controlled expression of homogeneous VEGF levels in vivo, we recently developed a high-throughput FACS-based technology to rapidly purify populations of transduced human adipose-derived mesenchymal stromal cells (ASC) that produce only specific desired VEGF levels (15) (16). However, another key issue that severely

limits the therapeutic efficacy of this approach is the poor survival of delivered ASC after direct intra-myocardial injection (17) (18) (19). The global treatment of all affected areas is also difficult by cell injections. Delivery of cells following in vitro organization into engineered constructs may provide superior control over the targeted cardiac segments and enhance the implanted cell survival, thereby sustaining the delivery of the therapeutic signals (20) (21). Therefore, in this study as proof of principle we aim to combine a purified population of genetically modified ASC and a scaffold-based engineered patch to provide both spatial and dose control in VEGF delivery. Although three major splicing isoforms of VEGF exist (comprised of 120/121, 164/165, and 188/189 amino acids in rodents and humans, respectively) (22), in this study we focused on VEGF164 because it is the only isoform able to induce a physiologically patterned vasculature as a single factor in the absence of the others (23).

During in vitro 3D culture, bioreactors for direct perfusion of the medium were used to promote the reproducibility and the quality of cell-based patches by uniform distribution during seeding and efficient provision of nutrients and oxygen in mm-thick porous collagen scaffolds (24). In particular, we hypothesized that FACS-purified VEGF-expressing ASC pre-cultured in perfusion bioreactors on 3D sponges can provide a controlled and sustained VEGF release to induce safe and efficient angiogenesis both within the engineered patch (intrinsic) and in a surrounding area of clinically relevant size (extrinsic). Since the extrinsic angiogenic potential of the engineered tissues was assessed in a subcutaneous mouse model, we used a several mm-thick cell-free

collagen scaffold (empty) to provide a standardized and controlled region in which to investigate dynamics of vascular growth.

2 Materials and methods

2.1 Cell transduction and sorting

Adipose tissue was obtained from a healthy donor undergoing plastic surgery after informed consent and according to a protocol approved by the Ethical Committee of Basel University Hospital. All investigations conform to the Declaration of Helsinki. Tissue was minced and digested with 0.15% collagenase (Worthington Biochemical Corporation, Lakewood, NJ) in PBS at 37 °C under continuous shaking for 60 minutes. Released cells were strained through a 70 µm nylon mesh, plated at a density of 105 cells/cm2 and cultured in high-glucose DMEM medium with 10% FBS. After 4 days, cells were transduced with retroviral vectors expressing rat VEGF164, linked in a bicistronic expression cassette to a truncated version of rat CD8a as a convenient FACS-sortable surface marker, as previously described (15). After 12 days, transduced ASC at p0 were FACS-sorted with a BD Influx Cell Sorter (BD Biosciences, Basel, Switzerland) with a gate determined by a reference clonal population of murine skeletal myoblasts expressing safe and specific VEGF levels (16). Two different cell groups were generated: (i) naïve ASC as control and (ii) cells expressing a specific safe VEGF level (VEGF-ASC).

2.2 Patch preparation and in vivo implantation

Engineered constructs (patches) were generated using either I) naïve ASC or II) VEGF-ASC. Bovine type I collagen scaffold (Ultrafoam™, Bard; size: 12mm diameter 3 mm thickness) were placed in the bioreactor chamber as previously described (25). Briefly,

ASC (2.2x106 cells/construct) were seeded and cultured throughout the inner 8 mm of the scaffold by a perfusion-based system at a speed of 3 ml/min for the first 18 hours and at 0.15 ml/min for the subsequent 5 days. Patches were then removed from the bioreactor, cut with 8mm punch to remove the not perfused rim of collagen and stitched with 2 points of surgical suture to a 8mm diameter and 7 mm thick empty scaffold (empty scaffold).

Animals were treated in compliance with Swiss Federal guidelines for animal welfare and all procedures were approved by the Veterinary Office of the Canton Bern (Bern, Switzerland) and conform to the Directive 2010/63/EU of the European Parliament. Male nude mice (Hsd: RH-rnu/rnu) were anesthetized by inhalation using a mixture of oxygen (0.6 L/min) and Isoflurane (1.5–3 vol%). Grafts were implanted in subcutaneous pockets in the back of the mouse. After 7, 14 and 28 days post-implantation, mice were anesthetized by intraperitoneal injection of a mixture of Ketamine (100 mg/Kg) and Xylazin (10 mg/Kg) prior sacrifice by total body vascular perfusion of 1% paraformaldehyde (PFA). The harvested constructs were further fixed in PFA 4% for 5 hours and left in 30% sucrose in PBS overnight, before embedding in OCT compound (Sakura Finetek, Torrance, CA) and freezing in liquid nitrogen-cooled isopentane vapors.

2.3 DNA assay

For DNA assay, patches (n=3) were collected from bioreactors, washed twice in PBS and digested overnight at 56 °C with protease K (0.5 mL of 1 mg/mL protease K in 50 mM Tris with 1 mM EDTA, 1 mM iodoacetamide, and 10 mg/mL pepstatin-A). Total DNA amount was measured with the CyQUANT® Cell Proliferation Assay Kit (Life

Technologies). DNA concentration was determined by reading the absorbance value at 485 nm using a Sinergy H1 Hybrid Reader (Biotek instruments Gmbh, Lucern, Switzerland).

2.4 Flow cytometer analysis

For phenotypic characterization of 3D-cultured VEGF-ASC, patches (n=3 per condition) were digested in 0.15% collagenase (Worthington Biochemical Corporation, Lakewood, NJ), liberated cells were collected by centrifugation and incubated for 20 min on ice, in PBS with 5% bovine serum albumin (BSA). The antibodies used were: CD90-FITC, CD73-PE, CD31-FITC, CD45-FITC, IgG1-FITC, IgG1-PE, IgG-APC (all from Becton and Dickinson Company, Franklin Lakes, NJ), CD105-FITC (Serotec Ltd. Oxford, UK), and VEGF-R2-FITC (R&D Systems). All the antibodies were used at a dilution of 1:50, except CD105-FITC, which was used at 1:20. Data were acquired with a FACSCalibur flow cytometer (BD Biosciences). For cell cycle analysis cells, retrieved from the patch, were fixed in 70% ethanol and incubated in a solution containing propidium iodide (Sigma-Aldrich) 10 µg/ml in PBS and RNAase 10 µg/ml for 20 minutes at 37 °C. Data were acquired with Fortessa II cytometer (BD Biosciences) and analysed by using FlowJo software (Tree Star, Ashland, OR, USA).

2.5 MTT staining

Qualitative spatial distribution of living cells was assessed by MTT (3(4,5-dimethylthiazol-2-yl)-2,5-diphenyltetrazolium bromide; Sigma-Aldrich) staining. Active mitochondria convert this tetrazolium salt into an insoluble formazan which stains cells purple. Samples were cut in half, rinsed in PBS and incubated at 37 °C for 2 hours with 3 ml of 0.12 mM MTT.

2.6 Histology

All histological analyses were performed on frozen sections. For basic histomorphological evaluation, sections were stained with hematoxylin and eosin (H&E) according to standard protocols. Color images were acquired with an Olympus BX63 microscope (Olympus, Volketswil, Switzerland) or a Zeiss LSM710 confocal microscope (Zeiss, Oberkochen, Germany). For immunofluorescence analyses cryosections were incubated for 1 hour in 0.3% Triton X-100 and 2% normal goat serum in PBS, and then for 1 hour in the following primary antibodies and dilutions: (1) anti-CD31 (AbDSerotec, Düsseldorf, Germany) at 1:100, (2) anti-NG2 (Millipore, Zug, Switzerland) at 1:200, (3) anti-α Smooth-Muscle Actin (Sigma-Aldrich, Basel, Switzerland) at 1:400, (4) anti-cleaved Caspase-3 (Asp175) (Cell Signaling Technology, Allschwil, Switzerland) at 1:100, (5) anti-Ki-67 (AbCam, Cambridge, UK) at 1:200, (6) anti-Human Nuclei clone 235-1 (Millipore, Billerica, MA, USA) at 1:100, anti-laminin (AbCam, Cambridge, UK) at 1:400, anti-VE-Cadherin (Santa Cruz Biotechnology Dallas, Texas, USA) at 1:200 . All secondary antibodies were used at 1:200 for 1 hour incubation (Life Technologies, Basel, Switzerland). Nuclei were stained using DAPI (Invitrogen, Switzerland). All antibodies were diluted in 0.3% Triton X-100 and 2% normal goat serum in PBS.

2.7 Vessel length density quantification

The amount of blood vessels was quantified on images taken from CD31-stained sections by determining the total vessel length density (VLD). Six representative fluorescent images per sample (4 samples per group) were acquired with a 20x objective on an Olympus BX61 microscope (Olympus, Münster, Germany), both in the

patch and in the empty scaffold areas (at the center and at the border). The total length of the capillaries was measured by tracing the CD31-positive vessels using CellSens software (Soft Imaging System, Münster, Germany). The vessel length density was then determined by dividing the total vessel length by the area of each field.

2.8 Human cell quantification

Human cell survival was evaluated by assessing the human cell density at 28 days post implantation. Six representative fluorescent images per sample (2 samples per group; n=12) were acquired both in the patch and in the area of the empty scaffold below the patch (100 µm away from the border with the patch) with 20x magnification on an Olympus BX63 microscope (Olympus, Volketswil, Switzerland) on cross-sections. Cells positive for human nuclei staining (see paragraph 2.6) were counted using ImageJ 1.47 software (Research Service Branch, NIH, USA) and divided by the image area to obtain the cell density. The in vivo percentage of proliferating ASC at 28 days was assessed by dividing the number of double positive Human Nuclei (HuNu) and Ki-67 cells by the total amount of human cells.

2.9 Elisa assay

The rate of VEGF production by ASC was quantified in the supernatant of 2D cell culture using a Quantikine rat VEGF immunoassay enzyme-linked immunosorbent assay (ELISA) kit (R&D Systems), as previously described (16). Briefly, 4 milliliters of fresh medium was added on Naïve or VEGF-ASCs cultured in 60-mm dishes in quadruplicate for 4h, collected, filtered, and frozen. Results were normalized by the number of cells in each dish and the time of incubation and expressed as ng/106 cells/day. For the estimation of VEGF concentrations in the patches during 3D culture,

patches were removed from the bioreactor after 4 days and immediately frozen. After homogenization of the patch in a PBS+1% Triton X-100 buffer, VEGF concentration was assessed with an ELISA kit (R&D Systems) and values were normalized by the estimated number of cells (according to the average of cell seeding efficiency) and the amount of the medium present in the bioreactor and expressed as ng/106 cells.

2.10 Statistics

Data were analyzed with the statistical software Prism 4.0a (GraphPad, La Jolla, CA) and SPSS 17.0 (IBM, Armonk, NY). Data are presented as means ± standard deviation. Comparison between groups was performed using a one-way ANOVA with Bonferroni correction for the VEGF quantification and a mixed-effects model for the angiogenesis quantification. $P<0.05$ was considered statistically significant.

3. Results

3.1 Engineered tissue characterization

Direct perfusion of culture medium through the scaffold allowed a uniform cell distribution through the entire thickness (top, center and bottom) of the collagen sponge (Fig 1A). Quantification of the nuclei by image analysis confirmed the homogeneous cell distribution (about 300-350 cells/mm2) throughout the entire construct cross-section (Fig. 1B). Seeding efficiency was measured by quantifying the amount of genomic DNA of the total amount of cells used for the seeding (as reference) and that retrieved from the scaffold 1 day after the loading and after further 5 days of perfusion culture (Fig 1C). The seeding efficiency was very high (98.3%±0.5% after 1 day compared with the reference amount of DNA). Macroscopic images of patches stained for metabolically active cells by using MTT excluded the

presence of a necrotic central core (Fig. 1 D), further confirming the homogeneous cell viability in the scaffold after 5 days of culture.

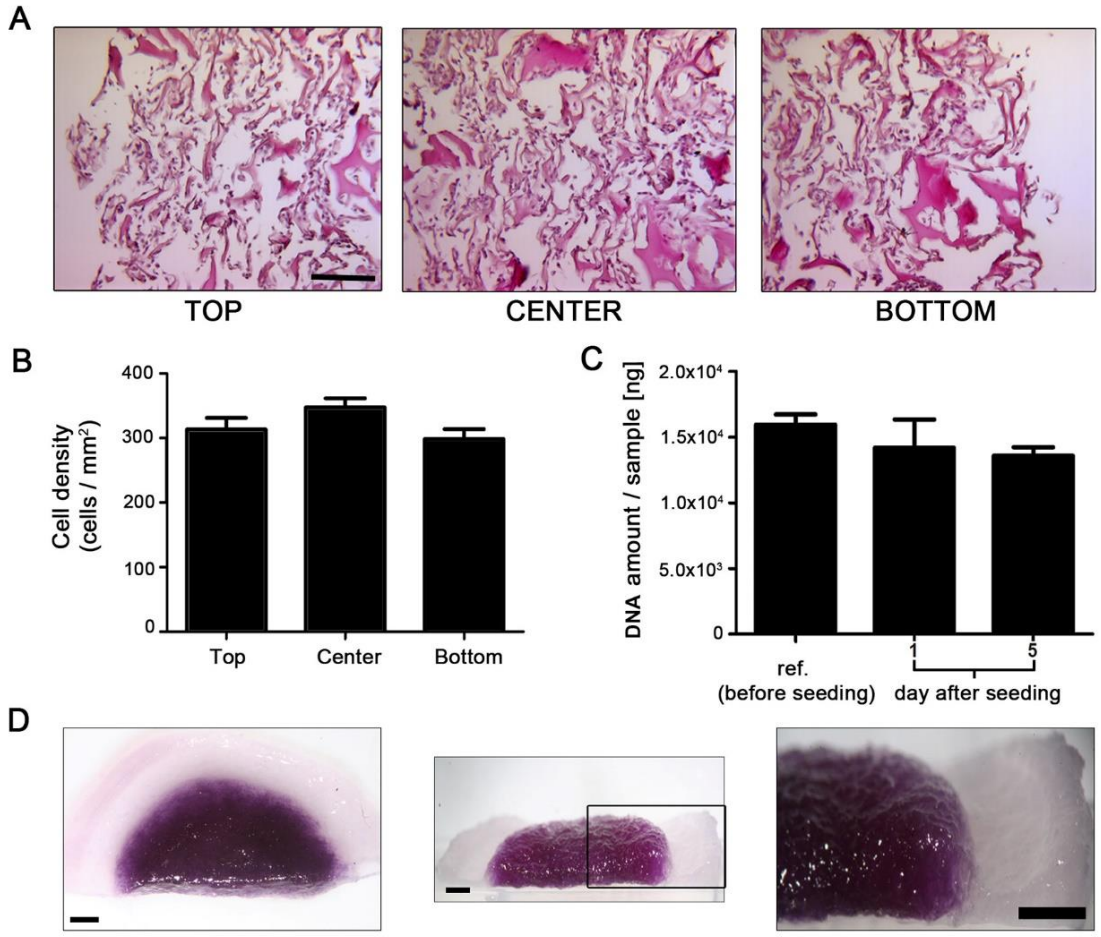

Fig 1 Characterization of the ASC-based patches. A) Representative pictures of hematoxylin and eosin staining taken at top, middle and bottom part of the scaffold (from the left to the right, respectively) (size bar=100 µm). **B)** Quantification of cell density distribution by image analysis of 9 random fields per sample (n=3 samples/condition). **C)** DNA amount Quantification of genomic DNA in the amount of cells used for the seeding (ref. after seeding) and present in constructs after 1 and 5 days of culture (n=3). **D)** Representative pictures of MTT staining on the entire scaffold after 5 days of culture (top and cross-section view at low and high magnification: from the left to the right; scale bar=1mm). Graphs are showed as mean ± Standard Deviation (SD).

3.2 Effect of VEGF expression on ASC

VEGF164 is a potent mitogen and affects cell survival, with effects being conserved across species. Therefore, we investigated its possible effects on human ASC proliferation, apoptosis and phenotype. No significant difference was found in the cell

density after 5 days of culture in constructs generated by VEGF-expressing and naïve ASC (Fig. 2A). Furthermore, cell cycle analysis with propidium iodide by cytofluorimetry showed that the majority of the cells (about 80%) was in G0/G1 phase in both experimental groups (Fig. 2B-C), thus confirming that VEGF expression did not increase ASC proliferation. Low doubling rates for both naïve and VEGF-ASC were also confirmed by immunofluorescence staining for Ki-67 protein, a marker expressed in actively proliferating cells in all phases of the cell cycle (Fig. 2D). VEGF expression by ASC appeared also not to affect cell apoptosis, since no relevant differences were found in the expression of caspase 3 (CAS-3), a key-protein in the apoptotic process (Fig. 2E). Cytofluorimetry analyses for hematopoietic (CD45+) mesenchymal (CD73+, CD90+) and endothelial (CD31+, VEGFR-2+) markers showed, as expected, that the near-totality of the ASC were of mesenchymal/stromal origin, with no hematopoietic cells and a minor amount of endothelium. Importantly, no relevant changes in the ASC population composition occurred when VEGF was expressed (Fig. 2F). Monolayer-expanded transduced ASC produced 58.5 ±11 ng/106 cells/day of rat VEGF (Fig. 2G), corresponding to the levels previously found to be safe and efficacious (16). Patches generated with ASC were then sutured on the top of empty collagen scaffold of critical size in order to assess their in vivo intrinsic and extrinsic angiogenic potential (Fig. 2H).

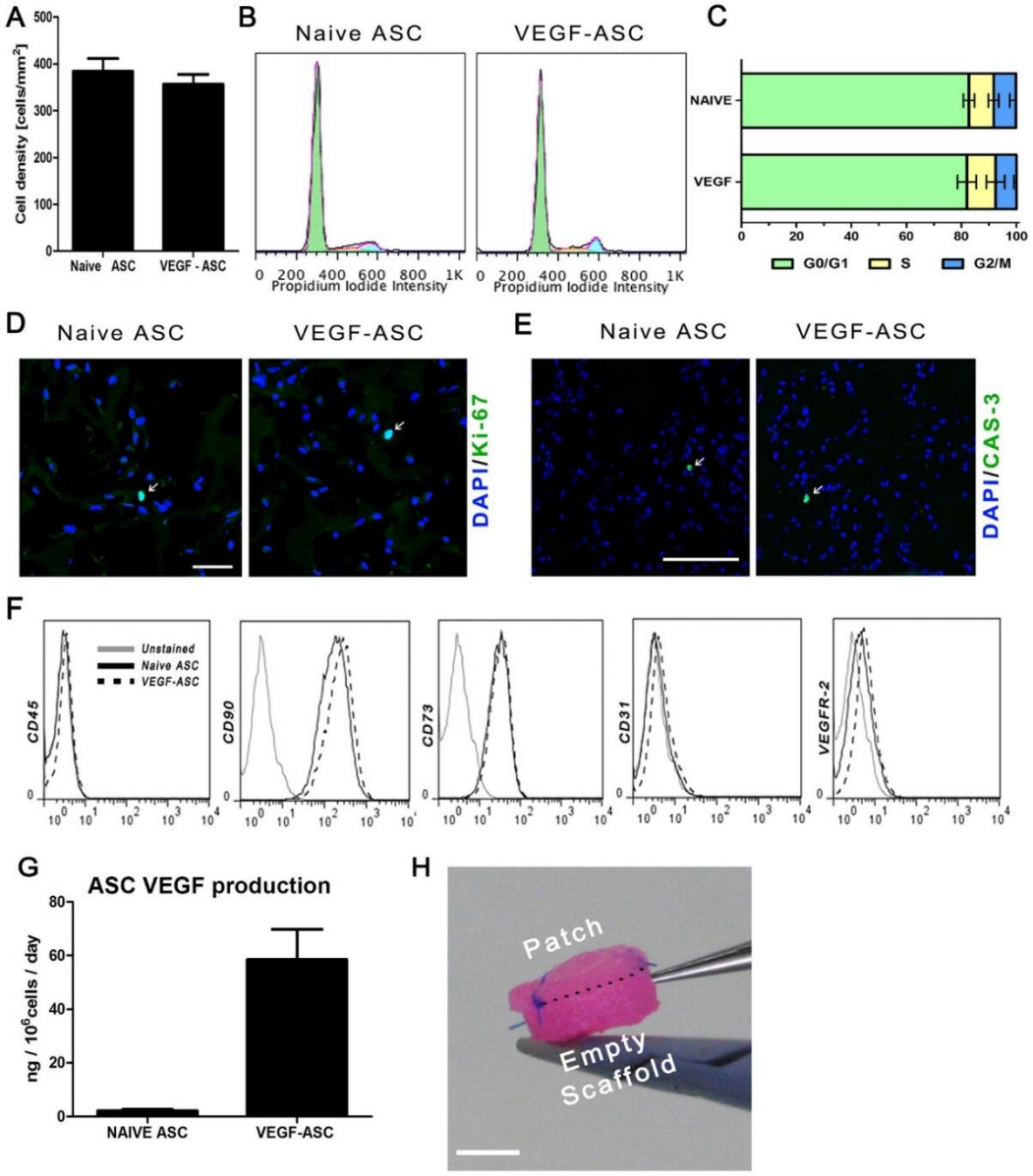

Fig 2 VEGF effects on ASC proliferation and phenotype in 3D *in vitro* culture. **A)** Quantification of cell density in VEGF and Naïve patches after 5 days of dynamic culture (image analysis performed on 6 random fields per sample; n=3 samples/condition). **B)** Representative histogram for flow cytometric analysis of cell cycle with propidium iodide emission for naïve (left) and VEGF- (right) ASC cultured on 3D collagen scaffold for 5 days. **C)** Quantification of percentage of cells present in either G0/G1 or S or G2/M cell cycle phase based on the flow cytometer analysis (n=3 per condition). **D,E)** Immunofluorescence staining for ki-67 and Cleaved Caspase-3 (green) and cell nuclei (blue) in the patches after 5 days in perfusion bioreactors (size bar=20 µm and 100 µm respectively). **F)** Phenotypic characterization of VEGF and naïve ASC by flow cytometry analysis for hematopoietic (CD45), mesenchymal (CD90, CD73) and endothelial (CD31, VEGFR-2) markers. **G)** Quantification of the amount of rat VEGF released by transduced cells either in monolayer or in 3D perfusion-based culture. Data are presented as mean ± SD (n=4). **H)**. Macroscopic view of the composed construct before implantation: the dashed black line distinguishes between the cell-based patch (patch) and the underneath cell-free collagen sponge (empty scaffold). At the border in blue there are the two surgical sutures (size bar= 5 mm).

3.3 In vivo vascularization of the patch

Before implantation, the amount of VEGF produced by transduced ASC after 3D perfusion culture was measured and was comparable to the rate of production measured during monolayer culture (41.9 ± 7.1 ng/106 cells). Upon implantation of mm-thick 3D patches, a prompt vascularization of the cell-seeded construct is essential to guarantee enough oxygen and nutrient provision to avoid cell loss. Moreover, in the scenario of angiogenesis induction through cell-based gene therapy, efficient survival of implanted cells is also crucial to achieve a sustained VEGF release. To investigate the kinetics of patch vascularization, we implanted cell-seeded patches ectopically in a subcutaneous pocket in nude mice and the resulting vascularization was analyzed at different time points (4, 14 and 28 days) by staining for the endothelial marker CD31. Vessel ingrowth was observed already after 4 days in VEGF-expressing patches and increased at 14 and 28 days in vivo (Fig. 3A-B). Branching points (white arrows in Fig. 3A), that indicate the formation of a well inter-connected and physiological microvascular network, were observed almost exclusively in VEGF-expressing patches and increased with time in vivo (Fig. 3A). Naïve ASC constructs contained few endothelial cells in the center and only few vessels were observed even at late time points (Fig 3A). The vessel length density (VLD) was statistically significantly greater at all time points in VEGF patches (Fig. 2B). Endothelial structure density in naïve cell-based constructs was similar at all time points. After 4 days in vivo, the vessel length density was 6-fold higher in the VEGF-ASC compared to control cell. A remarkable 4.9 fold increase in VLD was observed at 14 days and was maintained up to 28 days in the VEGF-ASC patches compared to the naive. In VEGF-releasing patches, the newly

formed blood vessels were also tightly surrounded by pericytes, as shown by immunofluorescence staining for NG2, confirming the formation of mature capillaries (Fig. 3C-D). Further, only morphologically normal capillary networks were observed and no instances of enlarged, aberrant angioma-like vascular structures could be detected. Taken together, these results indicate that patches seeded with transduced and purified ASC expressing controlled VEGF levels support the intrinsic induction of safe, efficient and mature angiogenesis.

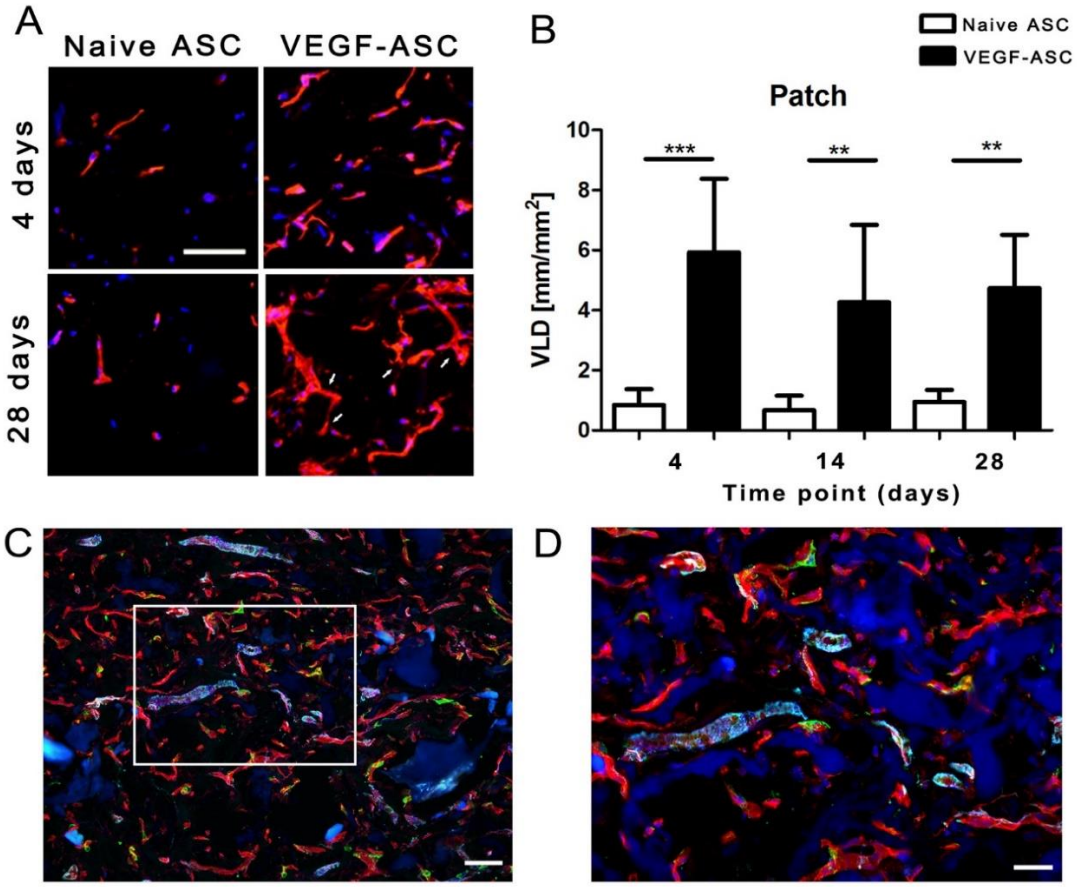

Fig 3 Fig. 3 In vivo vascularization of the ASC-based patches. A) Representative images of blood vessel density in patches seeded with naïve and VEGF-ASC after 4 and 28 days in vivo, assessed by immunofluorescence for CD31 (red) (size bar=20 µm)**. B)** Quantification of vessel length density (VLD) in the Naïve and VEGF patches at 4, 14 and 28 days upon implantation (image analysis performed on 6 random fields per samples n= 4 samples/condition; **p<0.01; ***p<0.001. **C, D)** Representative images of newly formed blood vessels stained for maturation markers at 28 days in VEGF-ASC patch al low (C) and high (D) magnification. Immunofluorescence staining for cell nuclei (DAPI; Blu), endothelial cells

(CD31; red), pericyte (NG2; green) and smooth muscle cells (SMA, cyan); (size bars=100 µm (C) and 20 µm (D)).

3.4 Angiogenesis induction outside the patch

To investigate the extrinsic pro-angiogenic potential of the engineered patches, the induction of vessel ingrowth was investigated in an empty collagen scaffold sutured underneath the cell-seeded patch and with a critical thickness of 7 mm. Host blood vessels reached the center of the empty scaffold only when VEGF-expressing cells were seeded in the patch sutured on top (Fig. 4A). In fact, at 28 days almost no vessels were present both in the center and at the border of the empty collagen scaffolds underneath the naïve ASC-based patches (Fig. 4A). At 4 days no host blood vessels reached yet the center of the acellular scaffold in both conditions (Fig 4A) and a negligible amount of sprouting capillaries was observed in the control sponge at later time points in vivo (Fig. 4A-B). On the contrary, VEGF-expressing patches induced a significant ingrowth of capillaries in the center of the underlying empty scaffold already by 14 days, which was maintained at 28 days (Fig. 4A-B, center). Host vessels start infiltrating the border of the empty patches of both conditions at 4 days. However, only in the presence of VEGF-releasing patches the VLD increased significantly at 14 and 28 days after implantation (Fig 4A-B, border). VEGF-expressing patches induced the formation of a mature capillary network with a physiologically branched morphology and the majority of new vessels were tightly associated with pericytes (Fig 4C). Moreover, no growth of aberrant structures was observed at either of the three time points, as expected with the delivery of controlled VEGF levels. Taken together, these results indicate that only VEGF-expressing patches have the ability to

efficiently induce safe and mature angiogenesis in an avascular volume placed at a significant distance from the engineered patch itself.

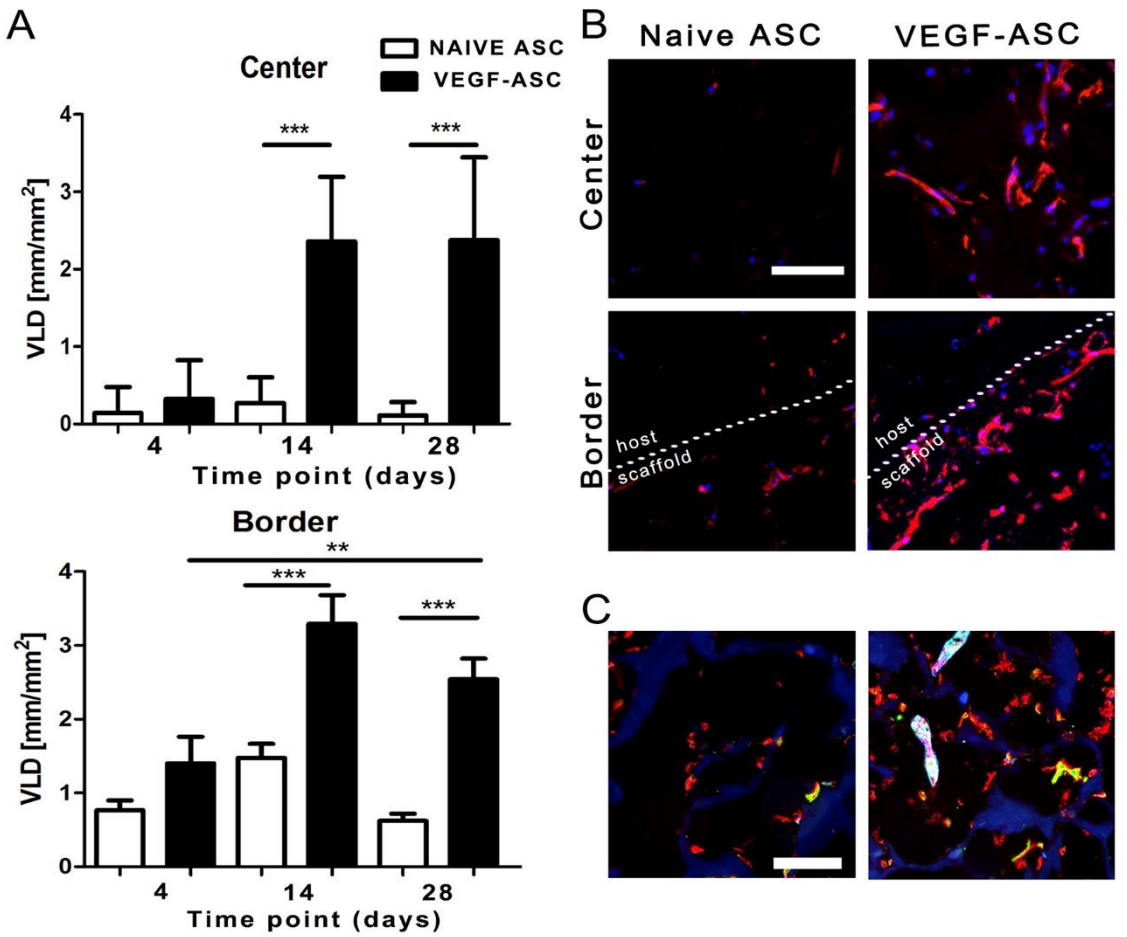

Fig 4 Induction of angiogenesis in the underneath empty collagen scaffold. A) Quantification of vessel length density (VLD) in the center and border area of the empty scaffold sutured beneath patches generated by either the Naïve or VEGF cells at 4, 14 and 28 days after implantation (image analysis on 6 random fields per area and per samples, n= 4 samples/condition; **p<0.01;***p<0.001. **B)** Representative images of blood vessel ingrowth in the center and border areas of the empty scaffolds 28 days after implantation, assessed by immunofluorescence for CD31 (red). Dashed line outlines the area of the empty scaffold which was in contact with the host tissue (size bar=20 µm). **C)** Representative images of blood vessel maturation in the inner area of the empty scaffolds sutured beneath Naïve (left) or VEGF (right) patches 28 days after implantation, assessed by immunofluorescence staining for cell nuclei (DAPI; blu), endothelial cells (CD31; red), pericyte (NG2; green) and smooth muscle cells (SMA, cyan); (size bar= 20 µm).

3.5 In vivo cell survival and migration.

To assess the functional consequences of the observed vascular ingrowth, we evaluated the survival of the human ASC seeded on the patches. After 28 days in vivo, control patches contained a lower amount of engrafted human cells compared to VEGF-expressing patches (Fig. 5A). Quantification of human cells (identified as staining positive for the Human Nuclei_HuNu antigen) cells showed that the density of human ASC in the presence of VEGF expression was significantly greater than in control conditions, with an 11-fold increase (Fig. 5B). Interestingly, the absolute cell density of VEGF-expressing ASC was similar to the one measured before implantation (Fig. 1B), showing that VEGF expression completely prevented the cell loss that took place in control conditions instead. Most of the implanted cells were retained inside the patch, with very low cell migration in the area of the empty scaffold just next to the patch (Fig. 5C-D). No human cells were detected in the distal portion of the empty scaffold as well as in the surrounding host tissue in any condition. After 28 days in vivo, most of the implanted cells did not differentiate into a vascular lineage, as human cells could not be observed inside the vessel basement membrane, identified by laminin, which defines the limit between vascular cells (endothelium and pericytes) and the surrounding tissue (Figure 5E). Blood vessels were therefore essentially of mouse origin. Lastly, only very few implanted ASC were proliferating after 28 days in vivo, with no difference between naïve or VEGF-expressing cells, as shown by the quantification of human cells positive for Ki-67 (Figure 5F).

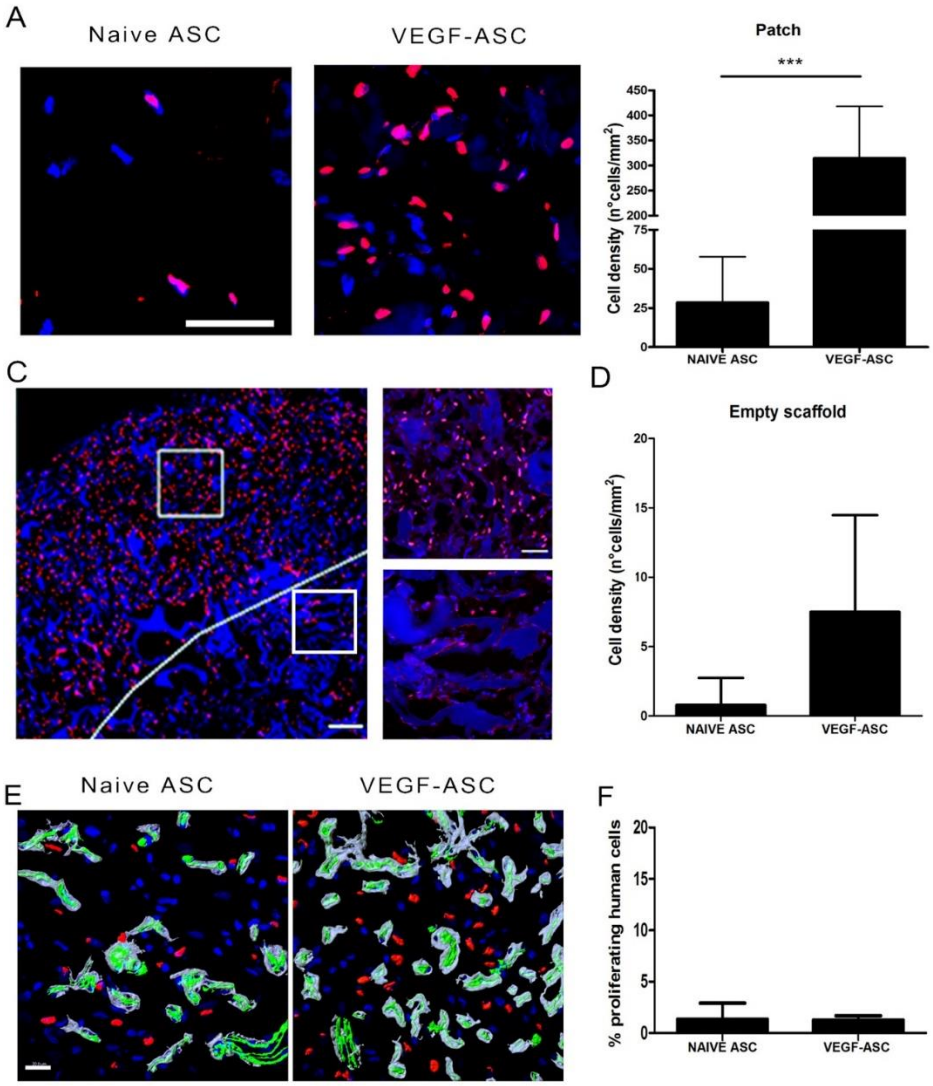

Fig. 5 ***In vivo*** **cell engraftment and migration**. **A)** ASC survival at 28 days was assessed by immunofluorescence staining for human nuclei (HuNu, in red) while all nuclei were visualized by DAPI (blue). White arrows indicate human cell nuclei in the naïve (left) and VEGF (right) patches (size bar 20µm). **B)** Quantification of human cell density in the naïve and VEGF patches at 28 days (image analysis on 6 random fields per sample; n=~~2~~ 4 samples/condition; ***p<0.001) **C)** (left): representative low-magnification image of specific human nuclei (red) and DAPI (blue) staining in the VEGF patch at 28 days. The white line represents the border between the patch and the empty scaffold (size bar=200µm). The small panels show higher magnification images of the areas in the white squares in the patch (top) and in the empty scaffold (bottom) (size bar=20µm). **D)** Quantification of human cell density at 28 days in the empty scaffold area below the naïve and VEGF patches (image analysis on 6 fields acquired randomly within 100 µm from the border line; n= 4 samples/condition). **E)** Representative images of immunofluorescence staining for human cells (in red), VE-Cadherin (in green), laminin (in grey) and DAPI (in blue) of patches generated by Naive or VEGF-expressing ASC after 28 days *in vivo* (size bar=20µm). **F)** Graph representing the percentage of human cells that are proliferating after 28 days *in vivo* in patches generated by Naive or VEGF-expressing ASC (image analysis on 6 random fields per sample; n=4 samples/condition; no statistic difference).

4 Discussion and conclusions

In this study, we showed that a patch seeded with a purified population of transduced adipose tissue-derived progenitor cells could function not only to attract intrinsic vascularization, but also as a device for delivery of controlled VEGF levels to induce extrinsic angiogenesis.

Several strategies have been investigated in the past years to promote angiogenesis for the treatment of ischemic diseases or the rapid vascularization of engineered tissue implants. The successful generation of in vitro engineered substitutes (e.g. skin, bone, fat and muscles) cannot be translated clinically if a prompt in vivo vascularization strategy is not envisioned to allow implanted cell survival, assuring their function also upon implantation (26). Efficient vascularization of engineered tissues is particularly important in the case of critical-size (several mm-thick) constructs. The most commonly adopted strategy consists in pre-vascularizing the engineered tissues by co-culturing mature or progenitor endothelial cells with mesenchymal stem cells or perivascular cells (27) or by the use of isolated (28) or pre-formed vessels (29). Moreover, the use of several biomaterials functionalized to release pro-angiogenic factors is an alternative promising method that is under investigation (30)(31).

Our approach, based on the long-term over expression of VEGF from implanted cells, favors the recruitment of blood vessels from the host, guaranteeing already after 4 days upon implant a dense vascularization of the entire cell-seeded construct (Fig. 3). On the opposite, patches prepared with naive ASC showed a few endothelial structures after 4 days: the fact that these were predominantly seen in the center of the patch, rather than at the border with the host tissue, suggests that these early

structures may depend on the few endothelial cells present in the ASC populations (Fig. 2F). Notably, the higher vascular density in VEGF patches compared to naïve ASC was maintained at 14 days, suggesting that VEGF expression was necessary for effective vascularization of the engineered patch. 28 days after implantation, vascular density was not further increased in VEGF-ASC patches and the newly induced capillary networks were associated with normal pericytes, indicating that they have achieved maturation and stabilization, as well as that angiogenesis induced by controlled VEGF levels is a self-limiting, non-progressive process. Particularly attractive is the perspective to implement this angiogenic strategy for the generation of different engineered tissue substitutes (e.g. muscle, bone) by co-culturing VEGF-expressing cells with a suitable progenitor cell source (32).

A consistent body of literature both in skeletal muscle and myocardium previously found that controlling the VEGF dose at the microenvironmental level, to express only therapeutic levels that induce efficacious and normal angiogenesis, is crucial to avoid the formation of aberrant structures, since VEGF remains tightly localized in the matrix around expressing cells (13,14,17). By correlating the production of VEGF with a FACS-sortable marker, it is possible to select and purify specific populations that homogeneously express only a desired safe and effective level of VEGF (16). It is however possible that the specific microenvironment of the 3D patch, in terms of scaffold composition and newly deposited extracellular matrix, might influence the spatial distribution of produced VEGF. Therefore, future studies will be necessary to investigate both the possibility of avoiding FACS-purification and the therapeutic

outcome of delivering non-purified transduced ASC expressing heterogeneous VEGF levels.

Beyond the ability to attract vascularization inside the patch, we hypothesized that a patch seeded with VEGF-expressing cells could also act as a factor-delivery device and induce angiogenesis in the surrounding tissue. To test this hypothesis, we sutured beneath the patch an empty collagen scaffold of critical size (7-mm thick and 8-mm diameter). At 4 days after implantation no vascular structures were observed in the inner part of the empty scaffold. Moreover the infiltration that was measured at the border was similar in the presence of both control and VEGF-expressing patches, suggesting no VEGF effect at this early time point. However, by 14 days a significant difference was observed in both regions of the empty scaffold: at the border vessel density increased 2- and 4-fold in the VEGF expressing conditions compared to naive (at 14 and 28 days, respectively), while at the center a striking 8- and 20-fold increase was observed in the VEGF-expressing conditions compared to naive (at 14 and 28 days, respectively). Remarkably, VEGF expression induced a similar vascular density both in the center and at the border by 14 days, whereas in its absence VLD in the center remained greatly lower than at the border at all time points. Furthermore, these extrinsic vascular networks reached maturation through association with pericytes, which is a necessary condition for their long-term persistence and functional efficacy. These observations indicate that: 1) VEGF diffused to the edge throughout the core of the empty scaffold, covering a quite unexpected distance from the source and guiding the recruitment of blood vessels from the host. 2) Sustained expression, ensured by the survival and the stable transduction of ASC with an integrating viral vector was

necessary to provide sufficient time for vessels to reach the core of the empty scaffold. In this experimental setup, ASC did not have a role in the formation of blood vessels, but they rather functioned as vehicle for VEGF delivery while embedded in the collagen scaffolds.

The engineered ASC-based patch described here represents an innovative device for controlled VEGF delivery that could be implemented to different fields, among which the treatment of cardiac ischemia might be a particularly suitable application, due to its specific requirements. In this future perspective, ASC are widely considered an ideal cell source for cardiac applications (18). In fact, skeletal myoblasts have been previously investigated as an attractive cell source for cardiac regeneration thanks to their capability to form contractile myofibers. However, they cannot acquire a cardiomyocyte phenotype and, most importantly, they form electrically active fibers that do not couple with the surrounding myocardium, causing dangerous arrhythmic events (33). On the other hand mesenchymal stromal cells, including ASC, do not form electrically active tissue and have been reported not to increase the risk of arrhythmias (34), providing therefore a more suitable cell source to deliver VEGF in the heart. In order to develop such an application, the functional properties of the extrinsic angiogenic potential described here would need to be further evaluated in an ischemic cardiac model to assess whether the sustained and controlled delivery of safe and effective VEGF levels to the ischemic tissue could improve perfusion, restoring local contractility and global cardiac function. Moreover, based on previous studies, the approach described here could also provide functional benefit through the further release of other paracrine factors, produced by ASCs, which can exert positive effects

on cardiomyocyte survival and on the ventricle remodeling after myocardial infarction (20).

In conclusion, our findings provide a proof of principle for generating an efficient angiogenic patch that has the potential to be used clinically. However, before a possible clinical translation, alternative vectors should be considered, since retroviruses raise safety concerns of neoplastic transformation of transduced stem cells by insertional mutagenesis (35). Self-inactivating lentiviral vectors with chromatin insulator elements represent a valid solution thanks to their capability to express a transgene in a stable and sustained manner, but without the oncogenic potential of retroviral vectors (36) (37).

5 References

1. *Stimulation of functional vessel growth by gene therapy*. **Korpisalo P. and Ylä-Herttuala S.** 2010, Integr. Biol. Camb. 2, 102-112.

2. *Therapeutic angiogenesis for critical limb ischaemia*. **Annex B. H.** 2013, Nat. Rev. Cardiol. 10, 387-396.

3. *Targeting angiogenesis to restore the microcirculation after reperfused MI*. **Van der Laan A.M., et al.** 2009, Nat. Rev. Cardiol. 6, 515-523.

4. *Cardiovascular gene therapy for myocardial infarction*. **Scimia M.C., et al.** 2014, Exp. Opin. Biol. Ther. 14, 183-195.

5. *Gene therapy for ischemic cardiovascular diseases: some lessons learned from the first clinical trials*. **Ylä-Herttuala S., et al.** 2004, Trends Cardiovasc. Med. 14, 295–300.

6. *Microenvironmental VEGF distribution is critical for stable and functional vessel growth in ischemia*. Von **Degenfeld G., et al.** 2006, FASEB J. 20, 2657-2659.

7. *Conditional switching of VEGF provides new insights into adult neovascularization and pro-angiogenic therapy*. **Dor Y., et al.** 2002, EMBO J. 21, 1939-1947.

8. *Biodegradable collagen patch with covalently immobilized VEGF for myocardial repair*. **Miyagi Y., et al.** 2011, Biomaterials, 32, 1280-1290.

9. *Endothelial cells guided by immobilized gradients of vascular endothelial growth factor on porous collagen scaffolds*. **Odedra D., et al.** 2011, Acta Biomater. 7, 3027-3035.

10. *Long-lasting fibrin matrices ensure stable and functional angiogenesis by highly tunable, sustained delivery of recombinant VEGF164*. **Sacchi V., et al**. 2014, Proc Natl Acad. Sci. U S A 111, 6952-7.

11 *Immune response to biologic scaffold materials*. **Badylak S.F. and Gilbert T.W.** 2008, Semin. Immunol. 20, 109-116.

12. *MSC-based VEGF gene therapy in rat myocardial infarction model using facial amphipathic bile acid-conjugated polyethyleneimine*. **Moon H.H., et al.** 2014, Biomaterials 35, 1744-54.

13. *Microenvironmental VEGF concentration, not total dose, determines a threshold between normal and aberrant angiogenesis*. **Ozawa C.R., et al**. 2004, J. Clin. Invest. 113, 516-527.

14. *Long-term VEGF-A expression promotes aberrant angiogenesis and fibrosis in skeletal muscle*. **Karvinen H., et al.** 2011, Gene Ther. 18, 1166-1172.

15. *High-throughput flow cytometry purification of transduced progenitors expressing defined levels of vascular endothelial growth factor induces controlled angiogenesis in vivo.* **Misteli H., et al.** 2010, Stem Cells 28

16. *Generation of human adult mesenchymal stromal/stem cells expressing defined xenogenic vascular endothelial growth factor levels by optimized transduction and flow cytometry purification*. **Helmrich U., et al.** 2012, Tissue Eng. Part C Methods 18, 283-292.

17. *Controlled angiogenesis in the heart by cell-based expression of specific vascular endothelial growth factor levels*. **Melly L.F., et al.** 2012, Hum. Gene Ther. Methods 23, 346-356.

18. *Transplantation of adipose derived stromal cells is associated with functional improvement in a rat model of chronic myocardial infarction*. **Mazo M., et al.** 2008, Eur. J. Heart Fail. 10, 454-462.

19. *Cell delivery and tracking in post-myocardial infarction cardiac stem cell therapy: an introduction for clinical researchers*. **Wei H., et al.** 2010, Heart Fail. Rev. 15, 1-14.

20 *Epicardial adipose stem cell sheets results in greater post-infarction survival than intramyocardial injections*. **Hamdi H., et al.** 2011, Cardiovasc. Res. 91, 483-491.

21. *Cell delivery: intramyocardial injections or epicardial deposition? A head-to-head comparison*. **Hamdi H., et al.** 2009, Ann. Thorac. Surg. 87, 1196-1203.

22. *The vascular endothelial growth factor VEGF, isoforms: differential deposition into the subepithelial extracellular matrix and bioactivity of extracellular matrix-bound VEGF*. **Park J. E., et al.** 1993, Mol. Biol. Cell. 4, 1317–1326.

23. *Spatially restricted patterning cues provided by heparin-binding VEGF-A control blood vessel branching morphogenesis*. **Ruhrberg C., et al.** 2002, Genes Dev. 16, 2684–2698.

24. *Perfusion seeding of channeled elastomeric scaffolds with myocytes and endothelial cells for cardiac tissue engineering*. **Maidhof R., et al.** 2010, Biotechnol. Prog. 26, 565-572.

25. *Three dimensional multi-cellular muscle-like tissue engineering in perfusion-based bioreactors*. **Cerino G., et al.** 2016, Biotechnol. Bioeng. 113, 226-236.

26. *Prevascularization in tissue engineering: Current concepts and future directions*. **Laschke M.W. and Menger M.D.** 2016, Biotechnol. Adv. 34, 112-121.

27. *Cell interactions between human progenitor-derived endothelial cells and human mesenchymal stem cells in a three-dimensional macroporous polysaccharide-based scaffold promote osteogenesis*. **Guerrero J., et al.** 2013, Acta Biomater. 9, 8200-8213.

28. *Vascularization strategies of engineered tissues and their application in cardiac regeneration*. **Sun X., et al.** 2016, Adv. Drug Deliv. Rev. 96, 183-194.

29. *Biodegradable scaffold with built-in vasculature for organ-on-a-chip engineering and direct surgical anastomosis*. **Zhang B., et al.** 2016, Nat. Mater. 15, 669-678.

30. *Vascularization strategies for tissue engineering*. **Lovett M., et al.** 2009, Tissue Eng. Part B Rev. 15, 353-370.

31 *Vascularization of three-dimensional engineered tissues for regenerative medicine applications*. **Kim J.J., et al.** 2016, Acta Biomater. [Epub ahead of print].

32. *The effect of controlled expression of VEGF by transduced myoblasts in a cardiac patch on vascularization in a mouse model of myocardial infarction*. **Marsano A., et al**. 2013, Biomaterials 34, 393-401.

33. *Cardiac cell therapy: lessons from clinical trials.* **Menasche P**. 2011, J. Mol. Cell. Cardiol. 50, 258-265.

34. *Cultured and freshly isolated adipose tissue-derived cells: fat years for cardiac stem cell therapy*. **Sanchez P.L., et al.** 2010, Eur. Heart J. 31, 394-297.

35.*Side effects of retroviral gene transfer into hematopoietic stem cells*. **Baum C., et al.** 2003, Blood 101, 2099-2114.

36. *The genotoxic potential of retroviral vectors is strongly modulated by vector design and integration site selection in a mouse model of HSC gene therapy*. **Montini E., et al.** 2009, J. Clin. Invest. 119, 964-975.

37 *Lentiviral hematopoietic stem cell gene therapy for X-linked severe combined immunodeficiency*. **De Ravin S.S., et al.** 2016, Sci. Transl. Med. 8, 335-357.

Chapter III: Scaffold composition modulates micro-environmental distribution of Vascular Endothelial Growth Factor over-expressed by transduced progenitor cells

1 Introduction

Over the last two decades, the concept of “therapeutic angiogenesis” emerged as a valid adjuvant treatment for patients affected by chronic cardiac ischemia following myocardial infarction (1)(2). Vascular Endothelial Growth Factor (VEGF)-based gene therapies have been extensively studied to boost the proangiogenic physiological response in order to restore the microvascular network, hence an adequate supply of oxygen and nutrients to the affected tissue (3); among the various isoforms, $VEGF_{165}$ has been determined as the most efficient in inducing functional and normal angiogenesis upon its over expression in vivo (4). Despite convincing pre-clinical studies, the efficacy of VEGF gene therapy, including the delivery of the gene for the isoform 165, has been highly questioned by controversial phase I/II clinical trial results (5). The inconsistent outcomes are mainly due to the low local transfection efficacy, resulting in limited amount and duration of protein expression (6). In fact, VEGF expression needs to be above a defined threshold and sustained for a period of at least four weeks to allow the maturation and the stabilization of the newly-formed blood vessels (7). A cell-based gene therapy approach might overcome these issues by transducing in vitro a suitable cell population to over-express the VEGF gene, ensuring a sustained release in vivo (8)(9). Nevertheless, intra-myocardial cell injection represents still the most used method in cell therapy, although is known to severely damage cells during the delivery leading to a poor survival (10)(11). In this context, epicardial delivery of in vitro engineered tissues has been shown to improve the survival of the implanted cells favoring their survival, favoring also the integration of the construct in the host myocardium (12)(13).

However, in order to fully exploit the therapeutic potential of the over expression of $VEGF_{165}$ by a cell population, a tight control over the microenvironmental dose around each producing cell is necessary to avoid adverse effects, such as the growth of aberrant structures induced by very high doses (14)(15). In particular, it is well-known that the biological effect of the VEGF is tightly regulated through a balanced interaction with the Extracellular Matrix (ECM) proteins as perlecans, agrins and syndecans through the heparan-binding domain at the C-terminal (16).

In the previous chapter, it has been reported the generation of an engineered VEGF expressing patch, by combining a tissue engineering strategy with a FACS-based purification technique that allows obtaining a population of retro-transduced adipose tissue-derived stromal cells (ASC) expressing defined and safe VEGF (17)(18). Although the cell purification step was optimized to be quite efficient, the procedure is still time-consuming, relying also on an extensive cell monolayer expansion to achieve the needed number of cells. Because the effect of $VEGF_{165}$ is strictly modulated by the interaction with the ECM proteins, it is rational to postulate that the biological composition of a scaffold could modulate the morphology of the blood vessels induced in vivo by a seeded cell population over-expressing the growth factor. In a previous publication, we observed that the collagen type I sponge (Ultrafoam) is characterized by a poor VEGF retaining ability (19). Therefore, in this study, we hypothesized that this collagen scaffold could act as buffer system at the microenvironmental level, diluting the very high concentrations of VEGF secreted by not purified ASC; this feature will prevent the formation of the toxic spots responsible for the growth of aberrant vascular structures upon implantation in vivo. In order to verify our hypothesis, we

compared the angiogenesis induced by the collagen-based patches with the one triggered by using a scaffold with a strong ability to bind the VEGF (19). We further tested the safety and the efficacy of the uncontrolled VEGF delivery through a collagen-based patch in a healthy nude rat heart model. Such proof of principle will open new perspectives on the use of the collagen scaffold as delivery tool and drastically reducing the procedure time and complexity avoiding as well the extensive monolayer-cell expansion needed to achieve an adequate number of cells.

2 Materials and methods

2.1 Cell transduction and sorting.

Adipose tissue was obtained from healthy donors undergoing plastic surgery after informed consent and according to a protocol approved by the Ethical Committee of Basel University Hospital. Tissue was minced and digested with 0.15% type II collagenase (Worthington Biochemical Corporation) in PBS at 37°C under continuous shaking for 60 minutes. Released cells were strained through a 70-µm and a 100-µm nylon mesh, plated at a density of 10^5cells/cm^2 and cultured in high-glucose DMEM medium with 10% FBS. After 4 days, cells were transduced with retroviral vectors expressing rat $VEGF_{164}$ linked to a truncated rat CD8a through an Internal Ribosomal Entry Site (IRES) (18). At the first passage, after 12 days, transduced ASC were Fluorescence-Activated Cell Sorting- (FACS) based purified with a BD Influx Cell Sorter (BD Biosciences) with a gate determined by a reference clonal population of murine skeletal myoblasts expressing safe and specific VEGF levels (17,18). Three different cell groups were generated: NAÏVE ASC as control (I) and cells expressing specific (SPEC ASC) (II) or uncontrolled (ALL ASC) (III) levels of VEGF.

2.2 Generation of the EGG WHITE (EW) scaffold

Chicken (Gallus gallus domesticus) eggs were collected freshly, not later than two first days of laying, broken manually and EW was deliberately separated from yolk without piercing the yolk. EW solution was then freeze-dried (Christ, Alpha 1–2 LD), milled to fine powders and kept in a freezer. The powder was later dissolved (6%, w/v) in acetic acid 2 M (Merck) and vacuum-degassed to remove air bubbles. Followed by molding the solution into 24-well plates, they were stored at 4 °C for 3 h. The samples were then freeze-dried overnight to form three-dimensional (3D) scaffolds EW scaffolds were subsequently cross-linked at 4 °C overnight using biocompatible, zero-length chemical crosslinker N-(3-dimethylaminopropyl)-N'-ethylcarbodiimide (EDC, 30 mM, Sigma-Aldrich) in presence of N-Hydroxysuccinimide (NHS, 30 mM, Sigma-Aldrich). Crosslinking reaction was performed in 4-morpholineethanesulfonic acid (MES, Sigma-Aldrich) buffer (50 mM, pH 5.5) in 70% ethanol. For sterilization, scaffolds were thoroughly washed with double distilled water, followed by sterile PBS and 70% ethanol for 24 h each. Prior cell seeding scaffolds were incubated in culture media overnight.

2.3 Physical characterization of the sponges

Structure and morphology of EW and collagen scaffolds were evaluated using a scanning electron microscope (SEM, FEI Nova NanoSEM 230, USA). Lyophilized samples were first sprayed with gold and then observed at an operating voltage of 15 kV. Average pore size of samples was calculated from at least 300 measurements on SEM micrographs using Image Analyzer software (Image J 1.44p by NIH). Since the density

(ds) and average protein density (dp, 1.3 g.cm-3)(1) of EW and collagen scaffolds are known, the porosity of scaffolds was measured according to the following equation:

Porosity (%)=(((d_p-d_s))/d_p)×100.

Biomechanical testing were performed to assess the compressive module and the equilibrium swelling properties. Uniaxial compression assays were performed on pre-hydrated (24 h at 37 °C in PBS) cylindrical scaffolds (12 mm in height and 6 mm in diameter) using a HCT-25/050 Zwick/Roell mechanical tester at 25 °C at a crosshead speed of 1.3 mm s-1 and 50% of the final strain level. Compressive modulus of EW and collagen scaffolds were determined using the tangent slope of the stress-strain curve. Four distinct samples were studied in triplicate for each group of scaffolds. Swelling properties of samples were determined at 37 °C in PBS for 24 h using gravimetric method. Lyophilized samples were first soaked in PBS, then blotted with a filter paper to remove excess liquid. Using the swollen (Ws) and dry (Wd) weights of scaffolds, the swelling ratio was calculated using the following equation:

Swelling ratio (%)=(((W_s-W_d))/W_s)×100.

Each swelling experiment was perfomed in quadruplicate and data presented as average and standard deviation.

2.4 Generation of the patches

For the generation of the patches, naïve, SPEC and ALL ASC were cultured on 8mm-diameter and 3mm-thick collagen (UltrafoamTM, Avitene) or EW scaffolds at the density of 20 x 10^6 cells/cm^3 (corresponding to 2.2 x 10^6 cells per scaffold). By using a perfusion-based bioreactor cells were perfused at a flow rate of 3 ml/min during the

cell-seeding phase (18 hours) and subsequently cultured at 0.15 ml/min for the following 5 days.

2.5 Implantation in nude rat model

To investigate the in vivo angiogenic potential of the engineered tissues based on collagen or EW, they were implanted ectopically (in subcutaneous pockets) or orthotopically (on healthy hearts) in 10-week-old male nude rats (Hsd: RH-rnu/rnu, Envigo RMS). In the ectopic model, half of the patches used for histological analysis (3/6) were sutured to cell-free (7 mm-thick) type I collagen scaffolds (as previously described in Chapter II, section 1 and 2.2). This served as clean systeml to investigate the extrinsic angiogenic potential of ASC expressing heterogeneous VEGF levels.

Animals were treated in compliance with Swiss Federal guidelines for animal welfare and all procedures were approved by the Veterinary Office of the Canton Bern (Bern, Switzerland) and conform to the Directive 2010/63/EU of the European Parliament.

In the ectopic model, nude rat were anesthetized by inhalation using a mixture of oxygen (0.6 L/min) and isoflurane (3 vol %). Samples (four per animal) were implanted in independent subcutaneous pockets in the back of the rat. At 7, 14 and 28 days post-implantation, animals were anesthetized by intraperitoneal injection of a mixture of Ketamine (100 mg/Kg) and Xylazin (10 mg/Kg) prior sacrifice by total body vascular perfusion of 1% paraformaldehyde (PFA). To investigate the vascular perfusion, some rats were intravenously injected with 250 µl of 1 mg/ml FITC-conjugated Lycopersicon esculentum lectin (Vector Laboratorie) each and 4 minutes later the tissues were fixed by vascular perfusion of 1% PFA and 0.5% glutaraldehyde in PBS pH 7.4.

The harvested constructs were further fixed in PFA 0.5% for 5 hours and leaved in 30% sucrose solution overnight before embedding in Optimal Cutting Temperature (OCT) compound (Sakura Finetek) and frozen in isopentane vapors cooled in liquid nitrogen. For real time RT-PCR and ELISA assays rats were euthanized with CO_2, samples collected and immediately frozen in liquid nitrogen and stored at -80° C for further processing.

In the orthotopic model, rats (about 400 g weight) were intubated and continuously ventilated with a mixture of oxygen (0.6 L/min) and isoflurane (3 vol %). After a conservatively dissection of thorax muscles (3 layers) collagen-based engineered constructs were fixed on the left ventricles with 2 sutures. Transthoracic echocardiograms was performed on rats under controlled anesthesia (at 1-1.5 vol % Isoflurane for maintenance) and spontaneous respiration at 7 and 28 days post implantation using a Vevo 2100 Ultrasound machine (VisualSonics). At 28 days rats were sacrificed and hearts collected and immediately embedded in OCT as described before.

2.6 In vitro VEGF quantification by ELISA assay.

To assess the VEGF binding capacity on different substrates, patches made by naïve ASC (n=5), cell-free collagen (n=5) and EW scaffolds (n=4) were incubated for 4 h at 37° C with 4 ml of culture medium, conditioned by monolayer-expanded ALL cells, containing 1.977 ± 0.36 ng/ml of $rVEGF_{164}$. The amount of rat $VEGF_{164}$ was quantified both in the supernatants and in the samples following two rinsing steps in PBS. Fresh culture medium with no VEGF supplementation was used as a control.

VEGF retention was also quantified in patches after 5 days of culture (n=4 per condition) or following in vivo implantation (n=3 per condition).

The VEGF concentration was measured by an ELISA kit (DuoSet, R&D Systems) according to manufacturer's instructions.

2.7 Quantitative real-time reverse transcriptase polymerase chain reaction (RT-PCR)

In vitro collagen or EW based patches were digested in TRI-Reagent (Sigma); total RNA was isolated following an adaptation of the method of Chomczyński and Sacchi (20). cDNA was reverse-transcribed from mRNA with the Omniscript Reverse Transcription kit (Qiagen) at 37 C° for 60 min. Quantitative real-time PCR (qRT-PCR) was performed with TaqMan® Assays master mix (Life Technologies) using a ABI 7500 Real-Time PCR system (Applied Biosystems). To investigate the expression of exogenous rVEGF gene we measured mRNA expression levels of the IRES sequence contained in the gene construct. Specific sets of primer and probe sequences were designed with Primer Express software 3.0 (Applied Biosystems, Zug, Switzerland):

Forward: 5'-GCTCTCCTCAAGCGTATTCAACA;

Reverse: 5'-CCCCAGATCAGATCCCATACA;

Probe: 5'-FAM-CTGAAGGATGCCCAGAAGGTACCCCA-TAMRA.

All primers were used at 400nM. Reactions were performed in triplicate for each template, averaged, and normalized to expression of the hGapdh housekeeping gene.

2.8 Histology

All histological analyses have been performed on frozen sections. For histomorphological evaluation, sections were stained with hematoxylin and eosin (H&E) and Masson Trichrome according to standard protocols. Color images were

acquired with Olympus BX63 microscope (Olympus). For immunofluorescence analyses, cryosections were incubated for 1 hour in 0.3% Triton X-100 and 2% normal goat serum in PBS, and then for 1 hour in the following primary antibodies: (1) anti-CD31 (AbDSerotec) diluted at 1:100, (2) anti-NG2 (Millipore) at 1:200, (3) anti-α Smooth Muscle Actin (Sigma-Aldrich) at 1:400, (5) anti-Ki-67(AbCam) at 1:200, (6) anti-Human Nuclei (MAB1281 Millipore, Germany, Antibody Registry identifier AB_94090) at 1:100, anti-fibronectin (AbCam) at 1:200 and anti-agrin (AbCam) at 1:100. All secondary antibodies were used at 1:200 for 1 hour incubation (Life Technologies). For CD73, CD105 and rCD8 staining, were used primary antibodies conjugated with PE APC and FITC fluorochromes respectively (Biolegend). Nuclei were stained using DAPI (Invitrogen) for 1 h. All antibodies were diluted in 0.3% Triton X-100 and 2% normal goat serum in PBS.

2.9 Vessel measurements

Vessel length density (VLD) and diameters were measured on 10 m-thick frozen cross-sections stained for endothelial cells ($CD31^+$ cells) of implanted patches or the surrounding myocardium. Briefly, VLD was measured in 5–10 fields per patch/heart (at least n = 3 per condition) by tracing the total length of blood vessels and dividing it by the total area of the field of interest (mm of vessel length/mm^2 of surface area).

Vessel diameters were randomly measured on six acquired images per sample (at least 3 per condition). Around 450 total diameter measurements were obtained from three independent experiments per condition.

All analyses were performed using the CellSens software (Soft Imaging System).

2.10 Human cell quantification

In vivo implanted human cell density was assessed at 0 (pre-implants) and 28 days post implantations. Six representative fluorescent images per sample (n=4 samples per condition) were acquired with 20x magnification with an Olympus BX63 microscope (Olympus) on patch cross-sections. Human nuclei positive cells were counted using ImageJ 1.47 software (Research Service Branch).

2.11 Statistics

Data were analyzed with the statistical software Prism 5.0a (GraphPad). Data are presented as means ± standard deviation. Comparison between groups was performed using a one-way ANOVA with Bonferroni correction. $P<0.05$ was considered statistically significant.

3 Results

3.1 Delivery of uncontrolled VEGF levels induces normal, mature and functional angiogenesis

To prove our initial hypothesis, we first assessed whether transduced ASC expressing uncontrolled (ALL) VEGF levels following 3D culture on collagen-based sponges could induce normal and efficient angiogenesis, in a subcutaneous rat model, similarly to cells purified to express only safe doses of the protein. During monolayer-culture, only SPEC and ALL ASC produced rat

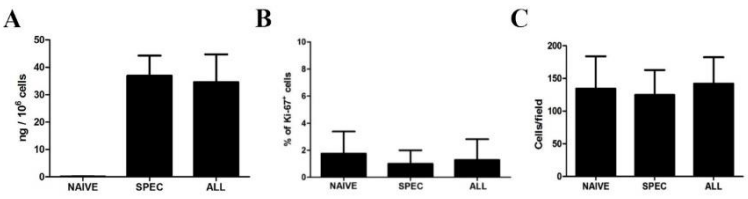

Supp. fig 1 A) rVEGF production by SPEC and ALL ASC-based patches after 5 days of dynamic culture (n=4) **B**) In vitro quantification of cell proliferation and density **(C)** in collagen-based patches generated by naïve, SPEC or ALL ASC after 5 days of culture.(n=3).

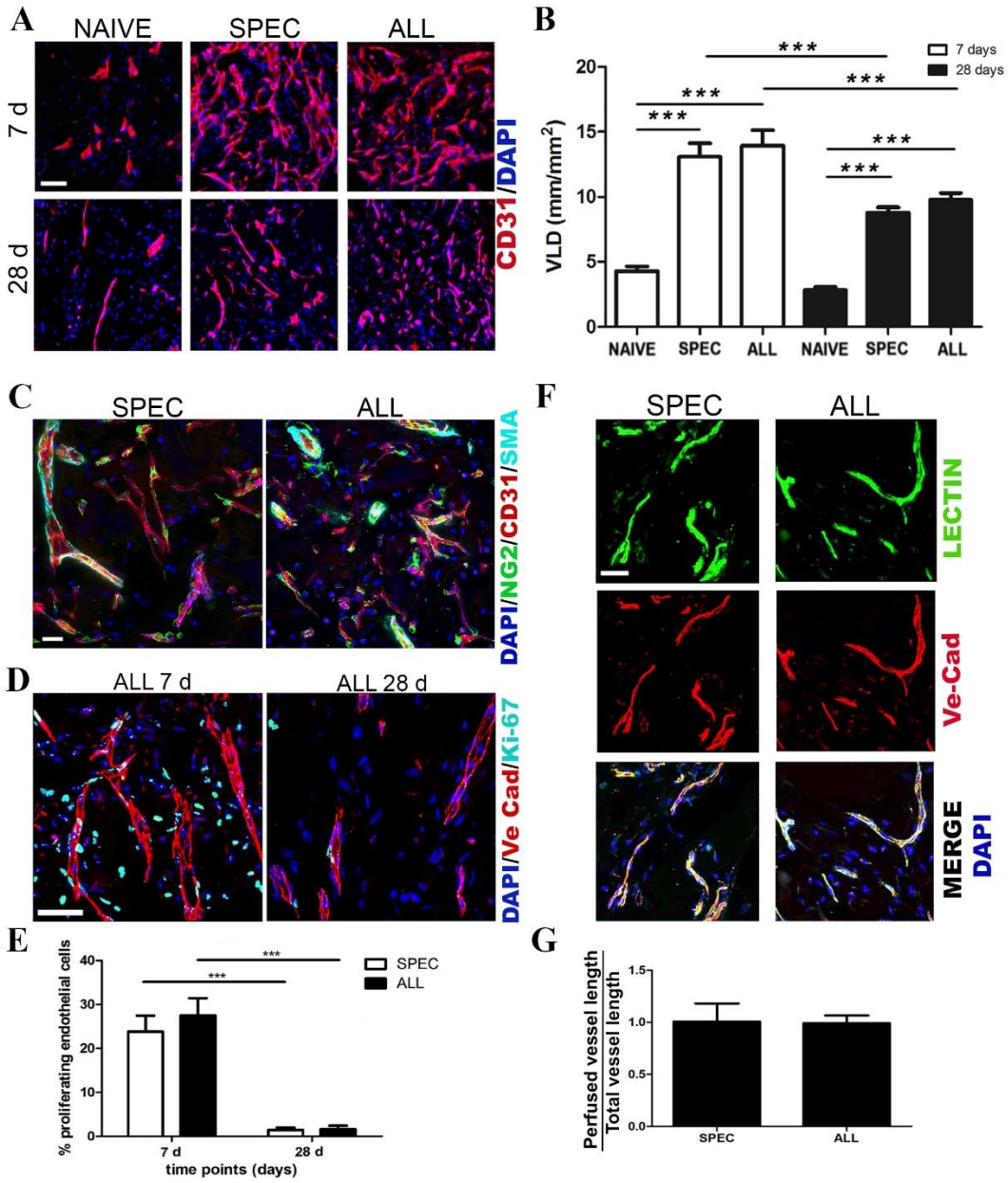

Fig. 1 Angiogenesis induced by collagen-based patches in an ectopic rat model. A) Representative images of blood vessels ingrowth in patches generated by naïve, SPEC and ALL ASC after 7 and 28 days *in vivo* (size bar =25µm). **B)** Quantification of vessel length density (VLD) in the naïve and both VEGF expressing patches at 7 and 28 days upon implants (n= 4 samples/condition; ***p<0.001). **C)** Representative images of newly formed blood vessels stained for maturation markers at 28 days in SPEC and ALL patches. Cell nuclei are stained with DAPI (blue), endothelial cells with CD31 (red), pericytes with NG2 (green) and smooth muscle cells with SMA(cyan) (size bar=20 µm). **D)** Representative images of growing blood vessels at 7 and 28 days in ALL patches. Proliferating cells are stained with Ki-67 (cyan) and blood vessels with VE-Cadherin (red) (size bar=20 µm) **E)** Quantification of proliferating endothelial cells at 7 and 28 days in vivo (n=3 per condition; ***p<0.001). **F)** Newly induced blood vessel in SPEC and ALL ASC patches stained by intravascular FITC-fluorescent lectin injection at the moment of sacrifice at 28 days (DAPI in blue; lectin in green; CD31 in red; size bar=20 µm). **G)** Ratio of perfused (lectin positive) vessels normalized to the total amount of vessels found in SPEC and ALL patches at 28 days post implantation (n=3).

VEGF in a similar amount (36.9 ± 7.3 and 34.5 ± 10.1 ng / 10^6 cells, respectively; Supp. Fig 1A). Importantly, VEGF expression did not affect the in vitro proliferation of human ASC, which resulted to be quite low in all experimental groups (Supp. Fig 1B). The cell density after 5 days of culture resulted also to be similar in all conditions (Supp. Fig 1C). Upon implantation, collagen-based patches generated by SPEC or ALL ASC showed an increased blood vessel ingrowth both at 7 and 28 days compared to control (Fig 1A). The quantification of vessel length density corroborated the histological observations by showing a significant persistent ~3-fold increase in VEGF-expressing ASC compared to NAIVE cells at 7 and 28 days (Fig 1B). Although no statistical significance was found in the VLD of patches generated by SPEC and ALL ASC within the same time point, a physiological regression of the number of vessels was observed from 7 to 28 days. Notably, we did not detected vessels displaying abnormal size or aberrant phenotype in the patches generated by ASC secreting heterogeneous VEGF levels at any time points. The newly-formed capillaries (Fig 1C, Red) in both SPEC and ALL ASC-based patches displayed a mature morphology with normal size and pericytes coverage (Fig 1C, green) and a thick layer of SMA positive cells (Fig 1C, Cyan) surrounding arterioles. Interestingly, at day 7 the blood vessel morphology induced by the ALL ASC patches was normal with no detection of proliferating enlarged vasculature structures (Fig 1D). At 28 days, the capillaries formed are in large part still present with very few endothelial cells dividing, which is most likely representing a complete shutdown of the angiogenesis process (Fig 1E). The amount of proliferating endothelial cells was similar in ALL and SPEC at both time points and statistically significant decreased at 28

days (Fig 1E). Moreover, the majority of the induced blood vessels were functionally connected to the host network, as showed by the co-localization of the green fluorescent signal (perfused circulating lectin) with the CD31 staining and the quantification of the ratio of the perfused versus the total amount of vessels (Fig 1F-G). Taken together these results showed that collagen-based patches efficiently prevented the formation of aberrant structures also when ASC were not FACS-purified to express safe VEGF levels.

3.2 Implanted human cell did not directly participate to the vessel formation

Implanted human ASC were homogeneously present throughout the patches, however, while the naïve ASC appeared mainly scattered, the cells expressing both specific and heterogeneous VEGF levels were denser (Fig 2A). In the VEGF-based constructs, an increased number of implanted cells were observed within the patch compared to control constructs. Quantification of cell density before and after implantation confirmed the histological observation: while the initial cell density was maintained in the VEGF-expressing patches at 28 days, the NAIVE cells significantly decreased in number (Fig 2B). The amount of rat VEGF entrapped in the implants generated by both SPEC and ALL was significantly higher than in the naïve samples at 7 days and decreased at 28 days, resulting to be similar to the control value (Fig 2C). Nevertheless, the expression of the IRES sequence (contained in the viral vector) was still detectable at 28 days, suggesting still an ongoing expression of exogenous VEGF (Fig 2D). Since ASC contain cell subpopulation capable to differentiate into endothelial/mural cells (21), their in vivo fate was investigated. In VEGF-patches, the

majority of the implanted cells resulted to be mainly close to but not embedded in the basal lamina of the newly formed capillaries (Fig 2E).

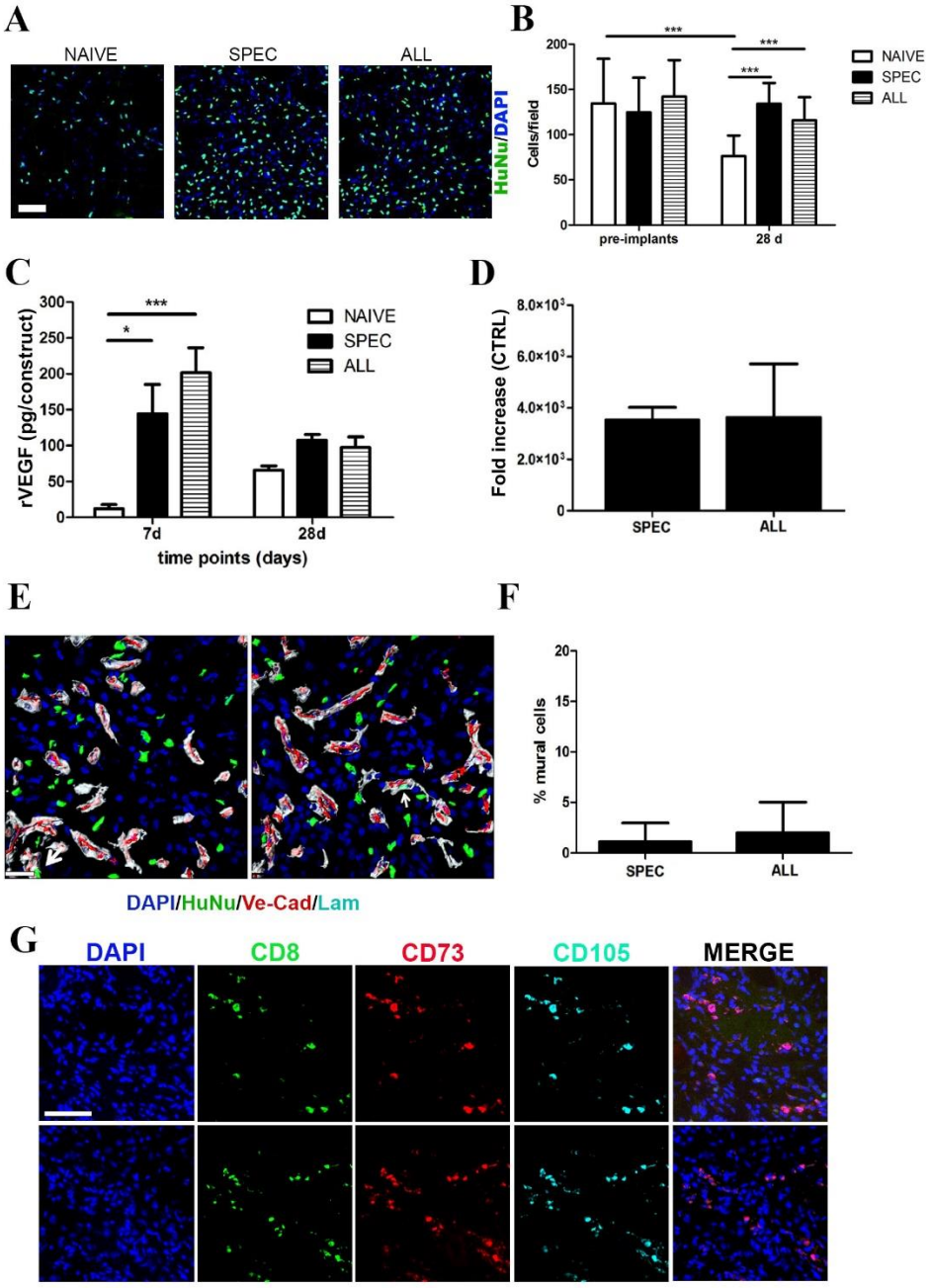

Fig. 2 Implanted cell fate in ectopic rat model. A) Representative immunofluorescence images of human cell distribution after 28 days *in vivo* in patches generated by naïve, SPEC and ALL ASC. Human nuclei were visualized in green (HuNu) and all nuclei in blue (DAPI) (size bar 20 µm). **B)** Human cell density in patches generated by naïve, SPEC and ALL ASC at day 0 (pre –implants) or 28 (post-implants) *in vivo* (n=4, ***p<0.001). **C)** rVEGF quantification in naïve and VEGF-expressing constructs after 7 and 28 days in vivo. (*p<0.05; ***p<0.001). **D)** RT-PCR analysis of IRES mRNA expression in SPEC and ALL constructs at 28 days *in vivo* presented as fold increase compared to the Control (naive patches). **E)** Representative immunofluorescence images for human cells (HuNu in green), VE-Cadherin (in red),

laminin (in grey) and DAPI (in blue) in patches generated by SPEC or ALL ASC after 28 days *in vivo*. White arrows indicate human cells embedded in the endothelial basal lamina (size bar=20µm). **F)** Percentage of human SPEC or ALL ASC with a role of mural cells (n=3 sample/condition). **G)** Immunofluorescence images for mesenchymal markers (CD73 in red; CD105 in cyan) in human transplanted cells identified with the rat CD8 (green) and DAPI (blue) at 28 days *in vivo* (size bar=25µm).

The number of mural cells of human origin was rather low and similar in the patches generated by either SPEC or ALL ASC (Fig 2F). The great majority of the implanted human ASC maintained the expression of the typical mesenchymal membrane markers as CD73 and CD105 at 28 days, suggesting that most of the cells retained the stromal phenotype (Fig 2G). Taken together these results showed that ASC per se might not have a key role in the normalization of abnormal structures.

3.3 Collagen-based scaffolds allow VEGF diffusion

To verify that the specific scaffold composition regulates alone the diffusion or not of VEGF, we compared the type of vessels formed in vivo by culturing ASC expressing heterogeneous protein levels on sponges made of either collagen or Egg White (EW).

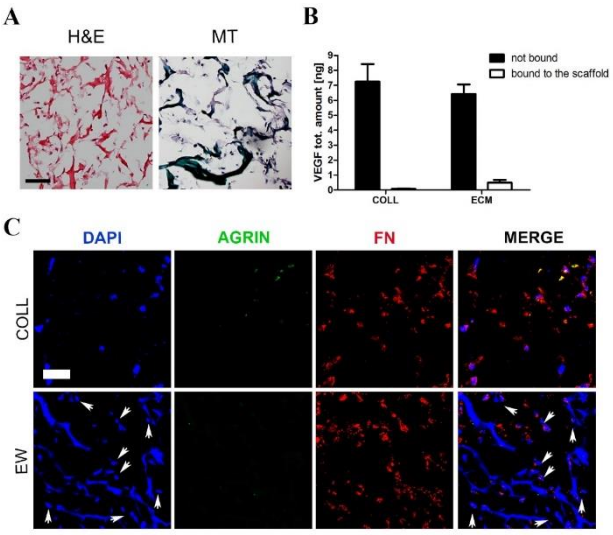

Supp. fig 2 A) Representative images of Haematoxylin and Eosin (H&E) staining and Masson Trichrome (MT) staining of naïve ASC-based patches after 5 days of dynamic culture (size bar=25 µm). **B)** Amount of rVEGF retained by collagen scaffolds either alone (COLL) or with extracellular matrix (ECM) deposited by naïve ASC. (n=5 per condition). **C)** Characterization of extracellular matrix composition of COLL- or EW- based patches generated by naïve ASC after 5 days of *in vitro* culture: DAPI (blue), agrin (green), fibronectin (FN, red) (size bar=20 µm).

While collagen is known to not bind the $VEGF_{164}$, EW has shown to have a high affinity to bind proteins including this specific isoform (19). By scanning electron microscopy imaging, the collagen and EW scaffolds displayed an analogous architecture with similar percentage of porosity and pore size (Fig 3A-B). The two sponges showed similar

swelling and degradation properties (Fig 3B). When incubated with $VEGF_{164}$ containing medium, collagen per se did not resulted positive for VEGF immunofluorescence staining,

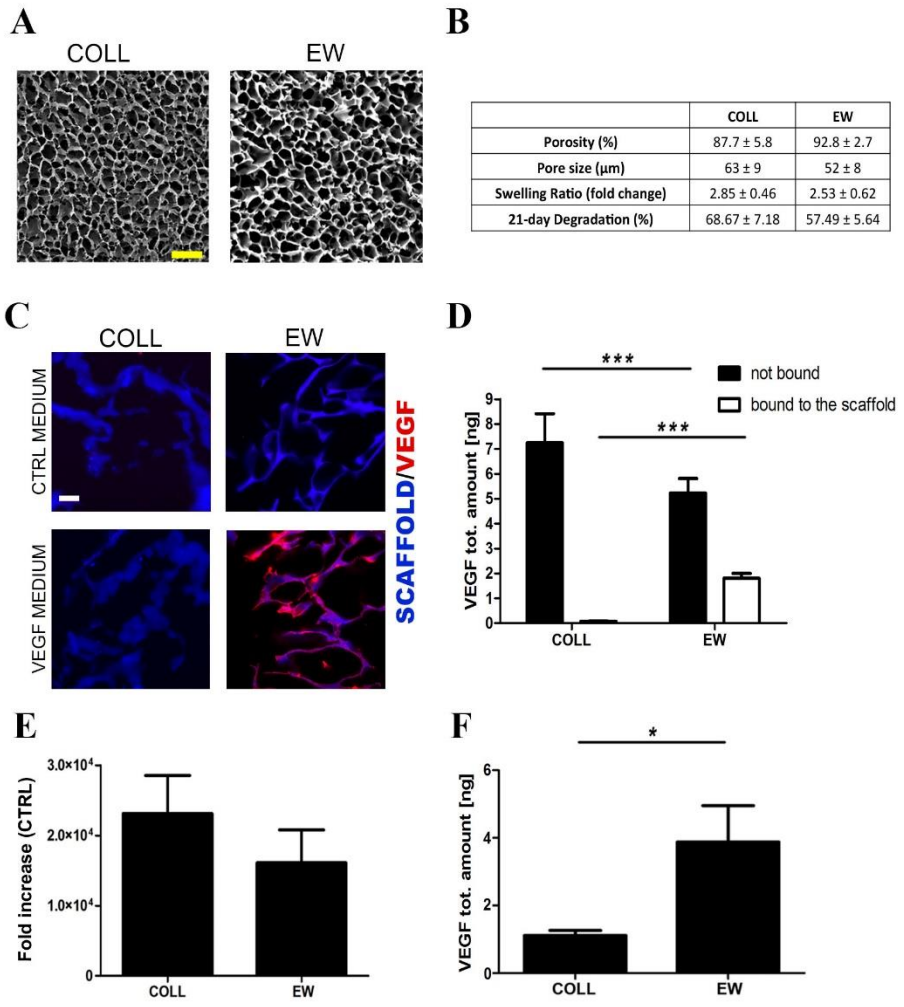

	COLL	EW
Porosity (%)	87.7 ± 5.8	92.8 ± 2.7
Pore size (µm)	63 ± 9	52 ± 8
Swelling Ratio (fold change)	2.85 ± 0.46	2.53 ± 0.62
21-day Degradation (%)	68.67 ± 7.18	57.49 ± 5.64

Fig. 3 ***In vitro*** **characterization of different scaffold composition. A)** SEM images of the porous architecture typical for collagen (COLL) and Egg White (EW) scaffolds (size bar=100 µm). **B)** Structural features of COLL and EW sponges. **C)** Immunofluorescence images for rVEGF (in red) bound to COLL or EW scaffolds (identified in blu by a high exposure time; size bar=20µm). **D)** Quantification of rVEGF trapped in the scaffolds (bound to the scaffold) and in the supernatants (not bound) after 4 hours of incubation in ALL ASC-conditioned medium. (n=5 for COLL, 3 for EW ***p<0.001). **E)** *In vitro* IRES mRNA expression in collagen or EW scaffolds seeded with ALL-ASC (n=3 per experimental group) has been normalized on the relative expression of h*gapdh* and presented as fold increase compared to the control (CTRL). **F)** Quantification of *in vitro* rVEGF present in COLL and EW sponge-based patches generated by ALL ASC after 5 days of culture (n=3 per condition; *p<0.05).

whereas EW showed a detectable amount of protein bound on the scaffold surface (Fig 3C). The quantification of rVEGF confirmed that most of the protein was not bound to the collagen scaffold, since it was found almost entirely in the supernatant. On the contrary EW-based sponges retained the 25% of the available VEGF (Fig. 3D). Importantly, after 5 days of perfusion-based culture ASC deposited a poor amount of extracellular matrix (ECM) mainly detected to the immediate surrounding area of the cells (Supp. Fig 2A). The ability of the naïve-based patches in retaining the VEGF was similar to the collagen sponge alone (Supp. Fig 2B). The ECM was deposited by naïve ASC in a scattered way both in collagen and EW sponges and was composed similarly by low amount of VEGF-binding proteins as agrin and fibronectin (FN). Agrin was indeed mainly undetectable, whereas FN was low and mainly expressed within the cytoplasm (Supp. Fig 2C). Moreover, although the expression of VEGF at the mRNA level of ALL-ASC after 5 days of culture in EW-based sponges was similar to that obtained in the collagen sponges (Fig 3E), the total amount of VEGF entrapped in the EW-construct was ca. 5-times superior (Fig 3F). These observations further confirm the ability of EW scaffold to bind the VEGF.

3.4 The scaffold composition controls the type of angiogenesis induced: normal versus aberrant.

When ASC expressing not controlled VEGF levels were cultured on EW-based scaffolds, numerous aberrant large blood vessels, a general dysfunction of pericytes and inhomogeneous coverage of smooth muscle cell layers were detected after 14 days in the rat subcutaneous pockets (Fig 4 white arrow). On the contrary, angiogenesis induced by the same donor cells expressing the same heterogeneous VEGF levels but

seeded on a collagen scaffold displayed a normal phenotype (Fig 4 ALL COLL, left column). Extended quantification of vessel diameters showed that the presence of large-in-size structures

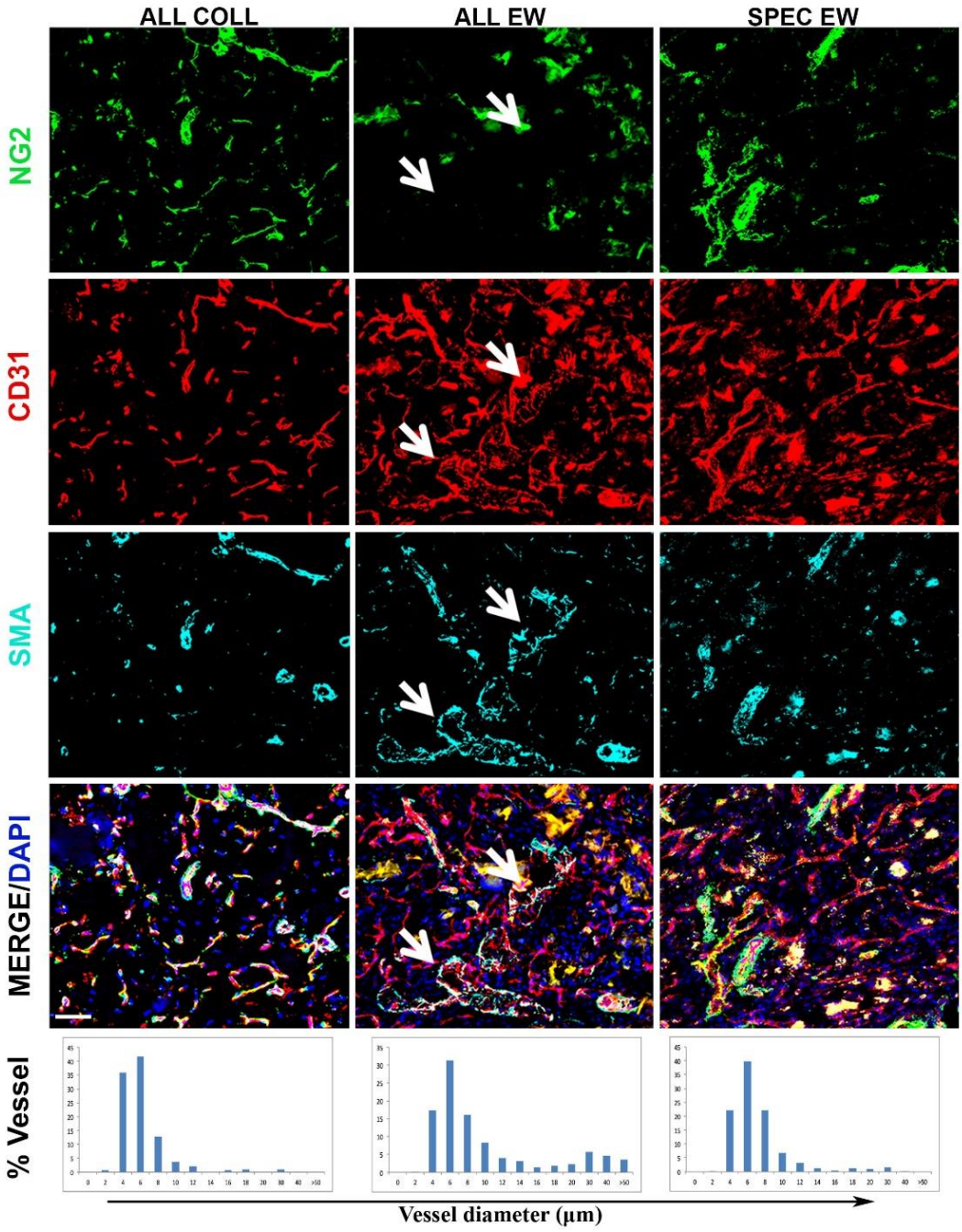

Fig. 4 Angiogenesis induced by egg white-based patches in ectopic rat model. Representative images with the relative distribution of vessel diameters of newly formed blood vessels in COLL or EW scaffold seeded with ALL ASC or in SPEC EW-based patches at 14 days upon implantations. Cell nuclei are stained with DAPI, pericytes with NG2, endothelial cells with CD31and smooth muscle cells with SMA. White arrows identify abnormal vessel structures (size bar=50 µm).

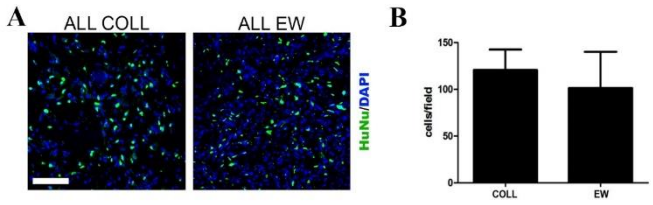

Supp fig 3. A) Representative images and **B)** quantification of human cell density in COLL- or EW-based patches generated by ALL ASC at 14 days in vivo (n=3; no statistically significant difference was found)

has a higher preponderance in EW-patches compared to COLL-constructs. These enlarged structures were consistently observed throughout the three replicates examined. Remarkably, when EW scaffolds were seeded with ASC expressing controlled VEGF levels, no aberrant structures were formed (Fig 4, SPEC EW, right column) and the vessel diameter distribution was similar to the one measured in the collagen-based patches (Fig 4). Importantly, the implanted human cells were uniformly distributed both in the collagen and in the EW sponge after 14 days in vivo and in a similar density (Supp. Fig 3 A, B).

3.5 Collagen-based patches act as efficient and safe VEGF delivery systems

The extrinsic angiogenic potential and the safety of the collagen-based patches releasing uncontrolled VEGF levels were assessed in both ectopic and orthotopic model of healthy myocardium. In rat subcutaneous pockets the angiogenesis was induced efficiently in the 7-mm-thick-collagen sponges with a higher vessel length density when ALL and SPEC VEGF-expressing patches were used compared to naive cells (data not shown). These results confirmed the previous extrinsic angiogenesis observed in mice when controlled VEGF levels were used (described in Chapter II,

section 3.4) and further demonstrated the efficacy of ALL ASC to induce normal angiogenesis in the surrounding area.

In healthy heart model, implants were found still in place on the top of the left ventricle after 28 days (Fig 5A H&E). However, while the cell-free collagen scaffolds showed no

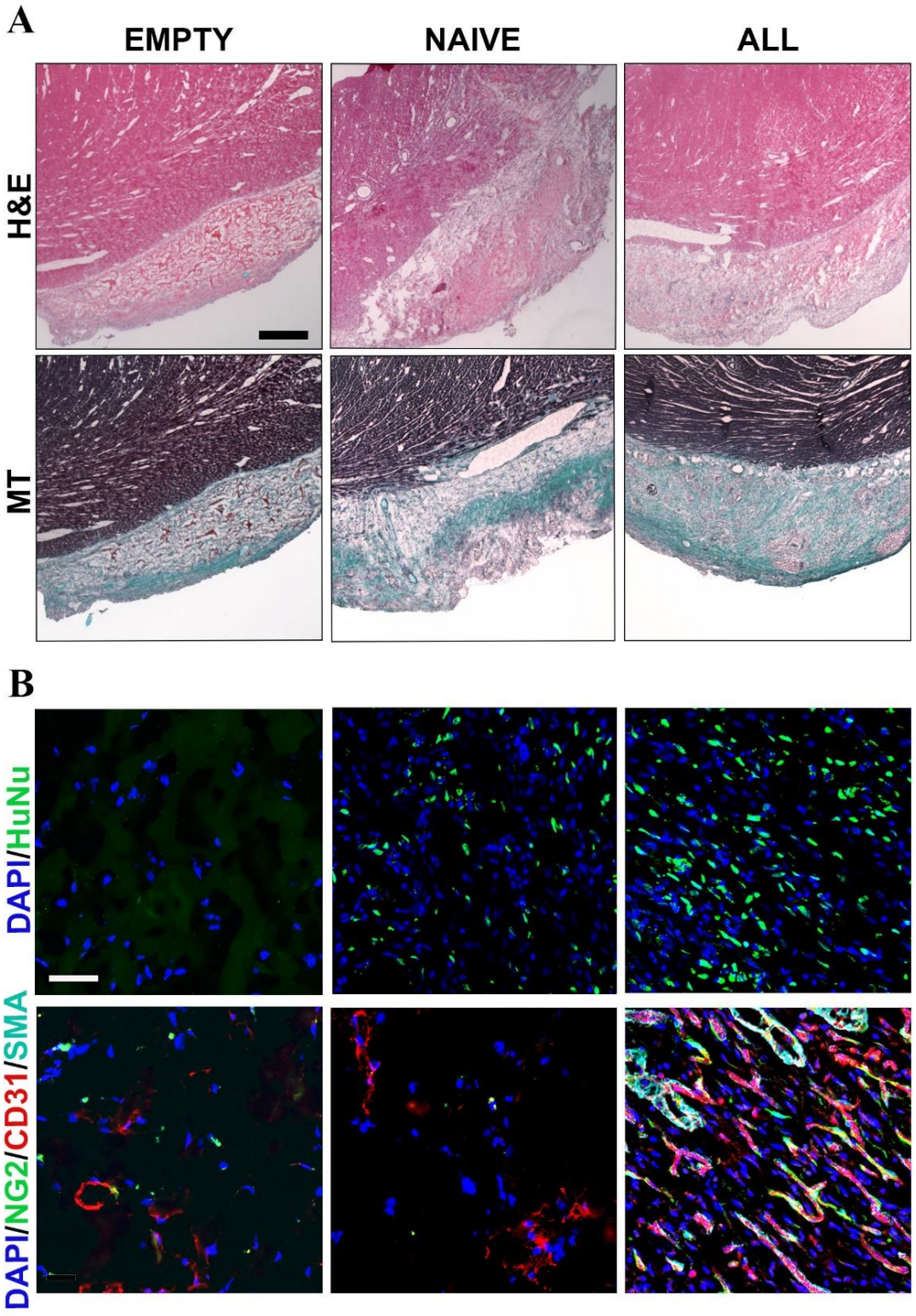

Fig 5 Collagen-based patches following implantation on healthy rat hearts. A) Representative images of Haematoxylin and Eosin (H&E) and Masson Trichrome (MT) of heart cross-sections implanted with cell free (EMPTY), naïve and ALL ASC collagen-based patches (size bar=500 µm). **B)** Representative images of human cell survival (in green) and patch vascularization at 28 days (DAPI blue, CD31 red, NG2 green, SMA cyan, size bar=50 µm).

important modification, the patches generated by ASC appeared to be quite remodeled, with a significant invasion of host cells and newly deposited extracellular matrix forming a fibrotic tissue within the constructs (Fig 5A, MT). Remarkably, human cells were still detectable in both naive and ALL ASC patches after 28 days. While cell-free scaffolds and naive ASC-based constructs were invaded by few blood vessels, VEGF-expressing patches were highly vascularized with mature blood vessels reaching the center of the implants. In the patch expressing heterogeneous VEGF levels, the abundant and newly formed vessels displayed a normal and mature morphology and consisted in both arterioles, surrounded by smooth muscle actin, and capillaries with the typical coverage with pericytes (Fig. 5B bottom panel). No abnormal vessel enlargements or morphology were observed in collagen-based patches generated by ASC releasing uncontrolled VEGF levels. Of note, the blood vessels significantly increased in the underlying myocardium only when VEGF expressing patches were used (Fig 6A). The quantification of the vessel length density showed a ~ 1-fold increase of VLD in the VEGF expressing patches compared to the controls. This angiogenic effect was observed up to 500 µm depth in the underlying myocardium of the VEGF-expressing engineered constructs.

The presence of the patches (either cell-free or cultured with naïve or VEFG- ASC) per se did not affect the functionality of the heart compared to the sham condition within a period of 28 days, as shown by the measurement of ejection fraction and fractional shortening recorded at 0 (pre-implantation baseline), 7 and 28 days post implantation. Taken together these results showed that collagen-based delivery of heterogeneous

VEGF levels induced an efficient and safe angiogenic process both in the patch itself and in the healthy surrounding myocardium, without impairing the heart contractility.

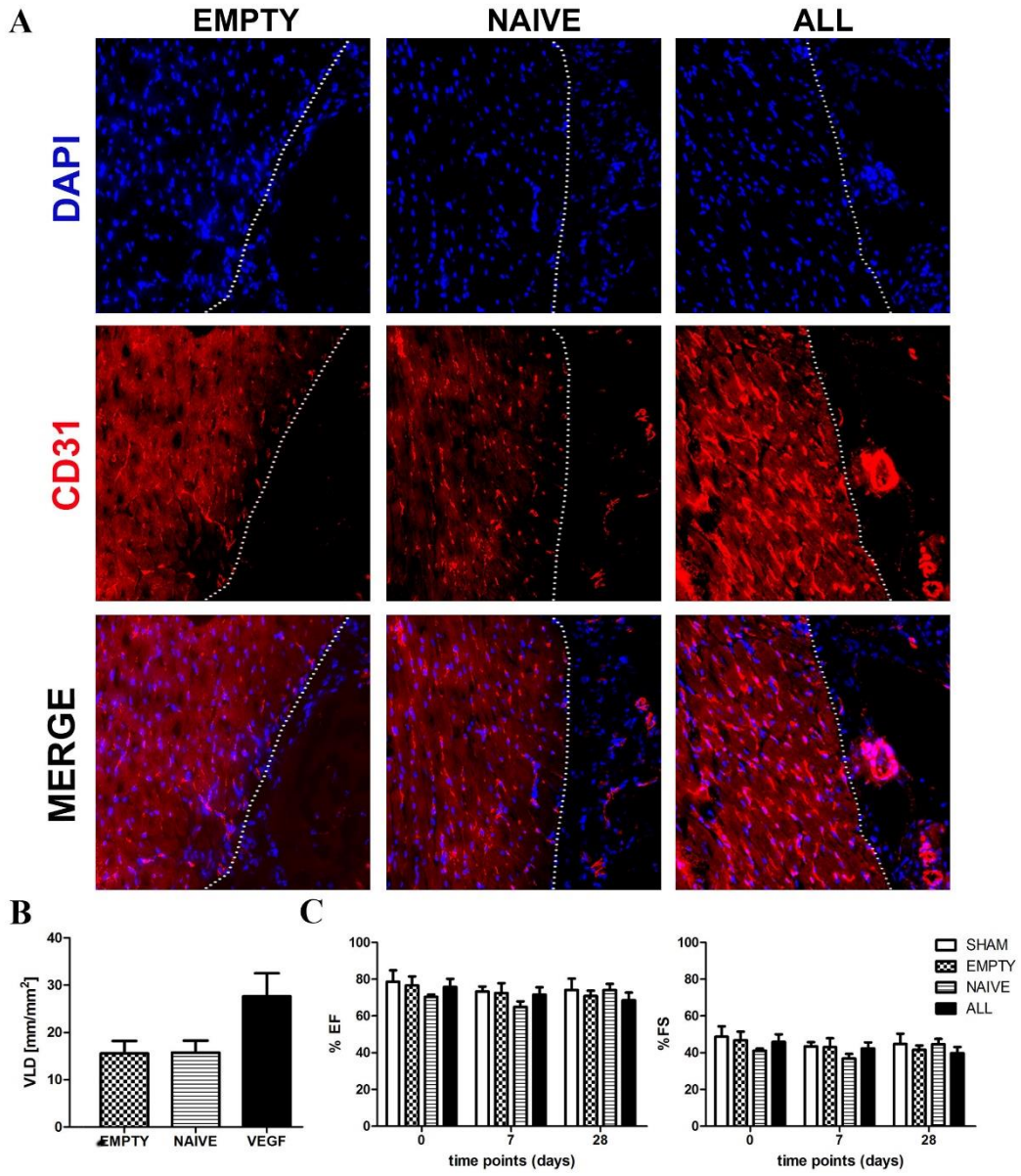

Fig 6 Induction of extrinsic angiogenesis in the rat healthy myocardium. A) Representative images of capillary density of the rat myocardium in the area acquired beneath the patches. Nuclei are stained in blue (DAPI) blood vessels in red (CD31). White lines represent the boundary between the myocardium and the implanted patch (size bar=50 µm). **B)** Quantification of VLD in the host underneath myocardium (EMPTY, n=3; NAIVE n=3 ALL n=4; ***p<0.001). **C)** Heart functionality measured as percentage of the Ejection Fraction (EF, left) and Fractional Shortening (FS, right) in the experimental groups (SHAM n=6, EMPTY n=3, NAIVE n=3 and ALL n=9) at 0 (pre-implant) 7 and 28 days post implantation.

4 Discussion and conclusions

In the present study, we demonstrated that a porous scaffold made of type I collagen, acting as a diffusion system, prevents the formation of toxic spots of VEGF caused by the uncontrolled overexpression of the protein from retro-transduced cells.

Analysis of cell survival showed the importance to prompt vascularize the scaffold in order to supply enough nutrients to the cells. In fact, in the patch that does not express VEGF we observed a drop in the cell density, overall suggesting that a tissue engineering approach without an intrinsic proangiogenic stimulus could fail because the premature death of the tissue implanted.

Efficacy in inducing angiogenesis is strictly modulated by the interactions between the VEGF and the extracellular matrix proteins; therefore, the biological effect, in particular the morphology of the new blood vessels, depends on the microenvironmental concentration to which are expose the next endothelial cells. In previous studies, a method based on the sorting of a population expressing only specific levels of VEGF has been tuned. Although the efficacy in preventing the formation of aberrant structures also in a 3D setting has been demonstrated, this method is not feasible for a translational approach because the high number of expansion and the in vitro manipulation required to achieve enough cells could affect their behavior. Recently, it turned out that a balanced co-delivery of VEGF and PDGF-BB, which is responsible for the recruitment of the pericytes, normalized abnormal vasculature suggesting a key role of mural cells in modulating the biological effect of the VEGF (22). In this study we showed that a collagen sponge used as scaffold to

generate a 3D patch acts as deliver system by diluting the toxic spots forming around cells expressing high levels of VEGF.

In particular this is possible on one hand because the inability of the collagen to retain the growth factor. On the other hand, the time of 3D perfusion culture (5 days) necessary to generate the patch is not sufficient for the cells to build a dense ECM. This concept is further support by the fact that the ECM produced by the ASC under perfusion lack completely of agrins, fibronectin (Supp. fig 2C) and perlecans (data not shown), which are the ECM proteins mainly responsible for the binding of the VEGF. In vivo it has been shown that in case of high levels of VEGF, aberrant structure growth within the first week and they became independent from VEGF signal continuing in proliferating. In this case, we observed inside the patch a normal angiogenesis proliferation at 7 days and any enlarged structures proliferating, although a sustained expression of the VEGF was maintained. ELISA assay confirmed a higher concentration of VEGF in the patches at 7 days in vivo as compared to the control, with a progressive decrease at long-term time point, as expected. In fact, although the viral construct is stably integrated in the genomic DNA, it is well-known that the promoter of the virus progressively becomes silenced in vivo due to the immune system recognition. Nevertheless, at 28 days RT-PCR analysis showed that it was still possible to detect copies of mRNA containing the IRES sequence, suggesting that ASC were still active in expressing exogenous VEGF. On the other hand, the effect on the endothelial cells decreased over a time leading to quiescence, where only few cells were still in the cell cycle. Based on these observations, we can speculate that the prevention of the growth of the aberrant structures is due mainly to the inability of the patch to retain

the VEGF, homogenizing the microenvironmental concentration. On the opposite when a scaffold that is able to efficiently retain the VEGF is used, we observed the growth of abnormal blood vessel with a spare dysfunction of the pericytes and a general increase in vessel diameters. Although the mechanism through this occurs has not been investigated, we can speculate that, once the blood vessels growth inside the patch within the first week attracted by the VEGF they get exposed to uncontrolled levels of VEGF. The blood vessels that meet high levels of VEGF grow abnormally, displaying the classical features of aberrant structures. Importantly, the collagen scaffold is able to prevent the growth of aberrant structures also when the patch is in contact with a highly vascularized tissue such as the myocardium. ALL patches not only do not cause aberrant angiogenesis but also increase the vascularization of the underneath tissue up to 500 μm, displaying an effective ability to provide an extrinsic proangiogenic stimulus. This could be a consequence of the diffusion capacity of the collagen. Future studies will aim to investigate the extrinsic angiogenic potential of these VEGF-expressing patches in chronic ischemic animal models and in particular for the treatment of the border zone of the infarct where there is a rarefaction of the microvasculature and the cardiomyocytes are not functional but still alive. It will be crucial to assess the VEGF capacity of diffusing through a fibrous scar tissue, present upon a myocardial infarction. Importantly, the functionality of the heart is not affected by the presence of the scaffold per se, further supporting the concept that this approach could be feasible in treating an ischemic myocardium. Further studies are also needed in order to deep investigate this aspect, focusing also on the paracrine effect that the ASC could have on the remodeling of the scar tissue.

In conclusion in this study, we demonstrated that composition of the scaffold in generating engineered tissues to deliver VEGF is a key to control the high potent angiogenic protein diffusion action, normalizing the microenvironmental concentration of the growth factor.

5. References

1. *Targeting angiogenesis to restore the microcirculation after reperfused MI*. **Van der Laan A.M., et al.** 2009, Nat. Rev. Cardiol. 6, 515-523.

2. *Therapeutic angiogenesis and vasculogenesis for ischemic disease. Part I: angiogenic cytokines*. **Losordo D.W. and Dimmeler S.** 2004, Circulation 109, 2487-2491.

3. *Cardiovascular gene therapy for myocardial infarction*. **Scimia M.C., et al.** 2014, Exp. Opin. Biol. Ther. 14, 183-195.

4. *Spatially restricted patterning cues provided by heparin-binding VEGF-A control blood vessel branching morphogenesis*. **Ruhrberg C., et al.** 2002, Genes Dev. 16, 2684–2698.

5. *Therapeutic angiogenesis for myocardial ischemia revisited: basic biological concepts and focus on latest clinical trials*. **Mitsos S., et al.** 2012, Angiogenesis 15, 1-22.

6. *Therapeutic angiogenesis for cardiovascular disease: biological context, challenges, prospects*. **Zachary I. and Morgan R.D.** 2011, Heart 97, 181-189.

7. *Conditional switching of VEGF provides new insights into adult neovascularization and pro-angiogenic therapy*. **Dor Y., et al.** 2002, EMBO J. 21, 1939-1947.

8. *MSC-based VEGF gene therapy in rat myocardial infarction model using facial amphipathic bile acid-conjugated polyethyleneimine*. **Moon H.H., et al.** 2014, Biomaterials 35, 1744-54.

9. *Baculovirus-transduced, VEGF-expressing adipose-derived stem cell sheet for the treatment of myocardium infarcti*on. **Yeh T.S., et al.** 2014, Biomaterials 35, 174-184.

10. *Cell delivery and tracking in post-myocardial infarction cardiac stem cell therapy: an introduction for clinical researchers*. **Wei H., et al.** 2010, Heart Fail. Rev. 15, 1-14.

11. *Cardiac cell therapy: lessons from clinical trials.* **Menasche P**. 2011, J. Mol. Cell. Cardiol. 50, 258-265.

12. *Cell delivery: intramyocardial injections or epicardial deposition? A head-to-head comparison*. **Hamdi H., et al.** 2009, Ann. Thorac. Surg. 87, 1196-1203.

13. *The effect of controlled expression of VEGF by transduced myoblasts in a cardiac patch on vascularization in a mouse model of myocardial infarction*. **Marsano A., et al**. 2013, Biomaterials 34, 393-401.

14. *Long-term VEGF-A expression promotes aberrant angiogenesis and fibrosis in skeletal muscle*. **Karvinen H., et al.** 2011, Gene Ther. 18, 1166-1172.

15. *Microenvironmental VEGF concentration, not total dose, determines a threshold between normal and aberrant angiogenesis*. **Ozawa C.R., et al**. 2004, J. Clin. Invest. 113, 516-527.

16*. The vascular endothelial growth factor VEGF, isoforms: differential deposition into the subepithelial extracellular matrix and bioactivity of extracellular matrix-bound VEGF*. **Park J. E., et al.** 1993, Mol. Biol. Cell. 4, 1317–1326.

17. *High-throughput flow cytometry purification of transduced progenitors expressing defined levels of vascular endothelial growth factor induces controlled angiogenesis in vivo*. **Misteli H., et al.** 2010, Stem Cells 28

18. *Generation of human adult mesenchymal stromal/stem cells expressing defined xenogenic vascular endothelial growth factor levels by optimized transduction and flow cytometry purificat*ion. **Helmrich U., et al.** 2012, Tissue Eng. Part C Methods 18, 283-292.

19. *Facile fabrication of egg white macroporous sponges for tissue regeneration*. **Jalili-Firoozinezhad S., et al.** 2015, Adv Healthc Mater. 4, 2281-2290.

20. *Single-step method of RNA isolation by acid guanidinium thiocyanate-phenol-chloroform extraction.* **Chomczynski P and Sacchi N**. 1987 Anal Biochem. 162, 156-159

21. *A perivascular origin for mesenchymal stem cells in multiple human organs*. **Crisan M., et al.** 2008, Cell Stem Cell 3, 301-13.

22*. Long-term safety and stability of angiogenesis induced by balanced single-vector co-expression of PDGF-BB and VEGF164 in skeletal muscle*. **Gianni-Barrera R., et al.** 2016, Sci. Rep. 6, 21546.

Chapter IV: Conclusions and future perspectives

VEGF cell-based gene therapy is a promising approach to induce therapeutic angiogenesis; however, the delivery of the cell population and the control over the protein expression levels still represent major issues. In this research project, we showed the possibility to generate *in vitro* a protein delivery platform (patch) based on genetically modified ASC cultured on a type I collagen sponge. We demonstrated that collagen based patches could induce physiological growth of new capillaries both within the construct itself and in the surrounding tissue also when ALL ASC were used, thanks to the poor affinity of the scaffold for VEGF. These promising results suggest numerous future studies. On one hand, it is crucial to investigate the effects of the angiogenesis induced by the patch also in animal infarction models in terms of micro-revascularization and eventually rescue of cardiomyocytes in low perfused areas of the hibernating myocardium. On the other hand, a specific study should be designed in order to understand whether such a diffused pro-angiogenic signal is enough to stimulate also the opening of the coronary collateral circulation (1) as already demonstrated in the hind limb ischemia model with other approaches (2).

Concerning the therapeutic potential, it is of primary interest to understand the limit of the VEGF diffusion from the patch placed on the epicardial surface of the heart into the myocardium. In fact, in cases of large infarction the ischemia can extend to the endocardium, damaging also the inner lining of the heart (trans-mural infarction). In this circumstance, it could be useful to support the action of the epicardial patch with several adjuvant intramyocardial injections of cells pre-organized in gels. In alternative, an attractive perspective derives from the possibility to exploit techniques that are used in cancer therapy to improve the diffusion of molecules through the ECM of solid

tumours, such as injection of proteases including trypsin, collagenase, hyaluronidas, metalloproteinase, relaxin and decorin (3)

Beyond angiogenesis induction, VEGF-A is directly involved in other physiological processes of repair after MI, such as pro-survival, adhesion and homing of c-kit positive bone marrow derived cells and inhibition of cardiomyocyte apoptosis (4). Therefore, it is critical to determine whether the prolonged VEGF over-expression might improve or impair these processes in a post-infarction heart failure condition.

Another important aspect, which should not be underestimated, is the use of ASC as delivery cell source; as briefly mentioned already in the discussion of the second chapter, ASC recently emerged as the "optimal" population in cell therapy for MI (5). Although in our experimental set-up we did not investigate any substantial paracrine-mediated angiogenic effect, we could not exclude the possible release of other factors affecting the scar composition, thus its stiffness, and the cardiomyocyte survival. Therefore, beyond the angiogenesis induction benefits, it would be interesting to investigate the cardioprotective effects of the factors released by the cells, regarding in particular the remodeling of the scar tissue and the survival of remaining cardiomyocytes at the border zone. Taking in account that our patch guarantees the survival of the cells up to 28 days upon implantations, the paracrine effects could be greatly improved as compared to what has been observed with the intramyocardial injections.

The final perspective of such study is undoubtedly to propose this model as adjuvant treatment for MI and start the first in human trial. The first "proof of principle" for the safety, in terms of survival after the treatment, and for the efficacy in triggering a

proangiogenic stimulus, has been evaluated in immunocompromised pre-clinical animal models. Moreover, functional data (2D echo, chapter III section 3.5) excluded any possible impairment by the scaffold on the normal contractile function of an healthy heart. However, beyond the necessity to investigate the therapeutic efficacy, major translational issues related to the safety and the scale-up of the model require deeper investigations. In particular, alternative gene vectors should be considered, since retroviruses raise safety concerns about neoplastic transformation. In this context, the new self-inactivating lentiviral vectors or new serotypes of AAV are valid solutions to be tested in our system (6). In this study the viral construct has been designed to be tested in rodent models; studies in larger animals (such as rabbit or pigs) will require increased size of the patch, with a consequent increment of the number of the cells needed. Therefore, an "*ad hoc"* study aiming at maximize the transduction efficiency of the new vectors will be necessary to limit the expansion of the cell population *in vitro*. In perspective, considering unessential the FACS purification step for the selection of safe VEGF expressing cells, the gene box for the CD8 marker could be replace by another growth factor in order to improve or accelerate the angiogenic stimulus (such as FGF-2 or PDGF-BB).

Importantly, the generation of several mm-diameter patches for large animal models will require a strict collaboration with engineers to develop a scale-up of the bioreactor. Moreover, in vision of clinical application, controlled bioreactor-based culture systems need to be designed conforming to the good manufacturing practice.

In parallel, the patch could be used as a "template" for the development of tissue engineering applications, where the prompt supply of oxygen and nutrients inside the

scaffold still represents a bottleneck for the survival of the implanted cells (7). Therefore, it will be appropriate to investigate the minimum amount of VEGF expressing cells needed to guarantee the fast vascularization of the patch, so that the remained space could be exploit for co-culturing a suitable cell population. In this context, the recent progresses in the field of stem cell biology offer several valid opportunities such as mature cardiomyocytes derived from embryonic or induced pluripotent stem cells, although the safety of these cell population still need to be addressed. This application could be further extended at other highly vascularized tissues, such as liver, skin and bone.

In conclusion, this work represents an optimal model to investigate fundamental angiogenic mechanisms, but also the starting point for different translational medicine projects that will open new perspectives in the field of cardiac regenerative medicine and vascularization in tissue engineering.

References

1. *The human coronary collateral circulation.* **Christian S.** 2003, Heart 11, 1352–1357.

2. *Long-lasting fibrin matrices ensure stable and functional angiogenesis by highly tunable, sustained delivery of recombinant VEGF164*. **Sacchi V., et al**. 2014, Proc Natl Acad. Sci. U S A 111, 6952-6957.

3. *Strategies to Increase Drug Penetration in Solid Tumors*. **Choi I., et al.** 2013, Front. Oncol. 3, 193.

4. *Vascular endothelial growth factor in heart failure.* **Taimeh Z., et al** 2013, Nat.Rev. Card. 10, 519-530.

5. *Concise review: Adipose-derived stem cells as a novel tool for future regenerative medicine.* **Mizuno H., et al.** 2012, Stem Cells 30, 804-810.

6. *Gene therapy returns to centre stage.* **Naldini L.** 2015, Nature 526, 351–360.

7. *Vascularization of three-dimensional engineered tissues for regenerative medicine applications*. **Kim J.J., et al.** 2016, Acta Biomaterialia [epub ahead of print].